M 2020

U.PORTO
FEUP FACULDADE DE ENGENHARIA
UNIVERSIDADE DO PORTO

IMMUNOMODULATORY AND ANTIMICROBIAL ACTIVITY OF SAAP-148 IN SOLUTION AND RELEASED FROM PLGA COATINGS

JÉSSICA AMORIM
DISSERTAÇÃO DE MESTRADO APRESENTADA
À FACULDADE DE ENGENHARIA DA UNIVERSIDADE DO PORTO EM 12/11/2020
BIOENGENHARIA

Immunomodulatory and antimicrobial activity of SAAP-148 in solution and released from PLGA coatings

Jéssica Ferreira Amorim

Integrated Master in Bioengineering

Branch Molecular Biotechnology

Supervisor: Dr. Sebastian A.J. Zaat

Co-Supervisor: Dr. Cristina Martins

October 2020

The work described on this thesis was conducted at:

Amsterdam UMC (location AMC) – Amsterdam University Medical Centers
(Academic Medical Center of the University of Amsterdam)

“If I have seen further

it is by standing on the shoulders of Giants.”

Isaac Newton

Acknowledgements

In first place I would like to thank my supervisor Dr. Sebastian A.J. Zaat for giving me this opportunity to work in his group. I would like to thank for all the guidance and support that he provided me. I would like to thank Dr. Martijn Riool for all the help and patience in answering all my questions. I would like to give a special acknowledgement to Clara Guarch Perez for the companionship and patience in working with me, answering my questions and discussing with me the results from this work. During my time in the AMC I was able to learn a lot and from this amazing team professionally, but also as a person.

In second place I would like to thank my co-supervisor Dr. Cristina Martins for the advices, help and support during this process. I would like to thank for the availability for meetings to discuss work or for a simple conversion.

Finally, I would like to thank to my parents and my brother for all support and sacrifices, that allow me to arrive to the place where I am today.

Abstract

Bone fractures are a common injury, just in the USA nearly 3.5 million of bone fractures are registered in emergency departments in 2017 (Control 2017). If bone fractures are not properly treated, they can lead to non-unions and/or infections resulting in suffering and ultimately permanent disabilities. Nowadays, the treatment of infections associated with biomaterials includes the use of antibiotics and removal of the implant. However, antibiotics have been losing their efficacy to treat infections, due to the rising of resistance of bacteria to antibiotics.

A promisor strategy to fight infections is to ally antimicrobial peptides (AMPs) to biomaterials. AMPs are known by its antimicrobial activity, however, they have other abilities, such as immunomodulation (Hancock, Haney et al. 2016). SAAP-148 is a synthetic AMP derived from the natural AMP LL-37. SAAP-148 has been shown to be effective against drug-resistant bacteria and biofilms (de Breij, Riool et al.).

In this dissertation, it was studied the modulatory potential of the peptide SAAP-148 on mouse macrophage cell line RAW 264.7 cells, through gene expression of pro and anti-inflammatory markers. It was also analyzed the effect of SAAP-148 on calcium deposition by precursor osteoblasts mouse cell line MC3T3-E1 cells. It was also studied the antimicrobial activity of the release of SAAP-148 from 3D-printed PLGA coatings prepared from two different formulations.

The results of this research are very promising and suggest that SAAP-148 can modulate both macrophages into a tissue healing environment and keeping its antimicrobial activity after released from the PLGA coating.

Table of Contents

Table of Figures

Table Index

Abbreviations and symbols

3D printing – three-dimensional printing, also known as additive manufacturing

ALP – alkaline phosphatase

AMP – antimicrobial peptide

AP - activator protein

APCs - antigen-presenting cell

Are - antioxidant response element

Arg I – arginase 1

B2m – beta-2 microglobulin

BAP – bone alkaline phosphatase

BCA – bicinchoninic acid

BMP2 – bone morphogenetic protein 2

BMP2R - bone morphogenetic protein 2 receptor

CCR7 – C-C chemokine receptor 7

CD206 – cluster of differentiation 206

c-FMS – colony-stimulating factor-1 receptor

CFU – colony forming units

Cox-2 - cyclooxygenase 2

Creb - cAMP response element-binding protein

COC – circulating osteoblast-lineage cell

CXCR – CXC chemokine receptor

DC – dendritic cell

D-PBS - Dulbecco's phosphate-buffered saline

Dlx – distal-less homebox

dsDNA - double strain DNA

eDNA – extracellular DNA

EMA – European Medicines Agency

EPS – extracellular polymeric substances

ERK1/2 - extracellular related kinases 1 and 2

FBC – foreign body capsule

FBGC – foreign body giant cell

FBR – foreign body response

FBS - fetal bovine serum

FDA – U.S. Food and Drug Administration

FnBP A/B - fibronectin binding protein A and B

FPR2 - formyl peptide receptor 2

FRI – Fracture related infections

GAPDH - glyceraldehyde 3-phosphate dehydrogenase

gp130 – glycoprotein 130

Gre - glucocorticoid response element

hBD3 - human β-defensin 3

HDPs - host defense peptides

HIF - hypoxia-inducible factor

HMBS – hydroxymethylbilane synthase

IDRs - innate defense regulators

IFN-ɣ - interferon gamma

IGF-1R - insulin growth factor 1R

IL – interleukin

iNOS – nitric oxide synthase

IRF - TRIF-interferon regulatory factor

LC 99.9% – lethal concentration killing at least 99.9% of the bacterial inoculum

LPS – lipopolysaccharide

LTA – lipoteichoic acid

MAPK – mitogen-activated protein kinase

MCC – myeloid calcifying cell

MCETs - mast cell extracellular traps

MCP - monocyte chemoattractant protein

M-CSF – macrophage colony stimulating factor

MDSC - myeloid-derived suppressor cell

α-MEM - minimum essential medium α

MIC – minimal inhibitory concentration

Min - minutes

MOMP – monocyte-derived mesenchymal progenitor

MRGX2 - mast-related gene X2

MSC – mesenchymal stem cell

MSCRAMMs – microbial surface components recognizing adhesive matrix molecules

NETs - neutrophil extracellular traps

NFAT – nuclear factor of activated T cells

NF-kB - kappa-light-chain-enhancer of activated B cells

NK cell – natural killer cell

NOD - nucleotide-binding oligomerization domains

OC – osteocalcin, also known as bone gamma-carboxyglutamic acid-containing protein

OIM – osteoimmunomodulation

OPG – osteoprotegerin

OSM - oncostatin M

PAMP - pathogen-associated molecular pattern

PGE2 - prostaglandin E2

PIA – polysaccharide intercellular adhesion

PJI – prosthetic joint infection

PLD-1 - phospholipase D-1

PLGA - poly(lactic-co-glycolic acid)

PMN – polymorphonuclear leucocyte

PSM – phenol-soluble modulins

qPCR – real time quantitative polymerase chain reaction

RANK – receptor activator of nuclear factor kappa-B

RANKL – receptor activator of nuclear factor kappa-B ligand

RPMI 1640 - Roswell Park Memorial Institute 1640

ROS – reactive oxygen species

Runx2 – runt related transcription factor 2

S. aureus – Staphylococcus aureus

S. epidermidis – Staphylococcus epidermidis

SAAP-148 - synthetic antimicrobial antibiofilm peptide 148

SCID mice – severe combined immunodeficient mice

SCV – small colonies variant

SERAMs – secretable expanded repertoire adhesive molecules

SigB - sigma factor

SP - specificity protein

SpA - staphylococcal protein A

SPS - sodium polyanethole sulfonate

SQSTM1 - sequestosome 1

STAT - signal transducer and activator of transcription

TA – teichoic acid

T_c – cytotoxic T cell

TGF-β – transforming growth factor beta

T_h – helper T cell

TLR - toll-like receptors

TNFR - tumor necrosis factor receptor

TNF-α – tumor necrosis factor alpha

TRAF6 – TNF receptor associated factor 6

TREM - triggering receptor expressed on myeloid cells

T_{reg} – regulator T cell

VEGF – vascular endothelial growth factor

WST-1 – 4-[3-(4-Iodophenyl)-2-(4-nitro-phenyl)-2H-5-tetrazolio]-1,3-benzene sulfonate, also known as water soluble tetrazolium salt

Chapter 1

1 General Introduction

1.1 Motivation and Aim

In the USA alone nearly 3.5 million of bone fractures were registered in the emergency departments in 2017 (Prevention 2017). In spite of current advances in in medicine, 10% of these bone fractures results in undesirable outcomes (Pajarinen, Lin et al. 2019). In the USA, 100,000 bone fractures per year result in non-unions (Pajarinen, Lin et al. 2019) and about 1% to 2% of closed bone fractures results in infection, while in open fracture it can reach up to 30% (Steinmetz, Wernly et al. 2019). Complications such as infection and non-union of fractures can lead to loss of function and amputation. In addition to the morbidity and suffering, this kind of complications are also big burdens socially and economically, for example, the average cost of a non-union is around 10,000 USD (Pajarinen, Lin et al. 2019). With this situation in mind, the need for orthopedic devices that prevent infections and promote bone regeneration becomes very clear.

Antimicrobial peptides (AMPs) are short peptides with many functions including antimicrobial and immunomodulatory activity (Haney, Straus et al. 2019). AMPs can kill bacteria and thereby help to clear infections, but also can act on immune cells modulating their behavior which can also potentiate healing and infection clearance (Hancock, Haney et al. 2016). For these reasons, AMPs become a very interesting agent to be used in biomaterial coatings for medical devices.

Macrophages are cells from the innate immune system that are involved in bone fracture healing due to their capacity to cross-talk with bone forming cells to reestablish the tissue and the homeostasis (Chen, Wu et al. 2017). Thus, macrophages become a very attractive target since they are present in both fracture and infection site, act to clear the infections and also have an important role in bone regeneration.

The main aim of this dissertation is to study the modulatory activity of the antimicrobial peptide SAAP-148 on macrophages and osteoblasts. As a secondary aim, this dissertation focuses on the antimicrobial activity of 3D-printed PLGA coatings releasing SAAP-148 on titanium samples.

In order to assess the immunomodulatory activity of SAAP-148, the gene expression of characteristic markers from classically and alternatively activated macrophages were studied in mouse macrophages RAW 264.7 cell line using real time PCR. To study the osteogenic activity of the peptide, the calcium deposition by the mouse osteoblast precursor MC3T3-E1 cell line was assessed using Alizarin Red S.

The antimicrobial activity of the SAAP-148 in free form and when incorporated in the coatings was evaluated against *Staphylococcus aureus* through determination of the minimal inhibitory concentration (MIC) and the lethal concentration killing 99.9% of the inoculum (LC 99.9%), release assays and the JIS Z for determining the antimicrobial activity of the coatings.

1.2 Dissertation Structure

This dissertation is organized in 6 chapters.

In Chapter 1, the motivation and the aim of this work is explained.

In Chapter 2, a literature review to present the state of the art on the topics that motivated this dissertation, such as bone fractures, fractures related infections, biofilm formation, tissue colonization and bacterial antimicrobial resistance are explored. Alternatives to antibiotic treatments, such as AMPs and their double performance as antimicrobial agents and immunomodulators, will also be further looked into.

Chapter 3 presents the Materials and Methods used during this work. The Results are described in Chapter 4 and discussed in detail in Chapter 5. Chapter 6 contains the conclusions of this work as well as the future perspectives.

Chapter 2

2 Literature Review

2.1 Bone fracture

A bone fracture can result from many situations in our daily life, due to a big accident or even a simple fall. The bone is one of the few tissues that can heal without making a scar. However, certain types of bone fracture can lead to loss of function(s) (Baht, Vi et al. 2018), that, if not treated properly, can trigger permanent disabilities.

There are two processes for bone healing: the primary (or direct) healing and the secondary healing. The type of healing will depend on the space between the bone extremities.

Primary bone healing. In this process, there is a direct bone formation with recruitment to the site of mesenchymal progenitor cells and osteoblasts. The intramembranous process occurs when there is a rigid bone fixation without displacement of bone extremities and reduction of bone fragments. Due to these conditions, the inflammatory response is very low or even null (Baht, Vi et al. 2018). Primary bone healing can occur through contact healing or gap healing.

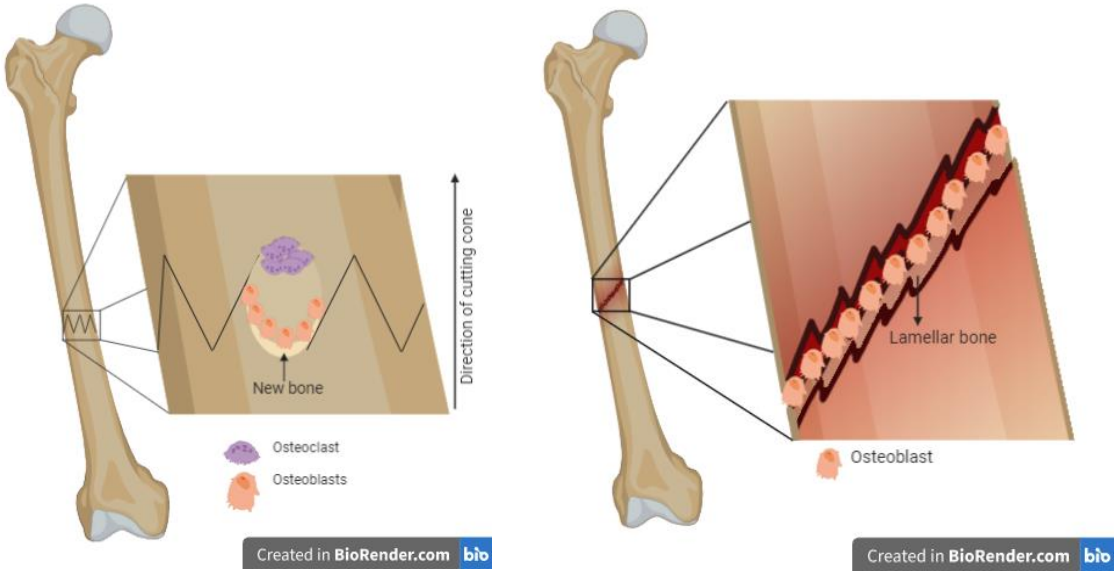

Figure 1 -Schematics of primary bone healing. (A) Contact healing with formation of a cutting cone. (B) Gap healing with formation of lamellar bone by osteoblasts.

Contact healing. Contact healing occurs in fractures which bone extremities are until 0,010mm apart. In this process, new bone is formed directly across the fracture line through extension of osteons. For that, there is the formation of cutting cones (Figure 1 A). In the tip of the cone there are osteoclasts which create cavities by reabsorbing the dead bone and in the rear of the cone there are osteoblasts which fill the cavities with new bone. Thus, the Haversian systems are retoured which allows the reestablishment of vasculature (Marsell and Einhorn 2011).

Gap healing. Gap healing occurs for gaps until 1mm. In this process, the gap is filled first with lamellar bone produced by osteoblast across the fracture line (Figure 1 B). This lamellar bone has a perpendicular orientation to the already existent bone and therefore has a weak mechanic stability. Thereby the new bone is remodeled in a process similar to the contact healing with the presence of cutting cones (Marsell and Einhorn 2011).

Secondary bone healing. This is the most common process and occurs in four phases: inflammatory phase, soft callus formation phase, hard callus formation phase and remodulation phase (Figure 2). Contrary to the primary healing, in the secondary healing the immune cells play an important role.

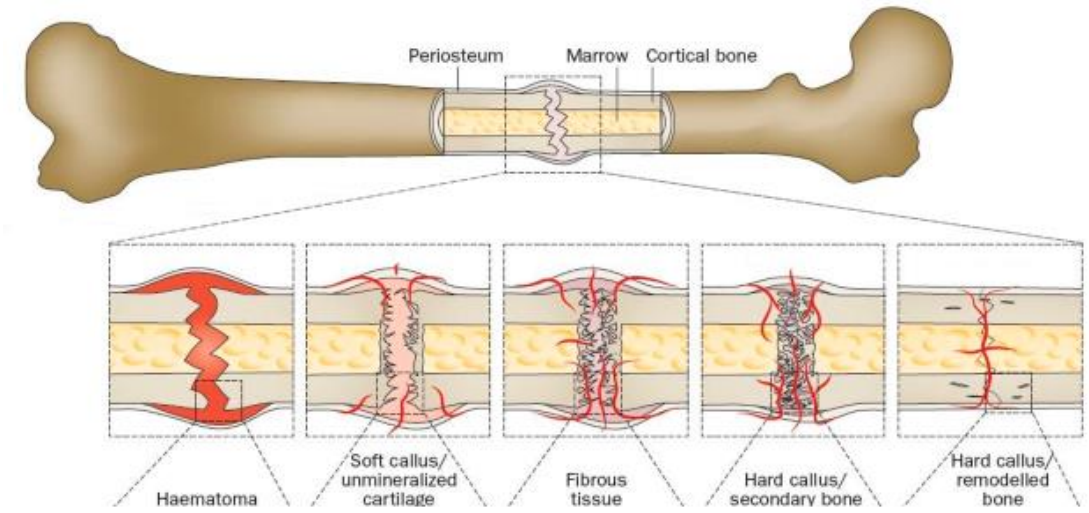

Figure 2 - Schematic of secondary bone healing with the four main phases. The first phase is the inflammatory phase with the formation of a hematoma. Followed by the soft callus with the formation of the fibrocartilaginous callus. The next phase is the hard callus, with formation of new bone. The last phase is the bone remodeling where the function and structures of the bone are reestablished. Image adapted from (Einhorn and Gerstenfeld 2015).

Inflammatory phase. A fracture is accompanied by disruption of the local vasculature and consequently the formation of a hematoma and the release of several cytokines and growth factors in order to recruit cells and promote angiogenesis. The hematoma serves as a template for the deposition of fibrin thrombus, which is infiltrated by capillary and substituted by granulation tissue (Baht, Vi et al. 2018). Neutrophils and macrophages are recruited to the site in order to clean the tissue and cellular debris and also to secrete several cytokines and chemokines for recruitment of mesenchymal stem cells (MSCs) from periosteum, bone marrow and the surrounding tissue. (Baht, Vi et al. 2018).

Soft callus formation phase. MSCs recruited in the early phase differentiate into chondrocytes. The chondrocytes will replace the granulation tissue for a fibrocartilaginous callus, which provides a better mechanical support. The fibrocartilaginous callus is later mineralized by chondrocytes. It is not yet certain if these chondrocytes later undergo through apoptosis or if they trans-differentiate into osteogenic cells (Baht, Vi et al. 2018).

Hard callus formation phase. In this phase, there are two different processes happening simultaneously: there is the osteoclast activation for reabsorption of the cartilaginous matrix and the recruitment of osteoprogenitor cells, which will differentiate into osteoblasts and start the osteogenesis process with the formation of new bone. Thereby, occurs the substitution of the cartilaginous callus for the bony callus, which

has a higher stability. In this phase the presence of immune cells such as macrophages, B cells and T cells is important, although the function of each cell type is not yet fully understood (Baht, Vi et al. 2018).

Remodulation phase. It is the last phase and the one that lasts the longest. In this phase occurs the substitution of the bony callus by lamellar bone with reestablishment of structure and functions of the original bone. In the remodulation phase the major players are the osteoclasts and osteoblasts, for bone reabsorption and bone formation respectively (Baht, Vi et al. 2018).

2.2 Bone fractures, host cells, biomaterials and infection

For the healing of a bone fracture, a crosstalk is necessary between many cell types like osteoblasts, osteoclasts, MSCs and immune cells, which are the major players. However, other cells such as endothelial cells are also very important because they allow the reestablishment of the vasculature and blood circulation in the bone (Lee, Byun et al. 2019). For that reason, it is more accepted that the bone healing is no longer only the activity of osteoblasts and osteoclast but the cooperation of multiple systems, such as skeleton, immune and circulatory systems (Chen, Wu et al. 2017).

2.2.1 Immune cells and biomaterial

When a biomaterial is implanted in the body the organism recognizes it as something strange and therefore triggers an immune response named foreign body response (FBR). The first event of this response is the adsorption of proteins from blood and interstitial fluids to the material surface. These proteins (fibrinogen, vitronectin, factor XIII, prekallikrein and high molecular weight kininogen and complement proteins) form a transient matrix in the surface, which will activate the coagulation process and the complement system, leading to the formation of a thrombus (Chen, Klein et al. 2016, Gorbet, Sperling et al. 2019). This interaction between the blood and material leads to an acute inflammation with recruitment of polymorphonuclear leucocytes (PMNs). PMNs will try to degrade the material through proteolytic enzymes and reactive oxygen species (ROS), but they get quickly exhausted and die by apoptosis (Chen, Klein et al. 2016). In the meantime, mast cells undergo through a degranulation which increases the chemokines and pro-inflammatory cytokine production. These molecules will amplify the inflammation as well as recruit monocytes to the site leading to their differentiation into macrophages. The macrophages will try to phagocyte the strange material. For materials until 5µm, macrophages can perform phagocytosis, for materials larger than that macrophages

fuse with each other by stimulation of IL-4 and IL-13, forming giant multinuclear cells named foreign body giant cells (FBGCs) (Chen, Klein et al. 2016). Due to the frustrated phagocytosis and therefore the failure of eliminating the foreign body, the organism will try to isolate it from the rest of the body by forming a fibrous capsule in order to contain any potential harm. However, this situation prevents the contact between bone cells and the material, which means that the fracture will be filled with a fibrotic tissue leading to the failure of the bone healing as well the osteointegration of the material (Chen, Klein et al. 2016).

2.2.2 Immune cells and bone cells

The healing of a bone fracture requires a balance between osteoblast and osteoclast activity. These activities are many times regulated by immune cells. The immune cells secrete cytokines and other molecules, which will trigger the activation of certain pathways and the production of specific proteins, resulting in bone cells' differentiation. Thereby, the immune cells are integral part of the bone healing process (Figure 3) (Baht, Vi et al. 2018).

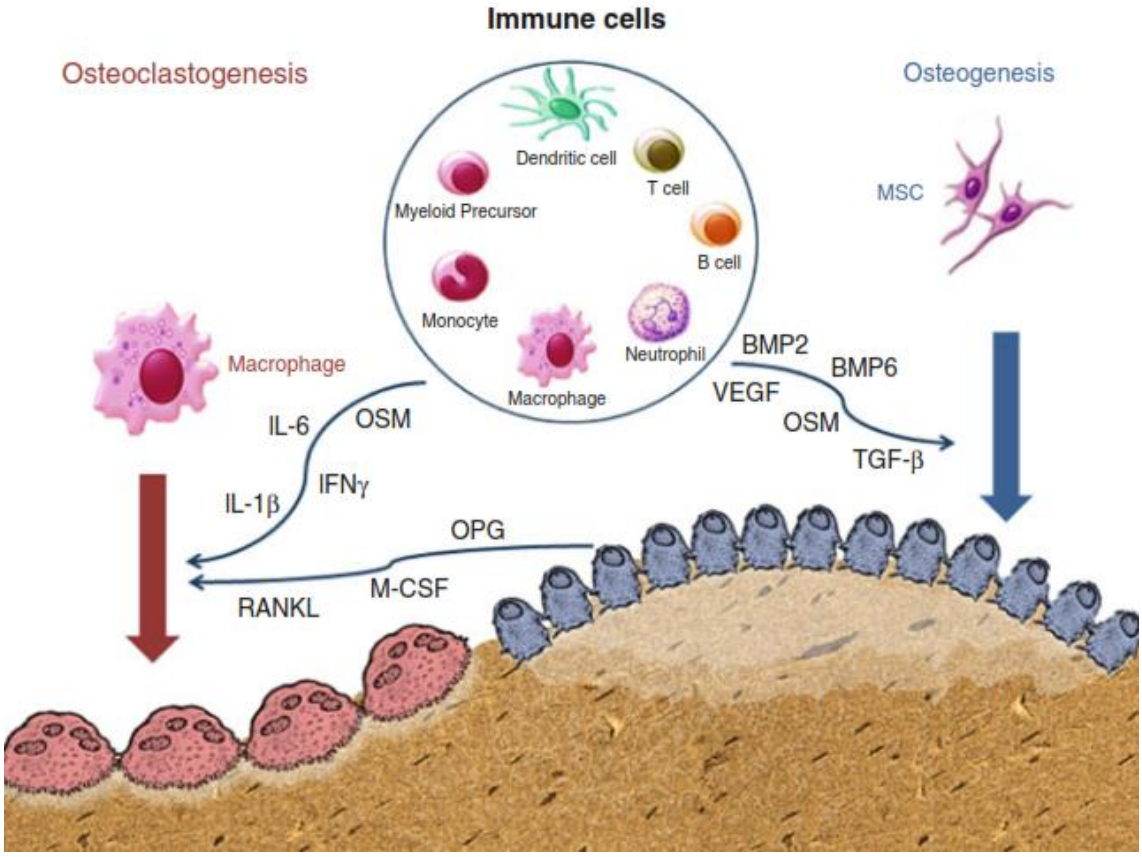

Figure 3 - Schematic representation of the influence of immune cells on bone dynamics. Immune cells are capable to regulate both osteoclastogenesis and osteogenesis via cytokine releasing (Chen, Wu et al. 2017).

Osteogenesis. Osteogenesis is the process of formation of new bone in which the effector cells are the osteoblasts. Osteoblasts differentiate from MSCs through the activation of many pathways. MSCs will differentiate into osteochondrocytes precursors. With help of Runx2, β-catenin and/or Dlx3/5/6 osteochondrocytes will differentiate into immature osteoblasts. For maturation of osteoblasts, molecules such as osterix, nuclear factor of activated T cells (NFAT) and β-catenin are very important (Lee, Byun et al. 2019).

In this process, it is thought that the macrophages play a very important role, although there is no consensus about which polarization of the macrophages is more supportive of osteogenesis, it is important to highlight that macrophages polarization and cytokines pattern is dependent of the microenvironment in which the macrophages are. The microenvironment of bone healing changes in space and in time. Therefore, the response of macrophages as well as its effect on osteogenesis and osteoclastogenesis is also dependent on the healing phase in question (Chen, Klein et al. 2016).

Macrophages with M1 polarization are associated with early phases of bone healing. M1 macrophages produce pro-inflammatory cytokines such as TNF-α, IL-6 and IL-1β, which are characteristic for stimulate osteoclastogenesis (Chen, Klein et al. 2016). Cytokines such as IL-1β suppress the synthesis of alkaline phosphatase (ALP) as well the mineralization of extracellular matrix (Lee, Byun et al. 2019). However, M1 macrophages also produce oncostatin M (OSM), which belongs to the IL-6 family, that induces the differentiation of MSCs and mineralization of the matrix (Guihard, Danger et al. 2012). Studies in mice also showed that the knockout of IL-6 leads to a delay in callus maturation and in the remodulation of the bone (Yang, Ricciardi et al. 2007).

Macrophages with M2 polarization are associated with later phases of bone regeneration. They are responsible for determining the success of the implant by osteointegration or the failure by developing a fibrous capsule (Chen, Klein et al. 2016). M2 macrophages produce anti-inflammatory cytokines such as IL-10 and IL-1RA, growth factors like TGF-β and VEGF and proteins like BMP-2/6, which will participate in recruitment of MSCs and their differentiation into osteoblasts (Baht, Vi et al. 2018). IL-1RA is an inhibitor of IL-1 and therefore inhibits and regulates the effects of IL-1 produced by M1 macrophages (Lee, Byun et al. 2019).

The adaptative immune system also has a participation in this process, although the exact role of T and B cells remains not fully clarified. Toben and co-workers showed that mice with depletion of adaptative immune system had an early

mineralization and remodeling as well as lower concentration of pro-inflammatory cytokines and a higher concentration of anti-inflammatory cytokines than the wild-type mice (Toben, Schroeder et al. 2011).

It is important to highlight that the effect of a cytokine is dependent on its concentration and presence of other cytokines. The same cytokine can have opposite effects depending the concentration and combination. For example, TNF-α can stimulate the ALP activity and matrix mineralization of MSCs through the NF-kB pathway. But TNF-α can also inhibit osteogenic differentiation by suppressing BMP-2 and inducing osteoblast apoptosis (Chen, Wu et al. 2017).

Osteoclastogenesis. Osteoclastogenesis is the process of bone reabsorption by osteoclasts. Osteoclasts are multinucleated cells that differentiate from monocytes, but they can also differentiate from macrophages (Baht, Vi et al. 2018). Immune cells can regulate osteoclastogenesis through cytokines, namely, macrophage colony stimulating factor (M-CSF), receptor activator of nuclear factor kappa-B ligand (RANKL) and osteoprotegerin (OPG) (Chen, Wu et al. 2017).

M-CSF promotes osteoclast differentiation by binding to its receptor named colony-stimulating factor-1 receptor (c-FMS) and triggering the mitogen-activated protein kinase (MAPK) pathway (Chen, Klein et al. 2016). Osteoblasts are producers of M-CSF when stimulated with IL-1 in order to inhibit apoptosis of osteoclasts and decrease osteogenesis through MAPK pathway (Lee, Byun et al. 2019).

The system RANKL/RANK/OPG. This is the main system to regulate the osteoclastogenesis. Osteoclast precursors have the receptor RANK on their surfaces which will bind to RANKL. This interaction activates the TNF receptor associated factor 6 (TRAF6) pathway through the activator protein 1 (AP-1) and the NFAT2. As a result there is an upregulation of genes to increase the survival of osteoclasts (Chen, Klein et al. 2016). RANKL is produced by osteoblasts, activated T cells and neutrophils. The other component of this system is OPG. OPG is a decoy receptor for RNAKL. OPG sequesters RANKL preventing its interaction with RANK and in this way, inhibits the differentiation and activation of osteoclasts. The major producer of OPG are B cells, but this molecule can also be produced by osteoblasts. T cells do not produce OPG, but they can act cooperatively with B cells for its production through co-stimulation via CD40/CD40L interaction (Chen, Klein et al. 2016).

There are other molecules which can regulate this system. IL-6 and IL-23 use the glycoprotein 130 (gp130) receptor to stimulate the RANKL production and indirectly

promote osteoclastogenesis. Similarly, OSM also binds to gp130 receptor and increases the RANKL production by osteoblasts (Chen, Wu et al. 2017). IL-15 produced by T cells stimulates osteoclasts differentiation too. It increases the RANKL expression as well the phospholipase D-1 (PLD-1) via MAPK and NF-kB pathways (Lee, Byun et al. 2019). On the other hand, IFN-ɣ promotes TRAF6 destruction and therefore the decrease of osteoclast survival. This allows to prevent an exaggerated bone destruction during the inflammation (Chen, Klein et al. 2016).

A chronic inflammation with presence of pro-inflammatory cytokines such as TNF-α, IL-1 and IL-6, skew the RANKL/RANK/OPG system for a higher concentration of RANKL, which results in an increase of osteoclastogenesis. This unbalance will shift the remodulation process to a higher bone reabsorption activity than bone formation activity which leads to a massive loss of bone (Chen, Klein et al. 2016).

2.2.3 Biomaterials, immune and bone cells

The characteristics of the biomaterials, especially, on their surface are very important and can change the fate of the implant. Some characteristics to pay attention to are the chemical and physical properties of the surface. The size and shape of the implant also play an important role. These characteristics might modulate differently the osteogenesis and osteoclastogenesis processes.

One important characteristic is **wettability**. For a good osteogenic activity, hydrophobic surfaces are associated with an increase of monocyte adhesion to the implant and consequently an immune response to the site of implantation (Chen, Wu et al. 2017). On the other hand, Hamlet and co-workers had shown that cultures of macrophages on hydrophilic surfaces promote a downregulation of pro-inflammatory cytokines such as TNF-α, IL-1α and IL-1β (Hamlet, Alfarsi et al. 2012). Bang and co-workers analyzed the influence of a hydrophilic sandblasted/acid etched surface of titanium on the differentiation of osteoblasts and osteoclast and concluded that the hydrophilic surfaces enhance the osteoblast differentiation. The same did not happen to osteoclast differentiation even when the macrophages where cultured with RANKL and M-CSF (Bang, Moon et al. 2014).

Another important characteristic is the **topography** of the surface. This aspect has been evolving with the advance of the technology, having nanopatterns different results than micropatterns. On a nanoscale, these patterns were responsible for MSCs producing mineralized bone *in vitro* without adding osteogenic supplements (Dalby, Gadegaard et al. 2007). Allan and co-workers demonstrated that the culture of MSCs

on nanopatterns leads to differentiation into osteoblasts and also demonstrated a good adhesion from mature osteoblasts (Allan, Ker et al. 2018). Costa and co-workers studied the influence of topography of hydroxyapatite (HA) coatings on polycaprolactone discs on osteoblasts and osteoclasts. They concluded that osteoblasts had a higher expression of osteogenic markers and adhere more to surfaces with increased roughness. In contrast, osteoclast presented higher reabsorption activity on smoother (Costa, Prowse et al. 2013). Furthermore, the topography of an implant can also modulate the immune system. Paul and co-workers showed that the polarization of macrophages was significantly affected by the micro-topography of the surface but not in the surface with nanotopography. On the micro-topography, the macrophages manifested characteristics of both M1 and M2 polarizations (Paul, Skazik et al. 2008). Smith and co-workers evaluated the influence of titania nanotubes arrays in titanium surfaces over immune cells. The study showed a decrease on the inflammatory response for the titania nanotubes *in vitro* via a reduced activity of immune cells such as monocytes, macrophages and neutrophils (Smith, Capellato et al. 2013).

The **charge** of the surface is also important, since positively charged surfaces have a higher chance to promote an inflammatory response than the negatively charged or neutral surfaces (Chen, Wu et al. 2017). The **release of ions** can also influence the immune cells. Magnesium (Mg) ions showed to suppress inflammation by inhibiting the production of pro-inflammatory cytokines. Contrary, cobalt (Co) stimulates an inflammatory response via hypoxia-inducible factor (HIF). Zinc (Zn) on the other hand stimulate the release of anti-inflammatory cytokines such as IL-10 and the decrease of TNF-α and IL-1β (Chen, Wu et al. 2017). The effect of metallic ions is very dependent on the charge of the ion, its concentration and role in the immune and bone cells pathways.

The **size** and **porosity** are also important aspects to have in consideration when designing a biomaterial. Studies have shown that the size of the material has an direct effect on FBR (Chen, Wu et al. 2017). Ward and co-workers compared the foreign body capsule (FBC) of polyurethane with silicone and polyethylene oxide (PU-S-PEO) materials with two thicknesses (300μm and 2000μm) and concluded that the FBC is thinner in thinner materials (Ward, Slobodzian et al. 2002). The porosity and the pore size also have an effect on FBR (Chen, Wu et al. 2017). Ward and co-workers also studied the FBC from solid materials and porous materials and verified that the FBC was more dense in solid materials, while porous materials presented microvessels (Ward, Slobodzian et al. 2002). Besides the presence or not of pores, it is also

important their size. A small pore size represents a limitation to nutrients and oxygen diffusion until the material core. Therefore, the material core will have an hypoxic environment, which will enhance the inflammatory response (Chen, Wu et al. 2017). Kuboki and co-workers sowed that a pore size between 90 and 100µm hamper vascularization and stimulates chondrogenesis, while 350µm pores enhance angiogenesis and osteogenesis (Kuboki, Jin et al. 2002).

Biomaterials can also release **biomolecules** such as proteins in order to modulate osteogenesis and osteoclastogenesis. Spiller and co-workers developed a system with a sequential release of IFN-ɣ and IL-4 in order to help the switch between M1 and M2 macrophages and enhance the bone healing (Spiller, Nassiri et al. 2015). The use of BMP-2 is also very common. Wei and co-workers showed that BMP-2 increases the recruitment of macrophages but decreases the expression of M1 markers. This team also demonstrated that macrophages previously stimulated with BMP-2 accelerated the differentiation of bone marrow stromal cells into osteoblasts (Wei, Zhou et al. 2018).

2.2.3.1 Osteoimmunomodulation

Osteoimmunomodulation (OIM) is a recent field that results from the combination of osteoimmunity and immunomodulation. OIM is a characteristic of a biomaterial that is implanted in the bone. It can be defined as the ability of a material to modulate the local immune environment to induce significant effects on bone cells functions. This ability is determinant to the success implant through bone regeneration and osteointegration (Chen, Klein et al. 2016).

A biomaterial with good OIM has the capacity to induce the correct immune response in the appropriate time. It is capable to induce a correct inflammatory response by immune cells with release of cytokines, chemokines and growth factors that will increase the recruitment and differentiation of MSCs into osteoblasts. This material also needs to have the ability to elicit the most appropriate osteoclast response, in order to maintain the balance of the bone dynamics by preventing an excessive bone reabsorption or lack of it (Chen, Wu et al. 2017).

To assess the OIM of a material, it is necessary to evaluate the interaction between the material, immune cells and bone cells. The usual manner to evaluate a material is by assessing the material effects on both cell types independently, but in order to evaluate the OIM that is not sufficient. A co-culture of immune cells and bone cells can be a good approach to determine the OIM of a biomaterial.

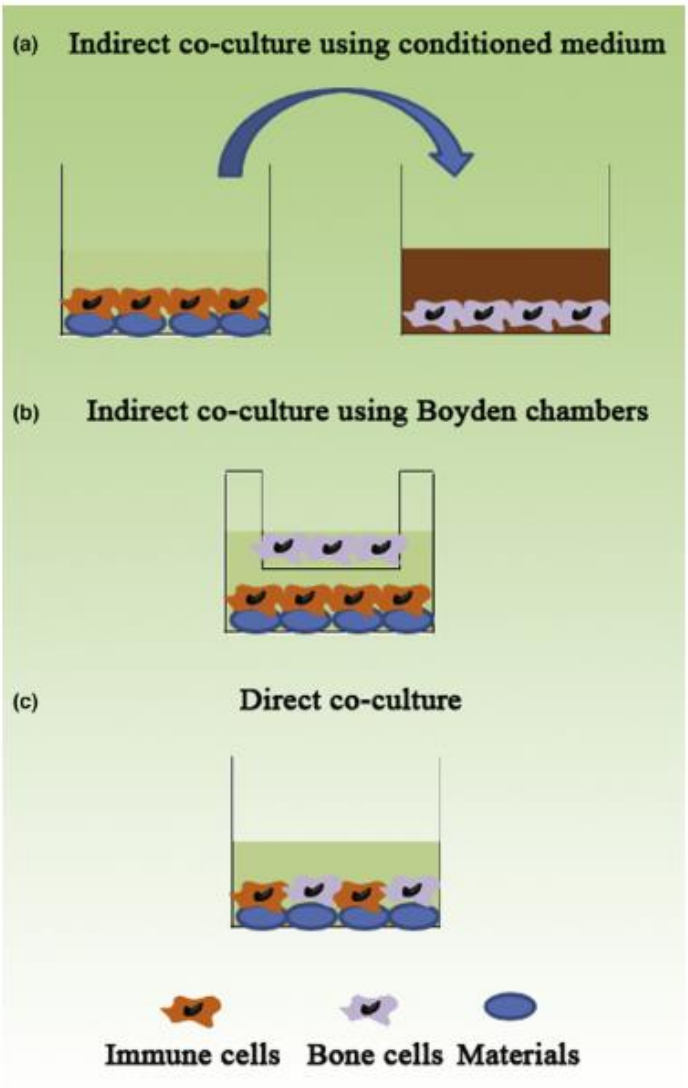

Figure 4 - Co-culture methods to assess OIM of a material. In order to evaluate the OIM of a material it is necessary to have the material, the immune cells and the bone cells together in the same assay, instead of only analyzing the response of both cell types to the material independently. Thereby the most suitable solution is the performance of co-cultures. Indirect co-culture using conditioned media (a) consists in the culture of immune cells with the material and then the culture of the bone cells with the conditioned media. This method only allows to test the influence that the immune cells have over the bone cells. Indirect co-culture using Boyden chambers (b) consists in culturing the immune cells in direct contact with the material in the well, while the bone cells are cultured in indirect contact in the insert. This allows to both cells types to play an active role over each other. The size of the pores of the insert will determine if it is analyzed only the influence of secreted molecules, like cytokines, chemokines and growth factors or if the migration of bone cells is also tested. Direct co-culture (c) it is the better representation of what happens *in vivo*. It consists in culturing both cell types on top of the material, allowing a direct contact between cells and material. Image from (Chen, Klein et al. 2016).

Indirect co-culture using conditioned media. This method is represented in Figure 4 (a) and consists in culturing immune cells, such as macrophages, with the biomaterial to obtain the immune response. Then, the bone cells are cultivated with the

conditioned media to see the influence of the immune response in the osteogenesis and osteoclastogenesis (Chen, Klein et al. 2016, Chen, Wu et al. 2017). This method has the advantage of being simple and to allow freezing the conditioned media and use the same batch of media in more than one experiment. However, this method only analyses one direction of the talk between immune and bone cells. This method assumes that bone cells have a passive role over the immune cells, which is not verified in *in vivo* (Chen, Klein et al. 2016, Chen, Wu et al. 2017).

Indirect co-culture using Boyden chambers. This method is represented in Figure 4 (b) and consists in cultivating the immune cells in contact with the biomaterial in the well and the bone cells in the insert (Chen, Klein et al. 2016, Chen, Wu et al. 2017). In this method, it is possible to control the size of the insert pores. A size such as 0,4µm allows the passage of biomolecules such as cytokines but not the cells. Then, it is possible to analyze the cross-talk between immune and bone cells, as well as the genetic and protein expression of the immune and bone cells separately (Chen, Klein et al. 2016). If a bigger pore is used, which allows the passage of the bone cells from the insert to the well, it is possible to evaluate the migration of bone cells due to the influence of immune cells (Chen, Klein et al. 2016). So, with this method there is not a direct contact between bone cells and biomaterial. However, depending on the design of the experiment, the pore size of the inserts and the immune response, this contact can happen in a later phase. The indirect co-culture using Boyden chambers method seems a better compromise between the representation of what happens *in vivo* and what is possible to analyze and mimic *in vitro*.

Direct co-culture. This method is represented in Figure 4 (c) and consists in cultivating both, immune and bone cells, over the material. This allows both cell types to be in contact with the material, mimicking better what happens *in vivo* (Chen, Klein et al. 2016, Chen, Wu et al. 2017). This method can be achieved by culturing first a layer of one type of cells and then the other on top the first one. This type of culture is hard to perform and makes it difficult to match the different effects to the different cell types (Chen, Klein et al. 2016).

The choice of which cells, media and molecular factors to use in the assessment of OIM depends on the phase of the healing that we want to act on, since different phases involve different cells and a different microenvironment (Chen, Klein et al. 2016).

2.2.4 Bone fractures, infection and biomaterials

Bone fractures related infections (FRI) occur due to access of bacteria to the bone through an open wound or open fracture. The risk of a bone fracture to become infected depends on the type of fracture and therefore can vary between 10%-50% (Seebach and Kubatzky 2019).

2.2.4.1 Osteomyelitis

Osteomyelitis is an infectious bone disease characterized by a strong inflammatory response and destruction of the bone due to the colonization by bacteria in the bone itself, bone marrow and surrounding tissue (Seebach and Kubatzky 2019). Osteomyelitis can have two different sources hematogenous or iatrogenic. In a hematogenous source bacteria arrive to the bone via blood stream from another infection site. In the iatrogenic source, bacteria arrive to the bone by the break of protective barriers like in an open fracture, an open wound or a surgical incision (Hofstee, Muthukrishnan et al. 2020). Thence, there is always a risk for orthopedic surgeries to develop infections due to the passage of bacteria from the skin to the bone.

In the early phase, osteomyelitis manifests itself by bacterial colonization and severe inflammatory response, associated with fever, pain and swelling. The exaggerated inflammation leads to an increase of TNF-α, IL-1β and IL-6, which promotes osteoclastogenesis and thereby bone destruction (Seebach and Kubatzky 2019). In this early phase a treatment with antibiotics usually is sufficient, having a success rate of 80% (Hofstee, Muthukrishnan et al. 2020).

In cases of chronic infections, the antibiotic treatment is not enough, being necessary to remove implant and infected surrounding tissue (Hofstee, Muthukrishnan et al. 2020). The recurrence of infections is associated with reservoirs of bacteria. Bacteria, such as *Staphylococcus aureus* are capable to survive inside of cells like osteoblasts and osteocytes (Hofstee, Muthukrishnan et al. 2020). Biofilm formation on the bone and/or implant surface also constitutes a bacterial reservoir. A recent study showed that bacteria can also colonize spaces in the bone such as canaliculi and osteocyte lacunae of cortical bone being hard to immune cells to reach these spaces (de Mesy Bentley, Trombetta et al. 2017).

The current treatments included the removal of implant and the infected tissue. For prosthetic joint infections (PJI), the removal of the implant can occur in one or two

phases, with an antibiotic treatment between explantation and re-implantation of the prosthetic (Seebach and Kubatzky 2019). For FRI, the decision of removing or not the implant will depend on the stage of infection, type of fixation applied and consolidation of the fracture. In fracture infection, bacterial clearance can be facilitated since the implant can be removed after the bone bridging happen. On the other hand, if the stability of the bone is treated, it might be necessary an external fixation and bone reconstruction (Seebach and Kubatzky 2019). All these processes are associated to long stays in hospital and huge economic burdens (Thakore, Greenberg et al. 2015, Metsemakers, Smeets et al. 2017). It also implies a lot of pain and suffering by the many surgeries with big impact on mobility and functionality of limbs (Seebach and Kubatzky 2019). The failure of treatment and recurrence of infection can result in non-union of the bone, stiffening of articulations or even the amputation of a limb (Seebach and Kubatzky 2019).

2.2.4.2 Biofilm

Biofilm formation is one of the major challenges in the field of medical devices. A biofilm is a community of microorganisms, in which aggregates are tightly adherent to the surface and encased in a matrix of extracellular polymeric substances (EPSs) produced by bacteria and the proximal host cells (Costa, Carvalho et al. 2011, Arciola, Campoccia et al. 2018).

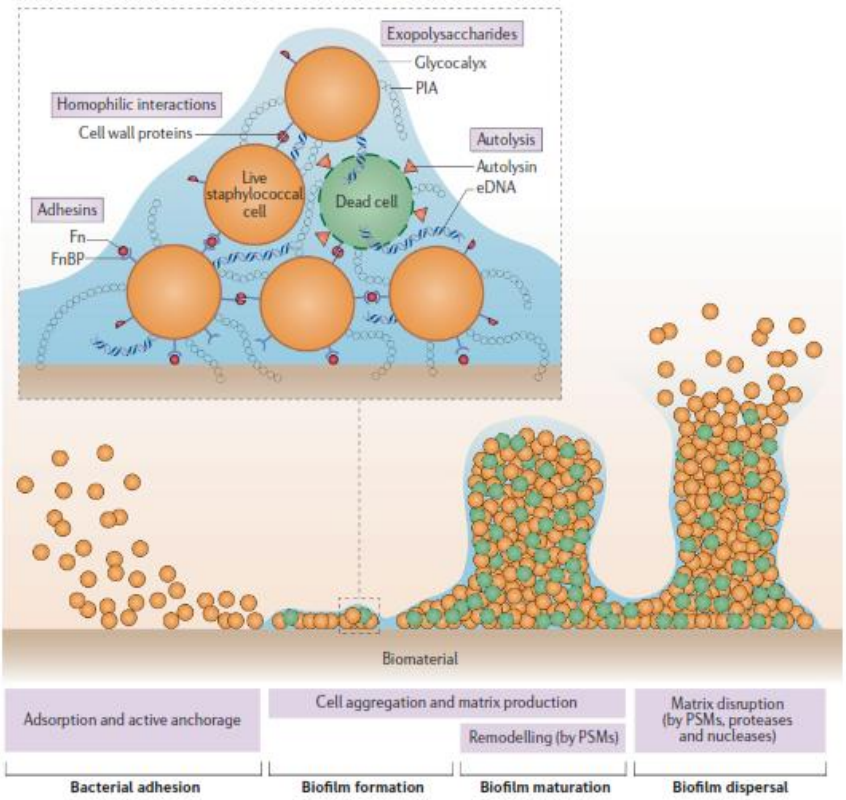

Figure 5 – Stages of biofilm formation. Biofilm starts with adhesion from bacteria to a surface, initially reversible adhesion, important to start the contact between bacteria-surface. Reversible adhesion involves forces such as electrostatic, Van der Waals and Lewis acid-base forces. The reversible adhesion proceeds irreversible adhesion where the interaction between bacterial wall proteins and the proteins adsorbed on the surface play the major role, leading to a stable anchorage of bacteria. Intercellular interactions through adhesins and wall proteins results in the aggregation of bacteria leading to clusters and microcolonies. Production of extracellular polymeric substances occurs during the biofilm's maturation process and promotes the formation of larger bacterial aggregates called macrocolonies. Some mechanisms involved in biofilm formation, for example of *Staphylococcic*, is the expression of polysaccharide intercellular adhesin (PIA) and the release of extracellular DNA (eDNA) from bacterial autolysis and from dead host cells. Phenol-soluble modulins (PSMs) are involved on water channels formation, characteristic from mature biofilms. In *S. aureus* and *S. epidermidis* biofilms PMSs are also responsible for biofilm disperser together with proteases and nucleases. (Arciola, Campoccia et al. 2018)

As shown in Figure 5, biofilm formation demands a certain order of events. It starts with adhesion of bacteria to the surface. It is followed by EPS production and aggregation of bacteria, forming microcolonies. The biofilm maturation is achieved with formation of macrocolonies. Once the biofilm is mature the last phase is disruption of the biofilm and dispersal of bacteria to other places (Pavithra and Doble 2008, Costa, Carvalho et al. 2011, Yang, Liu et al. 2012, Arciola, Campoccia et al. 2018).

Adhesion. The adhesion process starts with planktonic bacteria adhering to the surface in two stages. The first stage is named reversible adherence, in which the

major forces in play are Van der Waals force as well electrostatic and Lewis acid-base interactions (Pavithra and Doble 2008, Arciola, Campoccia et al. 2018). These forces, even though weak, allow the bacteria to get closer to the surface and to move to the second stage of adherence. The second stage is irreversible adherence, where the adhesion proteins on the bacterial membrane, like the autolysins in *Staphylococci*, bind to the surface of the material or to adsorbed adhesion proteins like fibronectin and vitronectin. (Arciola, Campoccia et al. 2018). *S. aureus* has many types of adhesins, such as microbial surface components recognizing adhesive matrix molecules (MSCRAMMs) and secretable expanded repertoire adhesive molecules (SERAMs). MSCRAMMs besides participating on adhesion can also modulate the immune system by acting as invasins, allowing bacterial internalization in host cells (Arciola, Campoccia et al. 2018).

EPS production. After the protein binding, the bacteria will start to produce the biofilm matrix, not only for a better adherence of the bacteria that are already bond to the surface, but also for other bacteria that are initiating the binding process, making the adhesion easier. As the bacteria adhere, they start to proliferate, recruit other bacteria and continue biofilm matrix production to form microcolonies that will grow into macrocolonies, leading to biofilm maturation (Arciola, Campoccia et al. 2018).

The biofilm matrix is the main shield of bacteria. It is composed of polysaccharides, proteins, extracellular DNA (eDNA) and lipids. EPS constitutes a physicochemical barrier against diffusion of the antimicrobial molecules. During the diffusion antimicrobial molecules can interact with proteins and enzymes that can change and/or inactivate them (Arciola, Campoccia et al. 2018).

A second way of protection is by establishing a reduced growth rate. Most antimicrobial agents target highly active cells; thus, a quiescent or low metabolic state prevents the uptake of these molecules by bacteria. These cells in this stage consist in a minor population called persister cells (Riool, de Breij et al. 2017, Arciola, Campoccia et al. 2018, de Breij, Riool et al. 2018). Persister cells are formed under conditions that activate stress signaling, like starvation and oxygen deprivation (Arciola, Campoccia et al. 2018), being this the main reason why they adopt a quiescent state. These cells do not grow or die during antibiotics treatments, but once the conditions are favorable again, they start dividing, causing a new infection. Therefore, persister cells contribute for recurrence and chronical infections (Seebach and Kubatzky 2019). The use and development of strategies and materials/molecules that assures the death of persister cells would help preventing the relapse of implant infections (Riool, de Breij et al. 2017,

Arciola, Campoccia et al. 2018, de Breij, Riool et al. 2018). These two types of protection confer tolerance to antibiotic treatments and not real bacterial resistance, since the bacteria can still be susceptible to antibiotic treatment once the biofilm is dispersed (VanEpps and Younger 2016).

A third way by which bacteria are protected in a biofilm is the bacterial cell-cell contact and communication promoted by the confined space of the biofilm. This proximity and contact promote the horizontal plasmid transference, where resistance genes can be encoded and, in this way, there is a resistance propagation through species (Donlan 2001). The presence of eDNA in the EPS also facilitates the transference of resistance genes between bacteria (Arciola, Campoccia et al. 2018).

Biofilm maturation and dispersal. During the maturation of the biofilm there is the rearrangement of the matrix with formation of new structures. Phenol-soluble modulins (PSMs) are proteins involved in water channels formation, so nutrients can reach the deepest parts of the biofilm (Arciola, Campoccia et al. 2018). For the formation of these channels, PSMs and other proteins such as nucleases and peptidases disrupt the bonds of the matrix, weakening the biofilm cohesion. This allows single cells or cell clusters to detach and migrate to other places and becoming the origin of another infection (Stoodley, Sauer et al. 2002, Pavithra and Doble 2008, Costa, Carvalho et al. 2011, Moriarty, Zaat et al. 2012, Yang, Liu et al. 2012, Arciola, Campoccia et al. 2018).

Biofilm modulation of immune cells. Biofilm has an acidic, hypoxic and starvation environment that can change the metabolism of the immune cells as well their activation (Seebach and Kubatzky 2019).

Although the biofilm represents a very strong protection to bacteria, it is not foolproof. There is a widow of action in the biofilm formation that immune cells can be successful. Günther and co-workers showed that PMNs can clear biofilms depending on their maturation. Immature biofilms (2-6 days) were phagocyted by PMNs, while mature biofilms (15 days) were not (Günther, Wabnitz et al. 2009). These results might be associated with the thickness of the biofilm, being a mature biofilm more thicker and therefore more difficult to penetrate (Seebach and Kubatzky 2019).

Biofilms can also modulate the polarization of macrophages. Thurlow and co-workers demonstrated that macrophages that penetrated into the biofilm had their M1 polarization changed to M2 pro-fibrotic type (Thurlow, Hanke et al. 2011). The formation of a fibrous capsule around the biofilm prevents the immune cells action over the biofilm and the bacteria in it (Seebach and Kubatzky 2019).

Myeloid-derived suppressor cells (MDSCs) are other type of cells compose by immature monocytes and granulocytes that have their behavior changed by the biofilm. These cells when arrive into the inflammation site differentiate into neutrophils, macrophages and dendritic cells (DCs) (Seebach and Kubatzky 2019). The immune system is negatively regulated by MDSCs in chronical infections. They inhibit polarization of macrophages into M1 phenotype. In biofilms there is an accumulation of MDSCs by a mechanism not yet known (Seebach and Kubatzky 2019).

2.2.4.3 Bacteria and bone cells

The presence of infection in the bone leads to interactions between bacteria and bone cells. For example, *S. aureus* in a general manner increases the osteoclast activity and inhibits the new bone formation which results in loss of bone.

S. aureus can adhere and invade bone cells such as osteoblasts and osteocytes. When comparing the internalization of these bacteria between osteoblasts and macrophages the macrophages have a higher percentage of internalization, but bacteria have a higher percentage of survival in osteoblasts than macrophages. This might be due to the lack of mechanisms for clearance of intracellular bacteria in osteoblasts since they are not professional phagocytes (Josse, Velard et al. 2015).

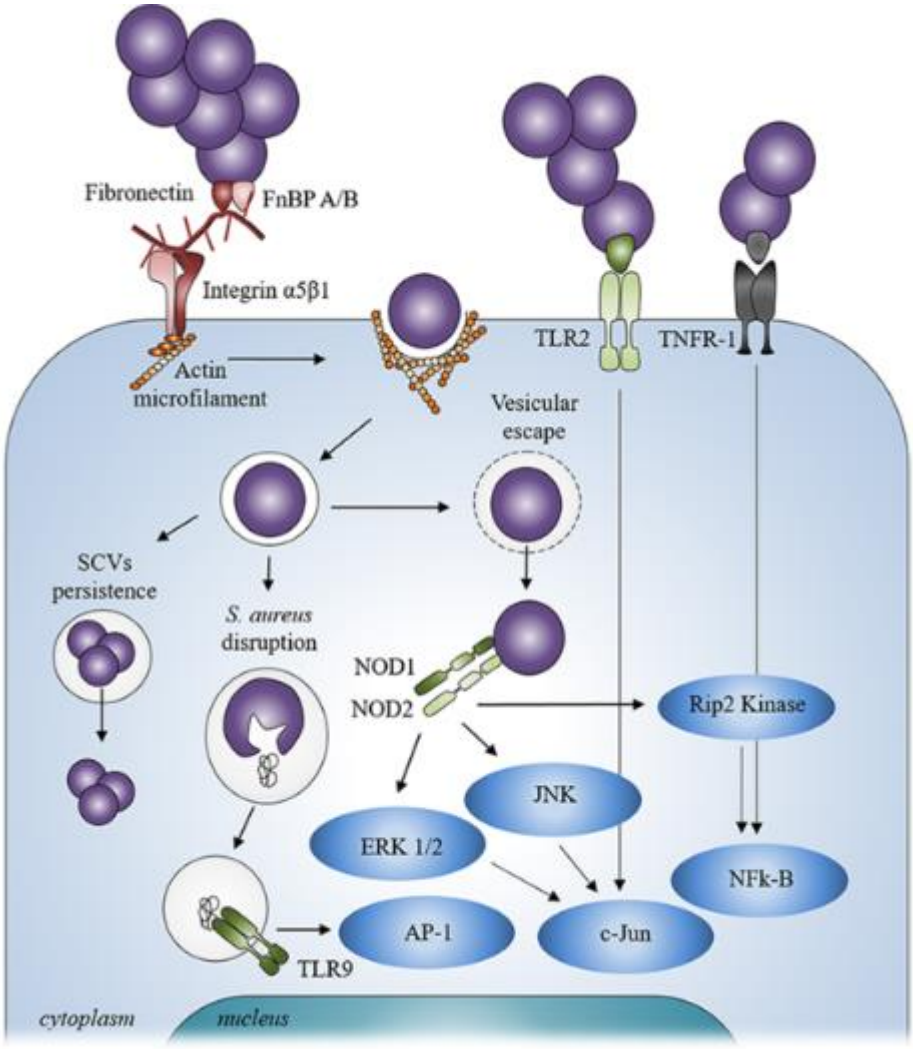

Figure 6 - Interaction between *S. aureus* and an osteoblast cell. Bacteria can interact with the osteoblast cell through membrane receptors, such as TLR-2 and TNFR-1, which will activate cellular pathways, that result in production of AMPs, cytokines and chemokines in order to clear the infection. Through the interactions with α5β1 integrin and actin filaments bacteria can be engulf in vesicles. Bacteria can escape from these vesicles by using membrane-damaging factors and then be recognized by intracellular receptors such as NOD-1 and NOD-2. If there is the disruption of the bacterial membrane the intracellular receptor TLR-9 can recognize the bacterial DNA and activate the AP-1 pathway. Bacteria can even adopt a SCV phenotype and therefore persist intracellularly without promoting danger signals. Image from (Josse, Velard et al. 2015)

Internalization of *S. aureus* in osteoblast occurs mainly via FnBP A/B – fibronectin – α5β1 integrin (Josse, Velard et al. 2015). Due to these interactions, the bacteria are engulfed and vesicles are formed. The natural fate of the vesicles is the fusion with lysosomes, therefore in order to survive bacteria need to escape from them. The exact mechanism by which bacteria escape from the vesicles is not yet known. However, *S. aureus* can use membrane-damaging factors such as hemolysin and PSMs, especially PSM-α and PSM-β, which can promote the escape from the vesicles. Although this

method allows an easier escape of bacteria to the cytoplasm, it also results in osteoblasts death, due to the contact of PSMs with the osteoblasts cytoplasmatic membrane (Josse, Velard et al. 2015).

Small Colony Variants (SCVs). After internalization instead of using membrane-damaging factors, bacteria can adopt a SCV phenotype. SCVs are bacterial colonies with abnormal morphology and biochemical characteristics (Josse, Velard et al. 2015). This phenotype allows the persistence of *S. aureus* intracellularly due to adaptation of their metabolism. SCV are smaller than the normal colonies and do not induce big changes in the colonized host cell, which allows them to be undetectable, making the diagnostic even harder (Zimmerli and Sendi 2011, Moriarty, Zaat et al. 2012). Cells with this phenotype tend to replicate very slowly and to inactivate or downregulate their virulence factors. These conditions allow the infected host cell to remain viable without showing any signs of danger (Zimmerli and Sendi 2011, Moriarty, Zaat et al. 2012). For *S. aureus* Sigma Factor (SigB) is very important, since it is responsible for the passage between the virulent phenotype to the SCV phenotype. An upregulation of SigB leads to an increase of adhesins and a decrease of virulent factors, which is characteristic from SCVs (Josse, Velard et al. 2015). The SCV phenotype can be reversed, since when bacteria leave the SCVs phenotype and the intracellular space, they resume their virulence factors and infect other cells (Josse, Velard et al. 2015).

Osteoblast also have receptor that can recognize pathogen-associated molecular patterns (PAMPs) such as Toll-like receptors (TLR), nucleotide-binding oligomerization domains (NOD) and tumor necrosis factor receptor 1 (TNFR-1) (Josse, Velard et al. 2015). TLR-2 is a membrane receptor that when activated with PAMPs it will activate the c-Jun pathway, which results in production of AMPs and in osteoblast apoptosis. The TLR-9 is an intracellular receptor that recognizes bacterial DNA and activates the AP-1 pathway. TLR-9 can have access to bacterial DNA, when there is the disruption of the bacterial membrane during the escape from the vesicles (Josse, Velard et al. 2015). NOD 1 and NOD 2 are also intracellular receptors, which recognize PAMPs and activate many pathways such as ERK 1/2,JNK, Rip2 Kinase, which results in production of immune molecules (Josse, Velard et al. 2015). *S. aureus* can also secrete a protein named staphylococcal protein A (SpA) which can affect osteoblasts. SpA interacts with TNFR-1, which increases the apoptosis and decreases the differentiation and mineralization of the matrix. This interaction also stimulates the production of RANKL, which will potentiate the osteoclastogenesis. (Muthukrishnan, Masters et al. 2019, Hofstee, Muthukrishnan et al. 2020).

S. aureus has a significant effect over osteoblasts. It inhibits osteoblasts differentiation and activation, decreases osteoblasts proliferation, decreases ALP activity, inhibits matrix mineralization and induces osteoblast apoptosis (Josse, Velard et al. 2015). *S. aureus* can promote osteoclastogenesis mediated by osteoblasts. These bacteria induce the production of RANKL by osteoblasts by the autocrine and paracrine action of prostaglandin E2 (PGE2) and cyclooxygenase 2 (Cox-2) that will be upregulated in osteoblasts themselves (Josse, Velard et al. 2015)

2.3 Antimicrobial Peptides

Antimicrobial peptides (AMPs) are small (until 50 amino acids), positively charged, amphiphilic peptides from innate immune system (Jenssen, Hamill et al. 2006). Many species produce AMPs such as bacteria, invertebrates, insets, mammalians, amphibians and even plants (Reddy, Yedery et al. 2004). Due to the AMPs diversity, it is difficult to classify them. Although it is possible to categorize AMPs according to their secondary structures, amino acids composition, size or even mechanism of action.

If we classify AMPs according to their structures, there are three main categories: α-helix, β-sheet and unique extended coil structures represented in Figure 7 (Guaní-Guerra, Santos-Mendoza et al. 2010, Kumar, Kizhakkedathu et al. 2018).

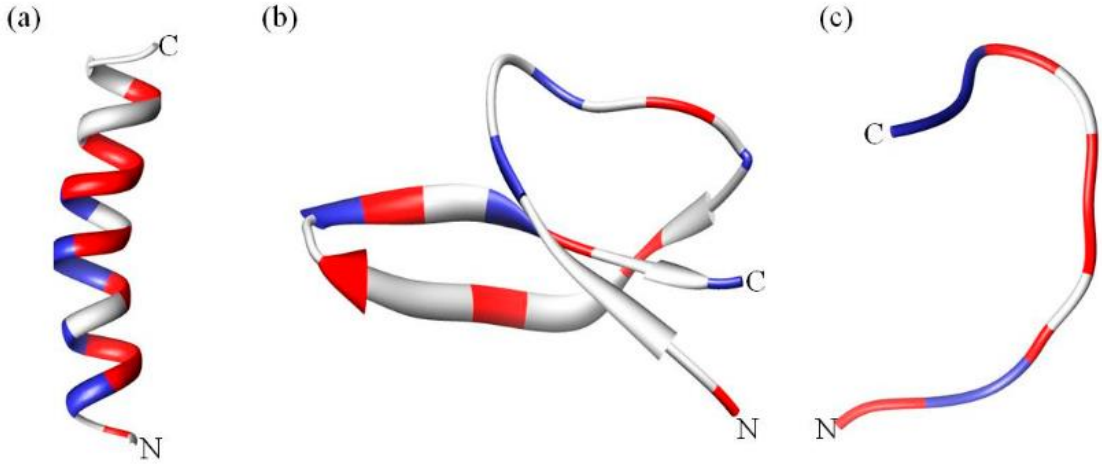

Figure 7 - AMPs representative structures classes. (a) α-helix structure is a typical structure of AMPs like magainins and from some members of the aurein and cathelicidin families (b) β-sheet structure is common for protegrins, defensins and tachyplesin. (c) Unique extended coil structure is found in most members of the cathelicidin family. The C represents the C-terminus of the peptide and the N the N-terminus. The red present the positive charged portions of the peptide and the blue represents the hydrophobic ones. Image adapted from (Kumar, Kizhakkedathu et al. 2018).

α-helix. The majority of the AMPs with this conformation are unstructured in water, but acquire their α-helix structure when in contact with bacterial membranes,

trifluoroethanol, detergents or surfactants above the critic micellar concentration, micelles and liposomes. Most AMPs with an α-helix structures need to amidate the C-terminus in order to obtain a higher antimicrobial activity. This modification increases the interactions between AMPs with a positive charge and the bacterial membrane with a negative charge. These interactions help to stabilize the α-helix structure. Magainins and some members of the aurein and the cathelicidin families are some examples of AMPs that adopt this structure (Kumar, Kizhakkedathu et al. 2018).

β-sheet. Most of these peptides have cysteines in their primary structure which allow the formation of disulfide bonds that reduces the activity of enzymes and gives stabilization to the structure. Contrary to what happens with the α-helices, β-sheets are able to keep they structure in water therefore they do not go under many conformational transformations when they are in contact with membranes. Some examples of β-sheets are protegrins, defensins and tachyplesin (Kumar, Kizhakkedathu et al. 2018).

Unique extended coil structure. The primary structure of these peptides normally has two or more residues of prolines, which leads to the break of the secondary structure of α-helix and β-sheet. Most members of the cathelicidins family and indolicidin have unique extended coil structure (Kumar, Kizhakkedathu et al. 2018).

Despite the variety of AMPs, there are some common aspects to all of them, like positive charge, hydrophobicity and amphipathicity.

Positive charge. This characteristic usually varies between +2 and +13. The positive charge of AMPs is due to the presence of residues like lysine, arginine and sometimes histidine, that can be placed in specific domains (Haney, Straus et al. 2019). Although counterintuitive, for the AMPs a higher charge does not necessarily means a higher antimicrobial activity, because it can induce stronger interactions between the AMPs and bacterial membranes preventing the translocation of the peptide (Kumar, Kizhakkedathu et al. 2018).

Hydrophobicity. Hydrophobicity can be achieved with the presence of residues like valine, leucine, isoleucine, alanine, methionine, phenylalanine, tyrosine and tryptophan. The quantity of these residues regulates the portion of the AMP that will interact with the membranes. An increase of hydrophobicity can lead to a loss of selectivity and antimicrobial activity and cell toxicity. The loss of activity due to the increase of hydrophobicity can be explained, for example, by the dimerization of AMPs, which restrain them to pass through the membrane (Kumar, Kizhakkedathu et al. 2018).

Amphipathicity. Amphipathicity is related with the relative abundance of hydrophobic and hydrophilic residues and domains in the AMPs. This characteristic is very important not only for primary structure but also for the secondary and tertiary structures. The best example for amphipathicity are α-helix because they can form two faces (inside and outside of the helix) being one hydrophobic and the other hydrophilic (Kumar, Kizhakkedathu et al. 2018).

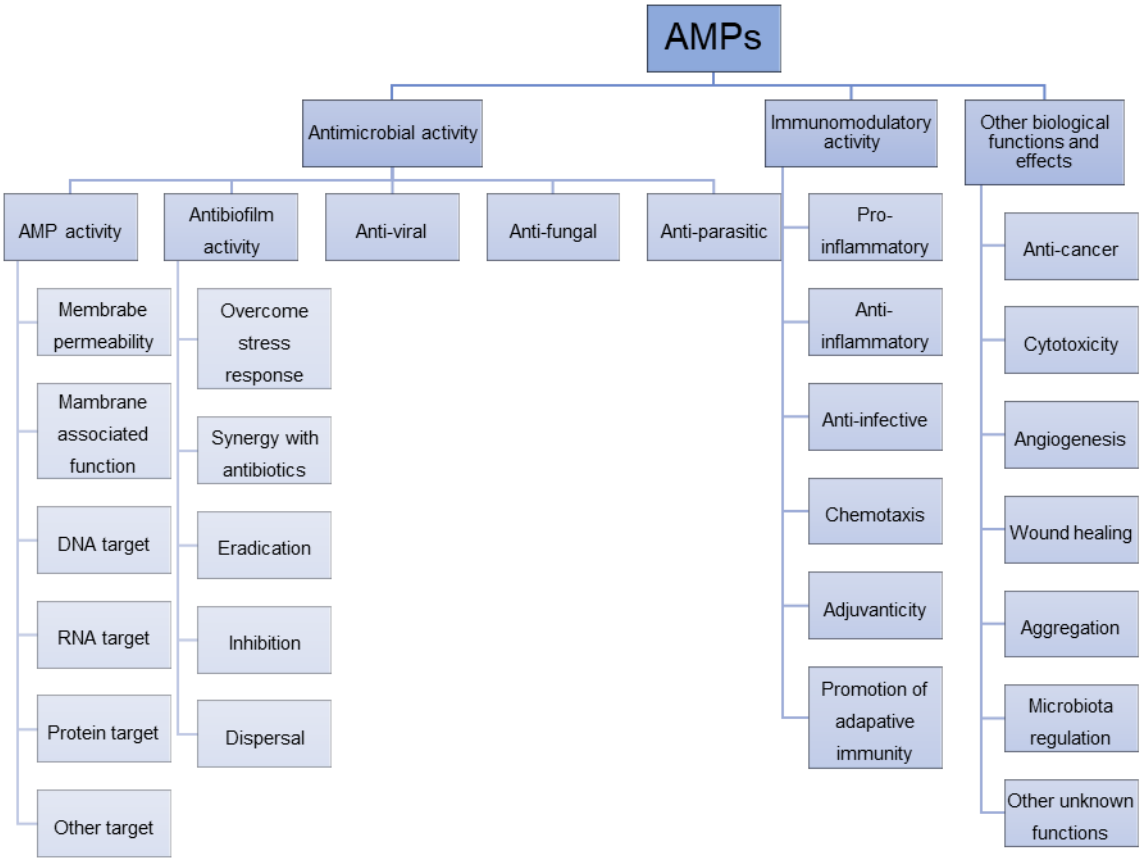

Figure 8 - Diverse functions of AMPs described in literature. Image adapted from (Haney, Straus et al. 2019)

AMPs are known by their biological activity against pathogens like bacteria (planktonic and in biofilm), fungi, virus and some parasites as shown in Figure 8. The antimicrobial activity is the main reason for the AMPs expression on sites where is more likely to get infections, like skin and mucosal epithelia, since they can act as the first line of defense against these organisms (Jenssen, Hamill et al. 2006). Nevertheless, the AMPs have other functions (Figure 8) like neutralization of endotoxins, chemokine-like activities, immunomodulatory properties, induction of angiogenesis, wound-healing, anticancer, microbiota regulation and adjuvanticity

(Guaní-Guerra, Santos-Mendoza et al. 2010, Ghosh, Sarkar et al. 2019, Haney, Straus et al. 2019).

2.3.1 Advantages and limitations of AMPs

In the last decades, the AMPs have attracted attention by their numerous advantages, like antimicrobial and antibiofilm activity, broad antimicrobial spectrum, fast and multiple mechanisms of action, low likelihood to promote resistance, neutralization of endotoxins and innate immune system enhancement for clearance of infection without a debris/septic inflammatory response (Hancock and Sahl 2006, Haney and Hancock 2013, Mansour, Pena et al. 2014).

In spite of the advantages, AMPs also present some limitations. High costs of production are many times highlighted as a limitation for the use of AMPs, although this argument is unfounded, because it is possible to optimize and adapt the synthesis process to a large scale and a lower cost (Hancock and Sahl 2006, Mansour, Pena et al. 2014, Haney, Straus et al. 2019). Another drawback is the AMPs' stability when they are present in a physiological environment. In a physiological environment, enzymes and proteases can inactivate AMPs by cleaving them, which affects their bioavailability. AMPs have an unusual pharmacokinetics when administrated systemically, which is characterized by a high distribution in the blood followed by the appearance of low concentration in certain tissues (Haney, Straus et al. 2019). These concentrations are too low for an antimicrobial activity; however, it can be enough for immunomodulating activities. For achieving higher local concentrations, AMPs can be protected by using a delivery systems like liposomes, dendritic peptides, DNA cages, solid core nanoparticles and carbon nanotubes (Haney and Hancock 2013, Haney, Straus et al. 2019). Other strategy is change the AMP chemically by using D-amino acids instead of natural L-amino acids together with the retro-inverse sequence in order to keep the orientation of the side chains while transforming the peptide into a peptide peptidase resistant (Easton, Nijnik et al. 2009). Another limitation is the potential toxicity *in vivo* due to the AMPs tendency to aggregate in presence of certain anions and body fluids. To little is known about the toxicity of AMPs *in vivo*, so it is necessary to perform more studies for pharmacokinetics, pharmacodynamics and activity profile for AMPs alone and in conjugation with other drugs (Hancock and Sahl 2006, Haney, Straus et al. 2019).

2.3.2 AMPs activities

2.3.2.1 Antimicrobial activity

AMPs antimicrobial activity can be defined as the use of AMPs "*to prevent or mitigate the growth of bacteria, to reduce the number of bacteria or to kill bacteria*" (Sjollema, Zaat et al. 2018). AMPs can modulate the immune system's response to protect an organism against infections, having an indirect antimicrobial activity, or they can act directly on the microorganisms promoting their death (Andersson, Hughes et al. 2016).

2.3.2.1.1 Mechanisms of action

AMPs are selective in their targets, since they are capable of killing pathogens and causing no damage to the host cells. This happens because of the cell membranes composition differences between bacteria and eukaryotic cells (Figure 9). In bacterial membranes there are anionic phospholipids stabilized by divalent cations in both layers of the membrane, while host cells have zwitterionic phospholipids conferring a neutral charge to the membrane's outer layer. In addition, eukaryotic cells distribute anionic phospholipids in the membrane's monolayer facing the intracellular space keeping the neutral charge of the outer membrane monolayer. Another difference is the cholesterol content in eukaryotic host cell membranes, which acts as a buffer for the phospholipid fluidity and stability against temperature differences. In short, AMPs specificity is based on the fact that electrostatic interactions between the anionic phospholipids in the outer layer of the bacterial membrane are stronger than the hydrophobic interactions with the zwitterionic phospholipids in the outer layer of eukaryotic cells (Andersson, Hughes et al. 2016, Kumar, Kizhakkedathu et al. 2018).

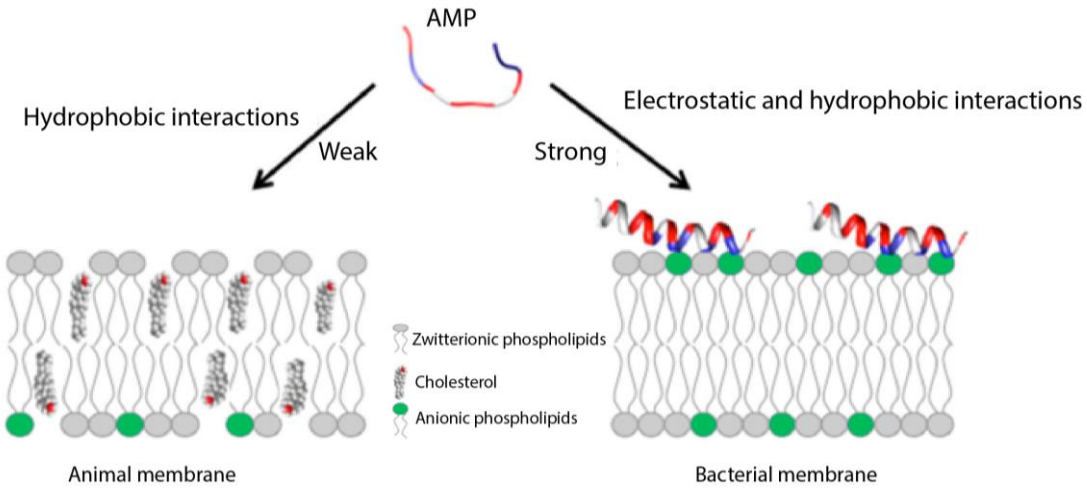

Figure 9 – The differences in composition of animal and bacterial membranes affects the interactions between AMPs and membranes. In animal membranes most interactions are hydrophobic interactions and

therefore weak. This is due to the outer layer of animal's membranes be composed of zwitterionic phospholipids and the anionic phospholipids being in the inner layer. Thereby there is a lack of negative charge for AMPs interact with the membranes. In addition to the asymmetric charge distribution, the presence of cholesterol also decreases the interactions between AMPs and membranes. The bacterial membranes have anionic phospholipids in the outer layer of the membrane which confers some negative charge to the membrane allowing electrostatic interactions between AMPs and the head groups of anionic phospholipids, being these interactions stronger than hydrophobic interactions. These differences are the basis to explain the selectivity of AMPs to bacteria instead of host cells. Image adapted form (Kumar, Kizhakkedathu et al. 2018).

In the beginning, it was thought that AMPs' mechanism of action was only through interactions with bacterial membrane, but recent studies have shown that AMPs can kill bacteria through both direct and indirect methods. The direct methods involve interactions with bacterial membrane with pore formation and disruption of the membrane, but also without pore formation by acting against intracellular targets like proteins, enzymes, RNA and DNA that are vital for the bacteria survival (Kumar, Kizhakkedathu et al. 2018, Ciumac, Gong et al. 2019). The indirect methods are related with AMPs' immunomodulation activities (Kumar, Kizhakkedathu et al. 2018).

Direct killing with pore formation in the membrane. Many AMPs are capable to interact with bacterial membrane without interacting with the receptors. AMPs use electrostatic interactions with the components present in the bacterial cell wall like teichoic acids (TA) and lipoteichoic acids (LTA) in Gram positive bacteria and lipopolysaccharide (LPS) present in bacterial membrane of Gram negative bacteria, which confer negative charge to it (Kumar, Kizhakkedathu et al. 2018). In this type of killing there are some steps that are common to all the mechanisms used by AMP, represented in the Figure 10 a) to c). First, AMPs approach the bacterial membrane through electrostatic interactions (Figure 10 a)) and then they adsorb to it and change their conformation (Figure 10 b)). The last common step is AMPs accumulation on the surface until the threshold concentration is reached and the AMPs self-assemble (Lee, N Hall et al. 2016). After these phases there are three possible mechanisms: barrel-stave model, toroidal pore model and the carpet model (Lee, N Hall et al. 2016, Kumar, Kizhakkedathu et al. 2018). Recent studies do not exclude other mechanisms or even a mixture or variations of the mechanisms mentioned above (Lee, N Hall et al. 2016, Kumar, Kizhakkedathu et al. 2018).

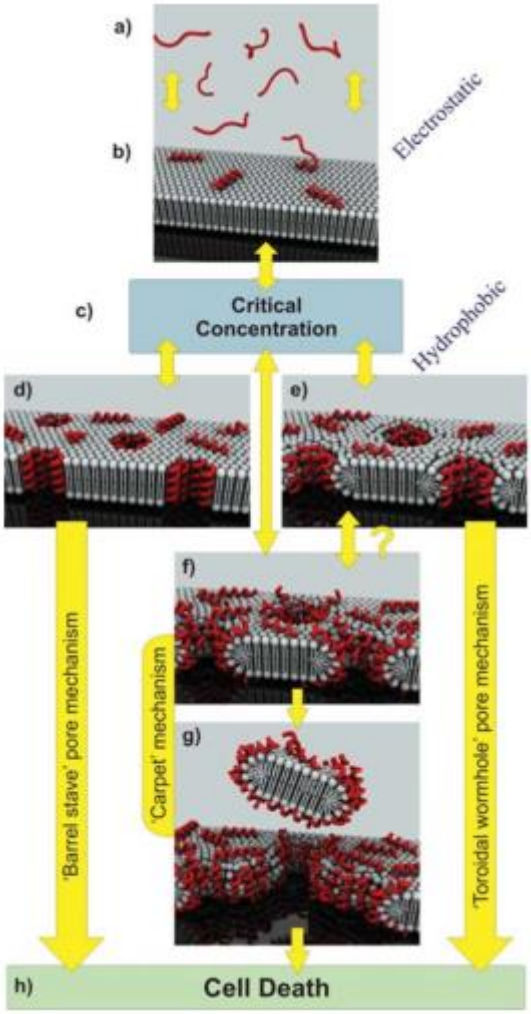

Figure 10 - AMPs' mechanisms of action. a) Initially there is an attraction of the AMPs toward the bacterial membrane through electrostatic interactions. b) Once the peptides get in contact with the membrane, they experience conformational changes. Thus, through hydrophobic interactions, an insertion of AMPs' hydrophobic portions into the membrane core could happen. c) The peptides continue to adsorb to the membrane's surface and to accumulate until the critical concentration is reached. Once the critical concentration is reached the AMPs start to self-assemble in one of three manners that lead to three different mechanisms. d) Barrel-stave model. After reaching the critical concentration the peptides self-assemble by inserting their hydrophobic portions perpendicularly in the membrane, where interactions between peptides are very important to form the pore. e) Toroidal pore model. In this model AMPs also insert their hydrophobic portions perpendicularly into the membrane promoting the formation of a curvature with partial pores formed by AMPs and the headgroups of the membrane's phospholipids. The nature of these pores is transient and therefore some AMPs can translocate into the cytoplasm and act on intracellular targets. f) Carpet model. AMPs adsorb in parallel to the membrane and accumulate until the critical concentration is reached, which ends with the loss of integrity of the membrane with a detergent-like effect, that eventually leads to the formation of micelles like shown in g). It has been hypothesized that the initial phase of the toroidal pore model can be the initial phase of the carpet model. Since both models hypothesize that AMPs adsorb in a parallel manner and accumulate on the membrane's surface until a critical concentration. It has also been hypothesized that it might be possible for AMPs to transit between

the carpet and the toroidal pore model. All these mechanisms end in the bacterial cell death. Image adapted from (Lee, N Hall et al. 2016).

Barrel-stave model (Figure 10 a) to d) and h)) – AMPs adsorb in a parallel way and suffer a conformational change which forces the perpendicular introduction of the hydrophobic part into the membrane bilayer (Andersson, Hughes et al. 2016, Ciumac, Gong et al. 2019). In this mechanism the interactions between AMPs and their amphipathicity are very important to the pore formation (Lee, N Hall et al. 2016, Kumar, Kizhakkedathu et al. 2018). AMPs associated to this type of mechanism usually have a size of 22 residues for α-helix and 8 residues for β-sheet (Lee, N Hall et al. 2016, Kumar, Kizhakkedathu et al. 2018). Some AMPs that use this mechanism are alamethicin, pardaxin and protegrins (Kumar, Kizhakkedathu et al. 2018).

Toroidal pore model (Figure 10 a) to c), e) and h)) – The peptides adsorb to the membrane, change their conformation and insert themselves perpendicularly to the membrane (Andersson, Hughes et al. 2016, Kumar, Kizhakkedathu et al. 2018, Ciumac, Gong et al. 2019). This will provoke membrane bending and the formation of a transient pore, by which the peptides can pass through and act on intracellular targets (Andersson, Hughes et al. 2016, Kumar, Kizhakkedathu et al. 2018, Ciumac, Gong et al. 2019). In this model, the pore can result from the curvature of one AMP, so the interactions between peptides are not important to the pore formation. The organization of hydrophobic and hydrophilic portions of the membrane is disturbed, while the same do not happen in the barrel-stave model (Kumar, Kizhakkedathu et al. 2018). The toroidal pore model is more transient and therefore not so stable as the barrel stave model. Thereby AMPs' charge has a bigger impact, since a higher charge leads to more repulsion between AMPs and consequently the pores will have a reduced half-time (Lee, N Hall et al. 2016). For using this mechanism AMPs need to have a discrete size and some ions selectivity (Kumar, Kizhakkedathu et al. 2018). Magainin, lactin Q, aurein 2.2 and meltittin are some examples of peptides that use this mechanism (Kumar, Kizhakkedathu et al. 2018). Both barrel-stave and toroidal pore models promote membrane depolarization, which ends with cell death.

Carpet model (Figure 10 a) to c) and f) to h))– AMPs adsorb in a parallel manner to the membrane and having covered enough area, they will promote unfavorable interactions. These interaction lead to loss of integrity of the membrane with transient holes (a detergent-like effect), which will form micelles resulting in cell death through lysis (Andersson, Hughes et al. 2016, Kumar, Kizhakkedathu et al. 2018, Ciumac, Gong et al. 2019). In this model interactions between peptides are not important and it is not required that the peptides introduce their hydrophobic portion into the membrane

to form transmembrane pores/channels or other specific structures (Kumar, Kizhakkedathu et al. 2018). The carpet model can be considered a pre-requisite for the toroidal pore model (Kumar, Kizhakkedathu et al. 2018). AMPs like cecropin, indolicidin, aurein 1.2 and LL-37 use this mechanism of action (Kumar, Kizhakkedathu et al. 2018).

Lee and co-workers described other mechanisms of action such as Shai-Huang-Matsazuki model, an interfacial activity model and an electroporation model (Lee, N Hall et al. 2016). It is important to highlight that the AMPs mechanisms of action mentioned above were only studied in membrane models, which means that different results might be obtained if different models are used and a direct translation of results might not be possible (Kumar, Kizhakkedathu et al. 2018).

There are differences between membranes of living bacteria and membranes of models. In living bacteria, there is a dynamism of the membrane and also mechanisms of compensation that are not replicated in membrane models. For this reason, studies of AMPs mechanism of action in live bacteria, have shown that these mechanisms are more complex than the ones observed in models. Omardien and co-workers studied the mechanism of action in live *Bacillus* (*B.*) *subtilis,* of TC-19, TC-84 and BP2. Primarily, it was shown that these peptides acted on the membrane leading to the displacement of membrane proteins connected with the cell wall synthesis, such as MurG, MraY, PonA, PBP2b and FtsW, making impossible for bacteria to recover the bacterial envelope (Omardien, Drijfhout et al. 2018). In another study, Omardien and co-workers demonstrated, also in *B.* subtilis, that TC-19, TC-84 and BP2 are capable of quickly increase the permeability of bacterial membrane by forming fluid domains without promoting cell lysis. This leads to displacement of proteins and due to the incapacity of the bacterium to prevent these harmful events, it will change the curvature of its membrane. The changes in the normal physiology of the membrane results in dissipation of membrane potential, which leads to AMPs internalization and leakage of cytosol (Omardien, Drijfhout et al. 2018).

Direct killing with non-pore formation in the membrane. AMPs can act on intracellular targets or on cell wall. Like antibiotics, AMPs can inhibit the cell wall synthesis, but unlike antibiotics, AMPs act interact with many precursors, instead of only one (Kumar, Kizhakkedathu et al. 2018). Human β defensin 3 and α-defensin 1 are examples of this mechanism (Kumar, Kizhakkedathu et al. 2018). The cWFW peptide is another example. Scheinpflug and co-workers studied the mechanisms of action of cWFW in *B. subtilis*. In live *B. subtilis*, the peptide quickly decreased the

membrane fluidity in the sites of contact, forming domains of different fluidities on the membrane. This phenomenon disrupts the protein organization in the membrane, with displacement of both peripheric and integral proteins, which leads to inhibition of cell wall synthesis and activation of the cell autolysis (Scheinpflug, Wenzel et al. 2017). AMPs can also interact with intracellular targets. First, these peptides interact with the membrane not causing any bacterial death and accumulate intracellularly, blocking vital cellular pathways like proteins and nucleic acid synthesis and interruption of enzymatic and protein activities (Kumar, Kizhakkedathu et al. 2018). AMPs such as indolicidin, human β defensin 4 and PR39 are capable to act intracellularly (Kumar, Kizhakkedathu et al. 2018). The exact AMPs' targets are uncertain and might be dependent on the local concentration to act against the membrane causing its disruption or be translocated to the cytoplasm and interfere with cell pathways (Andersson, Hughes et al. 2016).

2.3.2.1.2 Resistance to AMPs

As mentioned earlier, one of the appeals of AMPs is their low propensity to develop bacterial resistance, due to their co-evolution with bacteria, fast and physical mechanisms of action and due to having more than one target. However, studies have shown that bacteria have developed evasive mechanisms against AMPs (Ciumac, Gong et al. 2019, Haney, Straus et al. 2019). There are two types of resistance mechanisms to AMPs: passive and inducible. Passive resistance refers to mechanisms as a response to environmental changes that treat bacterial survival (Moravej, Moravej et al. 2018). These changes happen independently of the presence of AMPs (Moravej, Moravej et al. 2018). Inducible resistance refers to molecular changes that occurs as a response to the direct action of AMPs or to the stress provoked by them (Koutsopoulos 2017, Moravej, Moravej et al. 2018).

Bacteria resort to a variety of mechanisms to evade the AMPs attacks. But before bacteria defend themselves against AMPs, they need to sense them and for that they use sensing systems. These systems are capable to regulate the expression of target genes, once they contact with AMPs. The structures and different functions of sensing systems varies between Gram-positive and Gram-negative bacteria (Figure 11) (Moravej, Moravej et al. 2018).

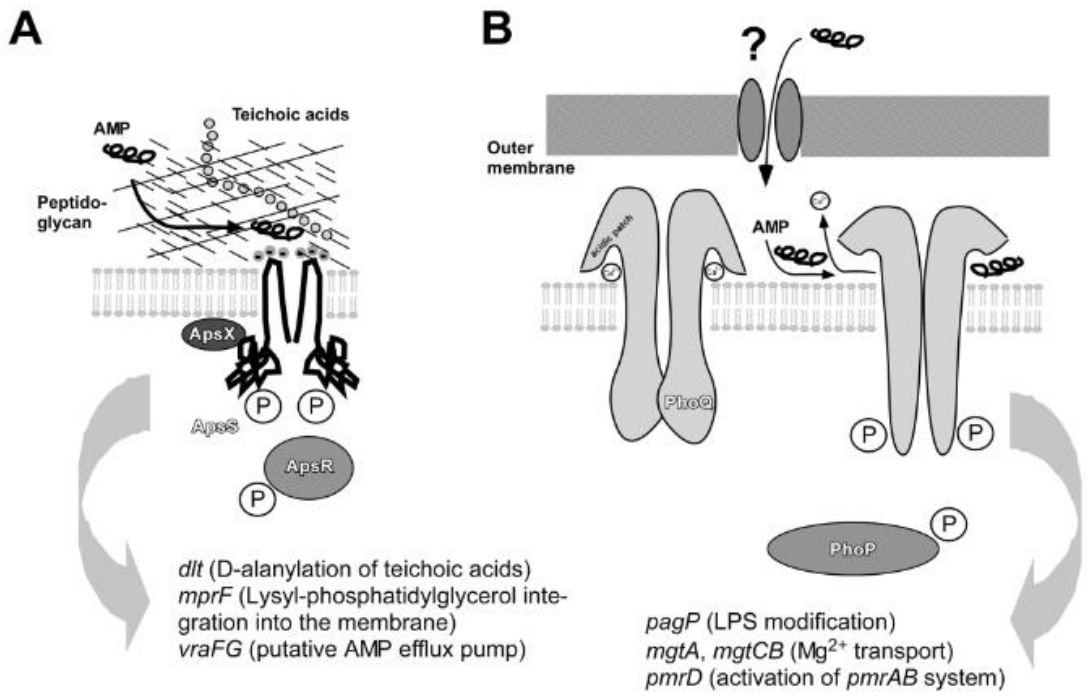

Figure 11 - AMPs sensing systems from Gram-positive and Gram-negative bacteria. A – Aps system of Gram-positive bacteria. It represented the bacterial envelope with a peptidoglycan cell wall with negative charged teichoic acid and the cytoplasmatic membrane. ApsS is in the membrane with a transmembrane domain and a very small extracellular loop with three negative charged residues, which might be important for the interaction with AMPs, although the mechanism for binding and activation is not yet known. A phosphorylation cascade might happen, typical for 2-component systems, in order to activate the transcription of target genes, such as *dlt, mprf* and *vraFG*. ApsX participates in the pathways, although in an unknown way. The formation of a dimer is not sure, but it is a common phenomenon of sensing systems. B – PhoP/PhoQ system of Gram-negative bacteria. Although it is not understood how AMPs pass through the outer membrane, they manage to reach the cytoplasmatic membrane, where the dimer PhoQ is present. Then occurs the substitution of divalent cations (Ca^{2+}) by AMPs in the acidic domain, that due to the size difference will promote conformational changes with movement of α-helices which leads to autophosphorylation of PhoQ and consequent phosphorylation of PhoP. The phosphorylated PhoP will interact with the promotors of the target genes, like *pagP, mgtA and mgtCB* and *pmrD* which activates the *pmrAB* system responsible for the regulation of lipid A modifications. Image adapted from (Otto 2009).

PhoP/PhoQ sensing system of Gram-negative bacteria. Gram-negative bacteria use a two-element system named PhoP/PhoQ, which is responsible for regulating cellular genes like *mgtA* and *mgtCB* for magnesium (Mg^{2+}) transport and for survival in macrophages, *pagP* for changes in LPS, transcription of *pmrD* for activating the regulation of the system *pmrA/pmrB* responsible for regulating modifications in the lipid A (Otto 2009, Shprung, Peleg et al. 2012, Moravej, Moravej et al. 2018). In this system there is a sensor PhoQ and a gene regulator PhoP (Figure 11). PhoQ is a histidine kinase and is present in the membrane as a dimer (Otto 2009). This component has two transmembrane α-helices, an extracellular loop of 145 residues and a

cytoplasmatic domain with a conserved site for autophosphorylation and for ATP binding (Otto 2009). PhoQ is stabilized by divalent cations, namely magnesium (Mg^{2+}) and calcium (Ca^{2+}) (Shprung, Peleg et al. 2012, Moravej, Moravej et al. 2018). When stimulated, PhoQ trans-autophosphorylates and a phosphate is transferred to a aspartate residue in PhoP, which is the protein responsible for the regulation of the target genes promoters (Otto 2009). PhoQ can be stimulated in three ways: concentration of divalent cations, low pH and presence AMPs (Otto 2009). High concentrations of magnesium (Mg^{2+}) and calcium (Ca^{2+}) can prevent PhoQ activation. These cations bind to the acidic residues next to the two transmembrane α-helices, being capable to reduce some repulsion between the acidic residues (Otto 2009). AMPs bind to the same site than divalent cations in PhoQ. Some studies even show that AMPs substitute the cations on the acidic site (Figure 11 B), but due to the AMPs' bigger size, AMPs will promote the helices movement and PhoQ activation (Otto 2009). PhoQ activation by low pH involve different mechanisms than the ones used by AMPs, being the effects of pH activation cumulative with the ones from AMPs activation (Otto 2009). A low pH will increase the PhoQ protein flexibility which allows the α-helices movement and phosphorylation in a similar model to the AMPs (Otto 2009). Despite the PhoP/PhoQ system had been study in detail, due to the AMPs' size it is possible that AMPs are sensed by other sensing systems before PhoP/PhoQ system. This suggests that more sensing systems can exist and they can work in a complex regulatory network (Otto 2009).

Aps sensing system of Gram-positive bacteria. In spite of Gram-negative bacteria have a well study sensing system, the same do not happen to Gram-positive bacteria. Li and co-workers studied a sensing system that confer *S. epidermidis* resistance to the AMP human β-defensin 3 (hBD3) (Li, Lai et al. 2007). *S. epidermidis* activated genes like *dlt*, *mprF*, overexpression of many transporters including the VraFG transporter, which is responsible for resistance to vancomycin and *S. aureus* also activated lysine biosynthesis, which is in line with the increased need of lysine because of the activation of *mprF* gene (Li, Lai et al. 2007, Otto 2009). What Li and her team found was that the *vraFG* gene was next to a three gene operon where the first two genes codified for a two-component system but the third gene did not have similarities with any gene which function was known (Li, Lai et al. 2007). This system was named Antimicrobial peptide sensor (Aps) and regulates most of the resistance mechanisms. The three components of Aps system are the sensor (ApsS), a gene regulator (ApsR) and a protein with unknown function (ApsX), all components are vital for the function of the system (Figure 11 A) (Otto 2009). ApsS is similar to PhoQ in

Gram-negative bacteria, it is a histidine kinase and it has two transmembrane α-helices and an extracellular loop with nine residues. The loop's sequence confers substrate specification and therefore resistance to a certain AMP or range of AMPs. In this system the divalent cations do not have a big impact in ApsS regulation, which suggests that ApsS and PhoQ have different mechanisms of activation (Otto 2009).

Once AMPs contact with bacterial sensing systems and activate them, resistance mechanisms are put in place in order to resist the AMPs action and survive the attack. The most common resistance mechanisms are the charge modulation of bacterial surface, overexpression of efflux pumps and AMPs degradation (Figure 12).

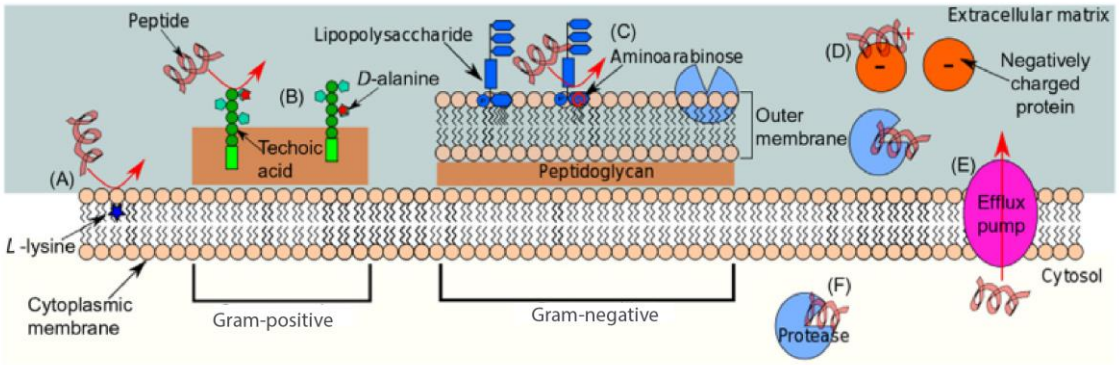

Figure 12 - Bacterial resistance mechanisms. A – Addition of L-Lysine residues to the phosphatidylglycerol groups of the phospholipids in the membrane. This leads to the neutralization of the overall membrane's negative charge, decreasing the AMPs electrostatic interactions with the membrane. B – Addition of D-alanine to teichoic acids by ester bonds in Gram-positive bacteria. This strategy has the goal to neutralize the negative charge of teichoic acids and to reduce AMPs' affinity to these molecules. C – Addition of molecules like aminoarabinose, glucosamine or phosphoethanolamine groups to the phosphate groups on the lipid A from lipopolysaccharide in Gram-negative bacteria, in order to neutralize surface charge. D – some bacteria secret negative charged proteins to sequester AMPs preventing their interaction with bacterial surface. E – Efflux pumps can be overexpressed in a stressful situation to remove any possible AMPs from the cytosol to the extracellular space preventing them to act over their intracellular targets. F – Bacteria have proteases and peptidases in the extracellular and intracellular space as well in the membrane. These proteins will act over the AMPs cleaving and inactivating them. Image adapted from (Koutsopoulos 2017).

Charge change of bacterial surface. Since the initial interactions between AMPs and bacterial surface are electrostatic, the change of the surface charge is a mechanism of resistance (Koutsopoulos 2017). The purpose of these changes is to reduce the negative charge of the bacterial envelope and consequently the AMPs affinity. (Maria-Neto, de Almeida et al. 2015, Ciumac, Gong et al. 2019). There are differences between Gram-positive and Gram-negative surfaces, which leads to different pathways to remodel surface's charge. In Gram-positive the molecule

responsible for the negative charge is TA, due to the presence of phosphate groups in the molecule (Koutsopoulos 2017). Bacteria are capable of adding D-alanine to TA by ester bonds (Figure 12 B). Thus, it is possible to neutralize some of the negative charge. Some bacteria, such *S. aureus*, have a protein named MprF which mediates the binding of L-lysine to the phosphatidylglycerol groups of the phospholipids in the membranes (Figure 12 A) (Koutsopoulos 2017). This is another strategy to neutralize the general negative charge of bacterial surface.

For Gram-negative bacteria, the molecule responsible for the negative charge is the LPS. Thereby, these bacteria add aminoarabinosamine (Figure 12 C), glucosamine or phosphoethanolamine groups to the phosphate groups on the lipid A from LPS (Koutsopoulos 2017). Through palmitoyl transferase (PagP), it is also possible to change the lipid A acetylation (Koutsopoulos 2017).

These mechanisms are bacterial adaptations to survive in stressful environments. Once the conditions become more favorable, bacteria can revert the changes. These remodulations can become a constitutive alteration of the surface molecules if the mutation of these genes occurs (Koutsopoulos 2017).

Efflux pumps. This is a mechanism very common against antibiotics not so much against AMPs (Koutsopoulos 2017). Efflux pumps are responsible for AMPs elimination from the intracellular space by moving them to the extracellular space and preventing its accumulation in the cytoplasm (Figure 12 E). It is due to these pumps that AMPs do not have time to exercise their function on their intracellular targets. In a stressful situation, like under AMPs attack, efflux pumps are overexpressed (Ciumac, Gong et al. 2019). Apart from efflux pumps, other transporters are involved in resistance to AMPs, like Sap uptake transporter that together with other uptake transporters such as dipeptide permease and oligopeptide permease are responsible for the uptake of AMPs into the cytoplasm with the intent of degradation and recycling (Bauer and Shafer 2015).

AMPs degradation by proteases or peptidases. These proteins can be secreted or can be found in the outer surface of the bacteria or in the cytoplasm in order to prevent the action of the AMPs against their intracellular targets (Figure 12 F) (Bauer and Shafer 2015, Maria-Neto, de Almeida et al. 2015, Koutsopoulos 2017, Ciumac, Gong et al. 2019). The type of proteins used against a certain AMP varies according to the strain in question. For example, for the AMP LL-37 different proteases and peptidases are used: *Enterococcus* (*E.*) *faecalis* uses gelatinases, *Proteus mirabilis*

uses metalloproteases and *Pseudomonas* (*P.*) *aeruginosa* uses elastases (Koutsopoulos 2017).

Additional mechanisms. Bacteria can also synthetize negative charged enzymes and proteins to sequester AMPs and prevent their activity (Figure 12 D)(Koutsopoulos 2017). For example, *S. aureus* produces an exoprotein named staphylokinase, which can bind to AMPs and prevent them to interact with *S. aureus* surface (Koutsopoulos 2017). Other bacteria like *E. faecalis* and *P. aeruginosa* secret proteases which will degrade proteoglycans and release anionic glycosaminoglycans which will bind to the AMPs inactivating them (Koutsopoulos 2017). Bacteria can still modify AMPs' intracellular targets by switching certain amino acids to turn vital proteins in a fundamental pathway resistant to the AMPs action (Ciumac, Gong et al. 2019).

In a pharmacologic perspective, bacterial resistance to peptides is not common due to multiple action mechanisms, targeting multiple precursors in multiple pathways with low affinity instead of having a specific target with very high affinity to it (Nijnik and Hancock 2009, Koutsopoulos 2017). Nevertheless, bacterial resistance mechanisms against AMPs create a limitation to AMPs use in clinic. However, the knowledge of the existence of these mechanisms allow the improvement of AMPs' design so they can evade these mechanisms and become more and more effective (Koutsopoulos 2017).

2.3.2.2 Immunomodulatory activity

As mentioned above, AMPs have many other functions besides antimicrobial activity (Figure 8), for this reason they can also be designated as host defense peptides (HDPs), if natural, or innate defense regulators (IDRs) peptides, if synthetic (Mansour, Pena et al. 2014, Hancock, Haney et al. 2016). Some of these other functions occur through the modulation of the immune system (cells and soluble molecules) and can consist in an indirect mechanism to kill a pathogen.

Before understanding how HDPs can modulate the immune system, it is important to understand the immune system's response to a microbial infection. There are two type of immunity: innate immunity and adaptative immunity. The innate immunity is the first to be activated and counts with epithelial cells and phagocytes (Hilchie, Wuerth et al. 2013). Epithelial cells act as a barrier to prevent pathogens entrance (Hilchie, Wuerth et al. 2013). Phagocytes can be residents in the tissue and/or recruited from the blood stream and their function is to phagocyte the pathogens (Hilchie, Wuerth et al. 2013). On a molecular level the cells recognize pathogen-associated molecular patterns (PAMPs) in their receptors, such as Toll-like Receptors (TLRs), which will activate signaling pathways, like mitogen-activated protein kinase (MAPK) pathway

(Hilchie, Wuerth et al. 2013). As a result cytokines and chemokines are produced to alert other host cells of the presence of infection and to recruit other immune cells to the infection site, respectively (Hilchie, Wuerth et al. 2013). Innate immune system activation can lead to a systemic response such as fever and also act directly as microbicidal through the production of reactive oxygen species as well reactive nitrogen species, antimicrobial peptides and proteins (Hilchie, Wuerth et al. 2013). The adaptive immunity is a response to specific molecular sequences and/or shapes named antigens. This type of immunity takes about three to seven days to be activated and relies on two types of cells antigen-presenting cells (APCs) and adaptative immune system cells (Hilchie, Wuerth et al. 2013). APCs, such as dendritic cells (DCs) and macrophages, are responsible for presenting the antigens to the adaptative immune system cells so they can develop and humoral response (Hilchie, Wuerth et al. 2013). The adaptative immune system cells are the T and B cells. T cells interact with the antigen presented by APCs which activate them. After activation, T cells pass through a differentiation process (Hilchie, Wuerth et al. 2013). They can differentiate into T_{Helper} (T_H) cells, which secret cytokines that will guide the immune response by interacting, for example, with B cells and induce them to produce antibodies for the specific antigen that was presented (Hilchie, Wuerth et al. 2013). T cells can also differentiate into $T_{Cytotoxic}$ (T_C) cells. These cells will bind to the infected and/or mutated cells and promote their death through cell death processes such as apoptosis (Hilchie, Wuerth et al. 2013). Another type of T cells is $T_{regulator}$ (T_{reg}), which are responsible for modulating and maintaining the balance of the immune response (Hilchie, Wuerth et al. 2013). B cells after being activated by T_H cells with a specific antigen will produce antibodies that will bind to the antigen on pathogens and enhance their recognition by phagocytes.

2.3.2.2.1 Mechanisms of action

The mechanisms used by the HDPs to modulate the immune system are complex and varies between the peptide in question, their concentration, the cell type that they interact with and the molecules that are present at that moment (Hancock, Haney et al. 2016).

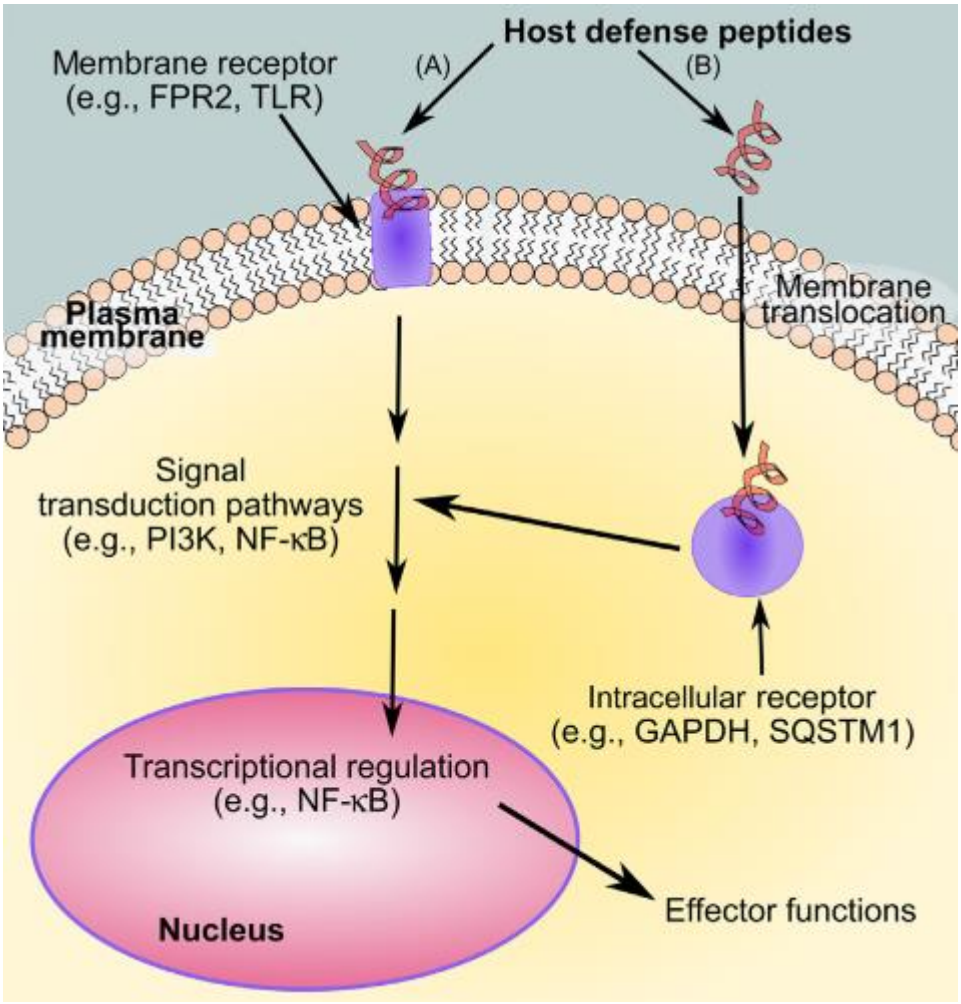

Figure 13 - Mechanisms of action of HDPs for modulation of immune cells, such as neutrophils and macrophages. The first step for modulation is the interaction of HDPs with receptors. The receptors can be (A) in the cytoplasmatic membrane, like FPR2 and TLRs, or (B) the peptide might need to translocate the cytoplasmatic membrane in order to bind to intracellular receptors such as GAPDH and SQSTM1. The choice between membrane or intracellular receptors is dependent of the molecular environment around the cell. After binding to the receptor, independently of the type, there is a stimulation of signal transduction pathways that leads to activation of transcription factors like NF-kB, AP-1 and STAT3. The transcription factors will activate or suppress the expression of target genes, resulting in chemokine production, skew of differentiation and other functions. Image adapted from (Koutsopoulos 2017).

For HDPs modulate the behavior of immune cells they need to bind to a receptor. As shown in Figure 13, HDPs can bind to membrane receptors like formyl peptide receptor 2 (FPR2), Mas-related gene X2 (MRGX2), tyrosine kinase receptor insulin growth factor 1R (IGF-1R), purinergic receptor P2X7, CXCR2 and Toll-like receptors (TLRs) (Hilchie, Wuerth et al. 2013, Koutsopoulos 2017). In an alternative, HDPs can translocate the cytoplasmatic membrane reaching to the cytoplasm and bind to intracellular receptors such as glyceraldehyde 3-phosphate dehydrogenase (GAPDH) and sequestosome 1 (SQSTM1) (Koutsopoulos 2017). Once bonded to a receptor,

HDPs can stimulate many signal transduction pathways as p38, extracellular related kinases 1 and 2 (ERK1/2), JNK MAPKs, nuclear factor kB (NF-kB), PI3K, TRIF-interferon regulatory factor (IRF), triggering receptor expressed on myeloid cells (TREM) and others (Hilchie, Wuerth et al. 2013, Koutsopoulos 2017). By activating these signaling pathways, AMPs induce the mobilization to nucleus of transcription factors like nuclear factor kappa-light-chain-enhancer of activated B cells (NFkB), cAMP response element-binding protein (Creb), interferon regulatory factor 4 (IRF4), activator protein 1 (AP-1), activator protein 2 (AP-2), antioxidant response element (Are), E2F1, specificity protein 1 (SP1), glucocorticoid response element (Gre), Elk, signal transducer and activator of transcription 3 (STAT3) and others (Koutsopoulos 2017). As a result from all this process there is expression of chemokines, such as monocyte chemoattractant protein 1 (MCP-1) e MCP-3 (Hilchie, Wuerth et al. 2013). There is also modulation of pathways and skew of differentiation of cells like DCs and macrophages. However, the direction of differentiation promoted by HDPs is hard to predict and depends on the microenvironment. LL-37 is an HDP and can direct macrophages polarization into M1 or M2. This direction depends on the state of polarization of the macrophages when the HDP interacts with them and also depends on the presence or not of PAMPs, like LPS (van der Does, Beekhuizen et al. 2010, Brown, Poon et al. 2011). Another example is IDR-1018 peptide. Macrophages exposed to IDR-1018 adopt a phenotype between M1 and M2 and 876 genes had their expression changed, some were upregulated others downregulated (Hancock, Haney et al. 2016).

Although the complex interactions and the many pathways that can be affected, some effects of the HDPs on the immune system are clearer, like modulation of pro- and anti-inflammatory responses, chemoattraction, enhancement of bacterial killing, cell differentiation, adjuvant activity, apoptosis, pyroptosis and wound healing.

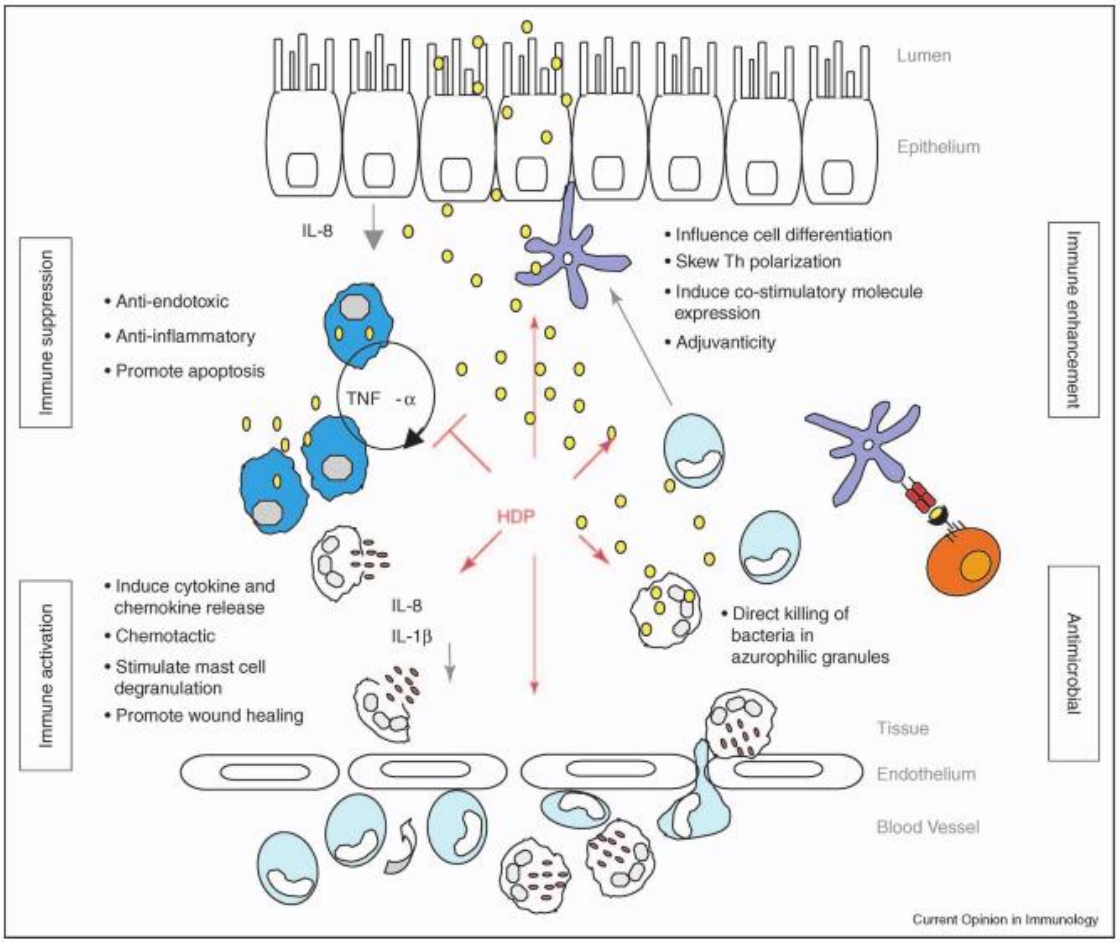

Figure 14 - Schematic representation of HDPs multifunction in an infection context (pathogens are represented by yellow circles). HDPs can be immune suppressors by stopping the immune response to endotoxins (anti-endotoxic function), by stimulating the production of anti-inflammatory cytokines and even triggering apoptosis in infected cells. HDPs can enhance the immune response already active by directing and skewing differentiation of immune cells such as macrophages, DCs and T cells and playing the role of adjuvant. HDPs can also activate the immune system by promoting cytokines and chemokines production, wound healing, by stimulating mast cell degranulation and influencing diapedeses. Finally, HDPs can act directly on pathogens leading to the death. Image adapted from (Brown and Hancock 2006).

Modulation of inflammatory responses. Do not exist pro-inflammatory or anti-inflammatory HDPs, but HDPs that selectively modulate the immune system and its mechanisms according to the microenvironment (Koutsopoulos 2017). HDPs can potentiate a pro-inflammatory response by enhancing chemokine production, influencing diapedesis, skewing macrophages, DCs and neutrophils differentiation into pro-inflammatory subtypes, increasing phagocytose and acting directly as a chemokine in order to recruit more immune cells to the site (Koutsopoulos 2017). HDPs can also promote an anti-inflammatory response by enhancing anti-inflammatory cytokines production, activating MAPK and PI3K signaling pathways and by blocking the bond between PAMPs and its receptors (Koutsopoulos 2017). LL-37 is capable to suppress

proinflammatory responses, like the production of TNF-α. The peptide acts in pathways, such as the MAPK pathway by binding to the intracellular receptor GAPDH, resulting in the inhibition of the expression of specific proinflammatory genes like NF-kB1 and TNF-α induced protein 2 (Lai and Gallo 2009, Mansour, Pena et al. 2014). LL-37 can also suppress STAT-1 pathway in monocytes, dendritic cells and macrophages inhibiting TNF-α and IL-12 production, which will suppress the T_{H1} response (Nijnik, Pistolic et al. 2009).

HDPs can directly binding PAMPs, making it impossible for them to bind to its receptor and trigger an inflammatory response (Scott, Vreugdenhil et al. 2000, Lai and Gallo 2009). LL-37 can directly bind to LPS, acting like a scavenger and preventing it to interact with the LPS-binding proteins of the receptor TLR4. Thus, pathways, such as MAPK, ERK and p38, will be modulated in order to suppress TNF-α production (Mookherjee, Brown et al. 2006). HDPs can also bind to nucleic acids, such as bacterial or viral double strain DNA (dsDNA) and form columnar crystalline complexes. The space between the columns of DNA is given by the HDP charge. This space is also responsible for a better or worse recognition of the TLRs and consequently a higher or smaller cytokine production (Lee, Lee et al. 2019). LL-37 binds to dsDNA forming a columnar crystalline complex with a spacing of 3-4 nm between, DNA columns. This space matches the steric site of TLR9 leading to an easier recognition of the dsDNA and a strong amplification of IFN production (Lee, Lee et al. 2019).

Chemoattraction. HDPs can indirectly act as chemokines by stimulating the production of cytokines, like IL-8 and MCP1, that will attract monocytes and macrophages, epithelium cells, mast cells and T cells (Mansour, Pena et al. 2014). For instance, it has been described that the IDR-1002 interacts with the Gi-protein-coupled receptors and the PI3K, NF-kB and MAPK pathways, which results in the enhancement of monocyte migration (Madera and Hancock 2012). HDPs can also act directly as chemokines, when in high concentrations. They promote the migration of epithelial and immune cells (Mansour, Pena et al. 2014). One explanation for this function of HDPs is their structural similarity to chemokines. Defensins have a similar size to chemokines, as well as structure, presence of disulfide bonds, positive charge and induction of interferon production (Koutsopoulos 2017). Niyonsaba and co-workers demonstrated that human β-defensin-2 can act as a potent chemoattractant to mast cells through the pertussis toxin sensitive and phospholipase C-dependent pathway and can also attract dendritic cells and T cells through the CCR6 receptor (Niyonsaba, Iwabuchi et al. 2002).

Adjuvanticity. In a vaccine there are two main components, the antigen and the adjuvant. The adjuvant is responsible for the activation and enhancement of the immune system response. The mechanism used by HDPs as adjuvants is not yet fully understood, but there are three mechanisms that stand out: enhancement of recruitment of APCs to the vaccine site, activation of APCs and formation of a compartment where the antigen concentration remains always high (Hilchie, Wuerth et al. 2013). These strategies can change the cytokines production and skew cellular differentiation of T cells and macrophages (Hilchie, Wuerth et al. 2013).

Enhancement of bacterial killing. HDPs can make part of traps like the neutrophil extracellular traps (NETs) from the neutrophils and/or the mast cell extracellular traps (MCETs) from the mast cells. The actual HDPs role in NETs and MCETs is not yet known, but it is hypothesized to be related to their antibiofilm potential in order to prevent bacterial growth on these traps (Mansour, Pena et al. 2014). HDPs can also enhance the intracellular killing, for example, IDR-1018 can enhance the trigger of neutrophils to kill *E. coli* and the production and release of HDPs by these same cells (Niyonsaba, Madera et al. 2013).

Cell differentiation. HDPs can promote cell differentiation in dendritic cells and macrophages. The direction of differentiation depends on the differentiation state of the cell and also on the presence of other soluble molecules (Hilchie, Wuerth et al. 2013, Mansour, Pena et al. 2014). Davidson and co-workers reported that LL-37 can influence dendritic cells differentiation, through the Gi protein-coupled receptor, into a phenotype that will privilege the T_{H1} cell differentiation, by regulating the amount of cytokines secreted, specially the IL-12, IL-6 and IL-4 (Davidson, Currie et al. 2004).

T and B cells. Besides the indirect influence that the HDPs can have in these cells, they can also interact directly with them (Mansour, Pena et al. 2014). HDPs can guide the T cells response into T_{H1}, T_{H2} or a mixture of both. Once again, the direction is decided according to the molecular environment present (Koutsopoulos 2017). A high concentration of defensins can promote a T_{H1} and T_C response, as well an enhancement of the activation of natural killer (NK) cells with an increase of IL-12 and IFN-ɣ production (Koutsopoulos 2017). Defensins can also stimulate a T_{H2} response with increase of IL-5 and IL-10 production (Koutsopoulos 2017). Hurtado and co-workers demonstrated that the LL-37 peptide improved the detection of bacterial DNA by the B cells, but not the detection of human DNA (Hurtado and Peh 2010). LL-37 can also instigate a granzyme-mediated apoptosis in T_{reg} (Mader, Ewen et al. 2011).

Wound-healing. HDP with good antimicrobial activity do not necessarily have a good wound healing activity and *vice-versa*. There are HDPs with poor antimicrobial activity but with good wound healing activity (Hilchie, Wuerth et al. 2013). The mechanisms for wound healing involve recruitment of epithelial cells and promotion of re-epithelization. HDPs can also promote production of extracellular matrix and control the synthesis of metalloproteinases to restructure the extracellular matrix, in order to improve the healing (Mansour, Pena et al. 2014). Niyonsaba and co-workers demonstrated the influence of β-defensins in keratocytes through the EGFR and the activation of the STAT-1 and STAT-3 pathways, thus, promoting the keratocytes migration and proliferation (Niyonsaba, Ushio et al. 2007). Oono and co-workers reported that defensin HNP-1 promotes matrix deposition by increasing the expression of proα1(I) collagen mRNA and protein in dermal fibroblast. On the other hand, the expression of the matrix metalloproteinase-1 (MMP-1) was reduced in the same cells. In this way, the wound-healing was promoted by matrix deposition and control of its degradation (Oono, Shirafuji et al. 2002). Another activity of HDPs related with the wound-healing is angiogenesis. HDPs are capable of promoting angiogenesis by acting directly on endothelial cells, their proliferation and the formation of vase-like structures. Koczulla an co-workers showed that LL-37 is capable of stimulate the endothelial proliferation and formation of new vessels through the FPRL1 path signaling (Koczulla, Von Degenfeld et al. 2003).

Autophagy modulation. Autophagy is the process to recover energy from cellular components. Through autophagy cells manage to recycle defected components and also survive longer in a starvation environment. The components are trapped in special vesicles called autophagosomes that will fuse with lysosomes to hydrolyze the components (Koutsopoulos 2017). HDPs can act on cellular pathways in order to induce or prevent the autophagy (Mansour, Pena et al. 2014). For example, Mayer and co-workers showed how IDR-1018 can modulate the AMPK-Akt signaling to stop the deregulated autophagy in cystic fibrosis cells (Mayer, Blohmke et al. 2013). On the other hand, Yuk et al. reported that LL-37 is capable to induce autophagy through a vitamin D mediated process in monocytes and macrophages, by activating the autophagy related genes *Beclin-1* and *Atg5* (Yuk, Shin et al. 2009).

Apoptosis modulation. Apoptosis is the programmed cell death. In this process caspases cleave their target proteins leading to the shrink of the cell and membrane bleb. Occurs, then, the degradation of DNA, RNA and other cellular components (Koutsopoulos 2017). HDPs can interfere with the cellular pathways in order to promote or delay the apoptotic process (Mansour, Pena et al. 2014). Nagaoka an co-workers

reported that LL-37 is capable of suppressing apoptosis in neutrophils through activation of the FPRL1 and P2X7 (Nagaoka, Tamura et al. 2006). Barlow et al. demonstrated that LL-37 is also capable to promote apoptosis in airways epithelium through the depolarization of the mitochondrial membrane, release of cytochrome c and the activation of caspases 3 and 9 (Barlow, Beaumont et al. 2010).

Pyroptosis modulation. Pyroptosis is a type of cell death induced by the presence of a pathogen, causing the release of proinflammatory cytokines. This type of cell death is considered to be highly damaging for the host (Mansour, Pena et al. 2014). A way to prevent this kind of exacerbated inflammatory response is by using HDPs. Hu and co-workers demonstrated both *in vitro* and *in vivo* that LL-37 is capable to inhibit the pyroptosis induced by LPS/LTA in macrophages (Hu, Murakami et al. 2014, Hu, Murakami et al. 2016).

The immunomodulation through the HDPs gives new ways of fighting not only infections and traumas, but also diseases related to inflammatory processes like cystic fibrosis, chronic obstructive pulmonary disease, psoriasis, atopic dermatitis and others (Hancock, Haney et al. 2016)

2.3.2.2.2 Osteoimmunomodulation

Osteoimmunomodulation is a recent field and therefore the application of HDPs in order to modulate the immune system to promote bone regeneration is something that is still in an incubator phase.

However, Zhang and co-workers have been studying the effect of the LL-37 peptide in monocytes and their effect in bone. This team discovered that LL-37 induce monocytes differentiation, in six days, into a novel type of bone-forming cells, which they named monoosteophils (Zhang and Shively 2010). In early phases of differentiation these cells present a morphology close to monocytes, they are large round and adherent cells. In later phases the cells adopt a morphology closer to osteoclast, they become giant multinucleated cells with an irregular shape (Zhang and Shively 2010). In addition, the differentiation of monoosteophils is sequential, since during the first 24 hours there is a decrease of cell numbers and then there is an increase of cell numbers from the second day to the sixth day (Zhang and Shively 2013). Although monoosteophils have a limited ability of proliferation, they have a longer survival capacity (Zhang and Shively 2013). Due to the proximity of osteoclasts in morphology, the monoosteophils were compared to osteoclast in function and cytokine releasing. To evaluate function, a bone reabsorption test was performed, where monoosteophils formed mineral granules of phosphorus, calcium, carbon and

sodium, while osteoclasts formed a pit (Zhang and Shively 2010, Zhang and Shively 2013). In addition, the cytokines analysis showed that monoosteophils produced more IL-1RA and less IL-1β, IL-6 and MCP-1 than osteoclasts. When challenged with LPS, monoosteophils produced more IL-1RA, IL-10, IL-12, IP-10 and GM-CSF than the osteoclasts, which suggests that LL-37 promotes an anti-inflammatory response in these cells (Zhang and Shively 2010). Because of the similar function to osteoblasts, monoosteophils were compared with MSCs, the precursors of osteoblasts. Monoosteophils shown differences in morphology, cells markers and different bone formation patterns (Zhang and Shively 2010). Since monoosteophils keep the phagocytosis function, they were compared with other cells that also differentiate from monocytes and have this function, such as DCs and macrophages. When compared with macrophages, monoosteophils produced more IP10 and IL-1RA and less IL-1β and IL-6 than macrophages (Zhang and Shively 2010). When compared with DCs, monoosteophils did not shared the same cell markers or the morphology of mature and immature DCs (Zhang and Shively 2010). In this way monoosteophils stand out as a novel type of bone-forming cells. In order to see if monocytes can differentiate into monoosteophils *in vivo*, human monocytes and LL-37 were mixed in a mixture of HA and TCP and transplanted into the dorsal surface of SCID mice. After seven weeks it was observed the differentiation into monoosteophils and the formation of epiphyseal-like structures (Zhang and Shively 2010).

Owing to the similarities of monoosteophils in morphology with osteoclasts and in function with osteoblasts, Zhang and co-workers analyzed the genetic expression of monoosteophils. By comparing monoosteophils' cell markers with macrophages and osteoclasts, monoosteophils presented higher levels of integrin α3, α3β1 and α6, which differentiate them from macrophages and osteoclasts (Zhang and Shively 2013). Monoosteophils lacked CD68, osteocalcin and bone alkaline phosphatase (BAP), which discriminate them from circulating osteoblast-lineage cells (COCs), myeloid calcifying cells (MCCs), monocyte-derived mesenchymal progenitors (MOMPs), as well as osteoblasts and osteocytes (Zhang and Shively 2013). When comparing the gene expression of monoosteophils with monocytes, the gene MAPK13 (p38MAPKδ) showed an upregulation while important genes from the BMP pathway such as Smad1-5, BMP2, BMP4, FOS, ATFs and p38MAPKα/β/ϒ were downregulated or unchanged (Zhang and Shively 2013). These results suggest that monoosteophils use different pathways from osteoblasts for bone formation. Other genes like APOC1 and CH1T1 were also upregulated and are associated with diseases such as atherosclerosis, Gaucher disease and tuberculosis (Zhang and Shively 2013). In order to prove the

efficacy of monoosteophils *in vivo,* an assay with SCID mice was performed. A hole was drilled in the mice's femur, monoosteophils were differentiate *in vitro* and then implanted in the defect. At the day 14th, in mice treated with monoosteophils the defect was almost healed and it was visible residues of a structure similar to the hard callus. The same situation was only observed at day 24th in mice treated with monocytes. By the day 24th, mice with monoosteophils had the defect completely healed (Zhang and Shively 2013).

Zhang and co-workers also studied the mechanisms behind the monoosteophils differentiation by LL-37. LL-37 interacts with the CXCR2 receptor in the monocyte's membrane and an endocytose process is started. The endocytose occurs via, both, clathrin and caveolae/lipid raft pathways resulting in small vesicles within the first two hours and larger vesicles after four hours (Zhang, Le et al. 2020). In order to detect which destiny these vesicles have, Zhang and co-workers used co-localization methods to determine which organelles these vesicles interact with. They discovered that after four and sixteen hours a small part of the vesicles was co-localized with lysosomes and a big part of the vesicles was co-localized with the trans-Golgi network (TGN) and the mitochondria (Zhang, Le et al. 2020). The co-localization between vesicles with LL-37 and mitochondria is very interesting, since in a previous study the mitochondria were co-localized with vesicles with calcium phosphate in osteoblast (Boonrungsiman, Gentleman et al. 2012). All this suggests that TGN and mitochondria have an important role in the monoosteophils differentiation (Zhang, Le et al. 2020). At the day six, the large vesicles with LL-37 are no longer co-localized with TGN and mitochondria, which suggests a sequential maturation of the monoosteophils. During the all process of differentiation the LL-37 peptide continues bond to the vesicles membrane, which leads to the conclusion that the LL-37 peptide plays an important role in directing the process of maturation (Zhang, Le et al. 2020).

2.4 Orthopedic devices

Orthopedic devices to treat bone fractures such as fixation plates, screws, nails, rods, wires, and pins are very important to assure the stabilization and immobilization of the bone to have a proper healing. These devices will be exposed to cyclic loading conditions, therefore they need to be resistant to high fatigue and have high stiffness in order to protect the fracture site from stress (Kim, See et al. 2020).

2.4.1 Titanium

The most common type of material used in orthopedics are metals, such as titanium alloys, copper-chromium alloys and stainless steel (Kim, See et al. 2020). Titanium and

stainless steel are the most used, because of high production costs of copper-chromium alloys (Kim, See et al. 2020).

Titanium alloys are a good option for orthopedic devices. Titanium presents characteristics such as light weight, excellent mechanical properties, good biocompatibility and high bone affinity (Takizawa, Nakayama et al. 2018). Briefly comparing titanium with stainless steel, titanium presents a higher maximum torque and fatigue resistance, a thicker oxide layer and faster regeneration of it, which implies a longer and better protection against corrosion and the metal ions released from the implant are less toxic (Kim, See et al. 2020).

2.4.2 Poly (lactide-co-glycolic) acid (PLGA)

Poly (lactide-co-glycolic) acid (PLGA) is a synthetic polymer compose by two monomers lactic acid and glycolic acid. This co-polymer is biodegradable and its degradation products are part of metabolic pathways from cells, such as Kreb's cycle (Figure 15) (Elmowafy, Tiboni et al. 2019). Different ratios from each monomer allow to obtain different physical, mechanical and chemical characteristics (Li, Cui et al. 2018).

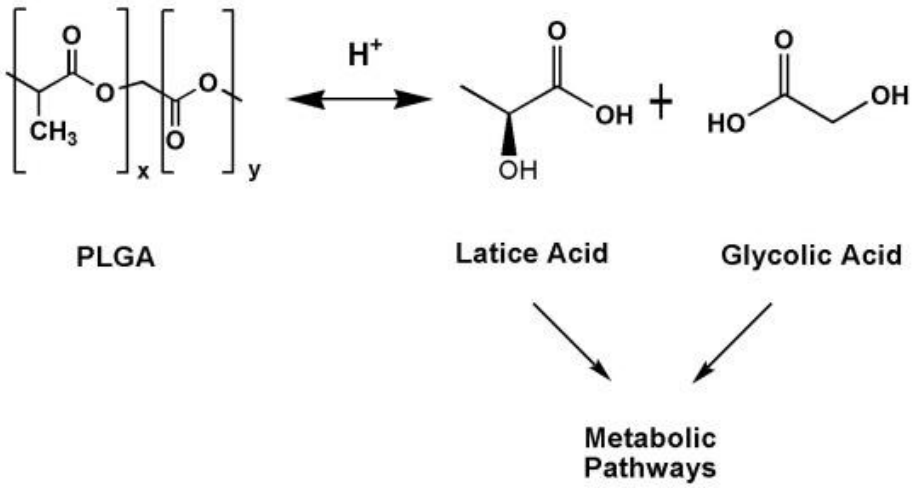

Figure 15 - Hydrolysis of PLGA. Image adapted from (Li, Cui et al. 2018).

The use of PLGA in clinic was already accepted by FDA and EMA and there are already PLGA products for orthopedic use, such as LactoSorb® (Biomet 2010) and RAPIDSORB® (Johnson 2020), two fixation systems.

However, PLGA has been also applied to drug delivery systems due to its safety and extensive characterization. It has been studied under the format of nanoparticles and coatings loaded with proteins, antimicrobial peptides and calcium phosphate to increase the osteogenic activity (Li, Cui et al. 2018).

2.4.3 Synthetic antimicrobial and antibiofilm peptide 148 (SAAP-148)

SAAP-148 is a synthetic antimicrobial and antibiofilm peptide inspired in the natural antimicrobial peptide LL-37.

Table 1 - Sequences of LL-37 and SAAP-148 peptides

Peptide	Sequence
LL-37	L L G D F F R K S K E K I G K E F K R I V Q R I K D F L R N L V P R T E S
SAAP-148	L K K L W K R V F R I W K R I F R Y L K R P V R

By using 24 amino acids from LL-37 C-terminal sequence as a template, some amino acids were substituted (Table 1) in order to increase the hydrophobicity and the positive charge, while keeping the α helix structure of LL-37 (Figure 16).

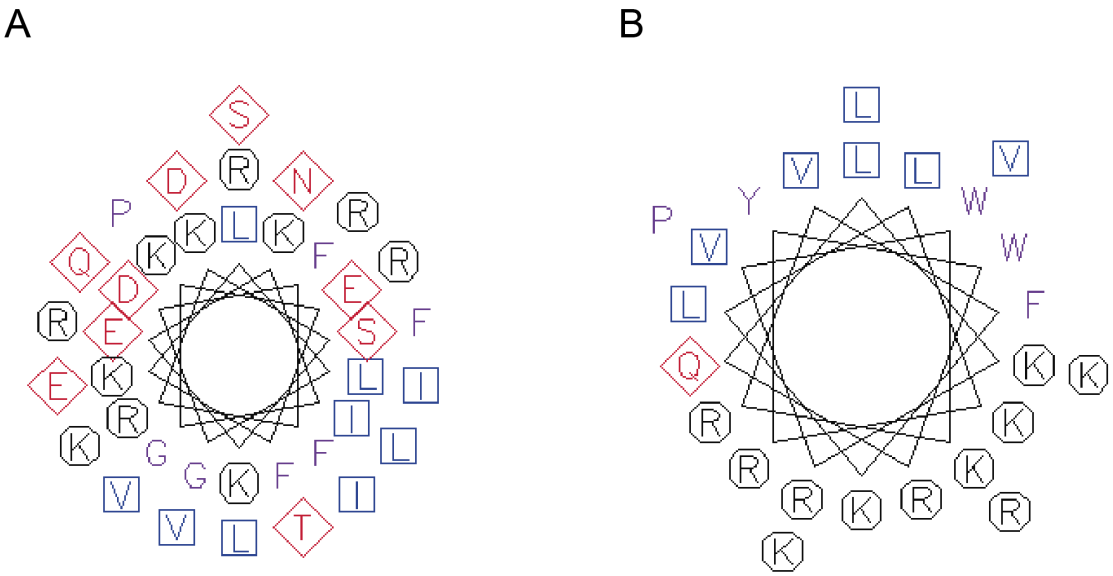

Figure 16 - Helical wheel projection of the peptides (A) LL-37 and (B) SAAP-148. These images were produced by the online program EMBOSS explorer (https://www.bioinformatics.nl/emboss-explorer/) Charged amino acids are in black and apolar amino acids are in blue.

According to de Breij and co-workers, SAAP-148 is a very promisor peptide, because SAAP-148 showed a higher activity than LL-37 even in plasma, it did not promote resistance after serial passages under subinhibitory concentrations for different strains such as *E. coli*, *A. baumannii* and *S. aureus* (non-multidrug resistant and multidrug resistant) and it was able to eradicate biofilms, including persister bacteria (de Breij, Riool et al. 2018).

As a mechanism of action, de Breij and co-workers described that SAAP-148 was able to strongly perturb the hydrophobic core of the membrane composed by lipid 1,2-dipamitoyldipalmitoyl-sn-glycero-3-phospho-rac-glycerol (DPPG). This perturbation lead to the membrane thinning, which results in the leakage of intracellular content (de Breij, Riool et al. 2018). A similar mechanism was described to the peptide LL-37 by Sevcsik and co-workers (Sevcsik, Pabst et al. 2007).

As for *in vivo* studies with SAAP-148, de Breij and co-workers showed that ointments with SAAP-148 were able to significantly reduce the number of viable MRSA and *A. baumannii* in murine models of abraded skin infections (acute and established) (de Breij, Riool et al. 2018). In contrast, Dijksteel and co-workers verified a poor antimicrobial activity for SAAP-148 (Dijksteel, Ulrich et al. 2019). However, Dijksteel and co-workers used a different wound model (incision wound models in rat) than he described by de Brij and co-workers, which leads to a different environment with a higher presence of proteins that might compromise the peptides efficacy. They needed higher concentrations of SAAP-148 for completely eradicate the bacteria not only in the rat model, but also in *ex vivo* experiments with skin. These differences can be due to the different susceptibilities of the different strains used in both studies. A final main difference between the two studies is the use of sodium polyanethole sulfonate (SPS) as a neutralizer of the peptide antimicrobial activity. The absence of a peptide-neutralizer in the studies performed by de Breij and co-workers may lead to an extended exposer to the peptide, resulting in an apparent effective eradication of bacteria (de Breij, Riool et al. 2018, Dijksteel, Ulrich et al. 2019).

2.4.4 Three-dimensional (3D) printing in orthopedic

Three-dimensional (3D) printing is a recent technology that has made its path through fields like aerospace, jewelry making and more recently medicine for plastic biomodels used for surgical planning, making implants formulations and even human tissues (Gubin, Kuznetsov et al. 2016, Iyer and Khan 2019).

3D printing is based on the additive manufacturing model, in which layers of raw material are added on top of each other, in order to achieve an accurate 3D object. 3D printers are capable to use many materials like plastics, polymers and metals. By adjusting the printing methods and conditions, it is possible to include biological components, such as peptides, proteins and even cells, in the inks for printing (Gubin, Kuznetsov et al. 2016, Ozbolat 2016).

In the orthopedic field, 3D printed materials can be a real advantage. Based in images such as computed tomography and magnetic resonance imaging, it is possible

to design a device adapted to each patient anatomic individuality, pathological condition and trauma. A personalized implant will provide a better fit and a better integration in the body (Ozbolat 2016, Iyer and Khan 2019).

Having in mind the advantages of 3D printing, materials produced by 3D printing are used in this dissertation. The bulk material used is a 3D-printed titanium with a 3D-printed coating of PLGA containing SAAP-148. This dissertation aims to study the antimicrobial activity of SAAP-148 in free form and incorporated in the coatings against Staphylococcus *aureus* through release assays and Lethal Concentration killing 99.9% of the inoculum and the JIS Z 2801 assay for assess the antimicrobial activity of the coating. Due to the AMPs modulatory activities, this dissertation aims to evaluate the effect that SAAP-148 has on macrophages gene expression, using the mouse macrophage cell line RAW 264.7 and on osteoblasts precursors calcium deposition, using the mouse osteoblasts precursors cell line MC3T3-E1.

Chapter 3

3 Materials and Methods

3.1 Peptide and materials

The peptide SAAP-148 (acetyl-LKRVWKRVFKLLKRYWRQLKKPVRamide; M= 3267.11Da) was produced at the Leiden University Medical Center, Leiden (LUMC), The Netherlands.

The 3D-printed poly(lactic-co-glycolic acid) (PLGA)-SAAP-148 coatings were produced at the Warsaw University of Technology, Faculty of Materials Science and Engineering, Warsaw, Poland. The difference between the coatings resides in the formulation of the bio-ink, therefore, the coatings will be referred to as coating A and coating B[1]. Both coatings were printed on titanium samples using the drop-on-command technique (Ozbolat 2016, Zhang and Song 2018). To make coatings with more than one layer, the layer-by-layer method was used (Ozbolat 2016).

3.2 Cell culture

RAW 264.7 cells were cultured in 75 cm^2 flasks (VWR) with Roswell Park Memorial Institute (RPMI) 1640 medium (Glibco) and supplemented with 10% of Fetal Bovine Serum (FBS), heat inactivated (Gibco), 1% of Penicillin-Streptomycin (PenStrep; 100.00 U/mL; Glibco) and 0.1% of 2-mercaptoethanol (2mE; Glibco) at 37°C with 5% CO_2. The cells were pass every three days by washing twice with Dulbecco's

[1] For intellectual protection of these materials, no further details about these materials will be revealed in this dissertation.

phosphate-buffered saline (D-PBS; Glibco), then 15mL of media was added and the cells were scraped using a 1.8 cm blade scraper (Falcon). One mL of cell suspension was added to 50 mL of fresh media in a new 75 cm^2 flask.

MC3T3-E1 cells were cultured in 75 cm^2 flasks with α minimum essential medium (α-MEM; Glibco) supplemented with 10% of FBS, heat inactivated, 1% of PenStrep (100,00 U/mL) at 37°C with 5% CO_2. The cells were passed every three days by washing twice with D-PBS, then the cells were incubated with 3 mL of Trypsin-EDTA 0.01% (Glibco) until detached. The trypsin was neutralized with 7 mL of fresh medium and 5 mL of this cell suspension was added to 41 mL of fresh media in a 75 cm^2 flask.

Both cell lines were used in experiments between passage 3 and 30.

3.3 Bacterial culture

S. aureus JAR060131 (clinical isolate from an infected hip prothesis, (Moriarty, Debefve et al. 2009)) was cultured by inoculating 1-3 colonies in 5 mL tryptic soy broth (TSB, prepared at the VOBO department of the AMC) and by incubating it overnight at 37°C while shaking (120 rpm). To achieve a logarithmic phase a 100 times dilution was made from the overnight culture into fresh TSB and incubated for 3 hours at 37°C and 120rpm.

3.4 Antimicrobial activity of SAAP-148 *in vitro*

Since the PLGA-SAAP-148 coatings were sterilized with gamma radiation, it was assessed if the gamma radiation affects the antimicrobial activity of SAAP-148 *in vitro*. Therefore, the antimicrobial activity of untreated SAAP-148, SAAP-148 gamma radiated in powder and gamma radiated in solution was tested.

The logarithmic phase inoculum in TSB was pelleted, washed twice with phosphate-buffered saline (PBS; prepared at the VOBO department of the AMC), and resuspended in RPMI medium supplemented medium with 20 mM HEPES and L-glutamine, without sodium bicarbonate (Sigma; further referred as RPMI) and diluted in RPMI to $1x10^7$ colony forming units (CFU)/mL, based on the optical density of the suspension at 620nm (OD_{620nm}) in a UV-Visible spectrophotometer (Genesys 180, Thermo Scientific). In a 96-wells polypropylene round bottom plate (Costar), 10 µl of the $1x10^7$ CFU/mL inoculum were added to 90 µl of SAAP-148 solution in RPMI (final peptide concentrations ranging from 0.06 µM to 60 µM; final concentration of bacterial suspension $1x10^6$ CFU/mL). As non-treated control the bacteria were incubated in RPMI without peptide. The plates were incubated for 24 hours at 37°C and 120rpm in a

humid atmosphere. Viable bacteria were determined in blood agar plates (prepared in VOBO department in the AMC).

Antimicrobial activity is expressed as the minimal inhibitory concentration (MIC), which refers to the lowest peptide concentration without visible growth, and as the 99.9% lethal concentration (LC 99.9%), referring to the lowest peptide concentration that killing ≥99.9% of the inoculum.

For time-killing assays, in a 96-well polypropylene round bottom plate, 25 µL of bacterial inoculum was added to 225 µL of peptide solution in RPMI for a total volume of 250 µL (final peptide concentration 3.75µM; final concentration of bacterial suspension $1x10^6$ CFU/mL). As untreated control, bacteria were incubated in RPMI without peptide. After incubation at 37°C and 120 rpm in a humid environment, a 20 µL sample was taken from the incubation every 5 minutes (min) up to 30 min, and subsequently added to 20 µL of 0.05% (v/v) SPS (Sigma) to inactivate the peptide's activity (Kwakman, Velde et al. 2010). Then, the number of viable bacteria was determined by quantitative culture.

FBS is known to reduce the antimicrobial activity of AMPs (Löfgren, Miletti et al. 2008). Thus, it is relevant to study which percentage of FBS can the medium contain without affecting the peptide's antimicrobial activity and yet support cell growth. The logarithmic phase inoculum in TSB was pelleted, washed twice with PBS, and resuspended in α-MEM alone and supplemented with 1%, 2% or 5% of FBS and diluted in the respective media to $1x10^7$ CFU/mL, based on the OD_{620nm}. In a 96-well polypropylene round bottom plate, 10 µL of the $1x10^7$ CFU/mL inoculum was added to 90µL of peptide solution with the respective FBS percentage (final peptide concentrations ranging from 0.06 µM to 60 µM; final concentration of bacterial suspension $1x10^6$ CFU/mL). As non-treated control the bacteria were incubated in the respective medias without peptide. The plates were incubated for 24 hours at 37°C and 120 rpm in a humid atmosphere. The number of viable bacteria was determined by quantitative cultures at blood agar plates.

3.5 Cell proliferation assay

The cytotoxicity of SAAP-148 was assessed by the water soluable tetrazolium salt 4-[3-(4Iodophenyl)-2-(4-nitro-phenyl)-2H-5-tetrazolio]-1,3-benzene sulfonate (WST-1) assay (Sigma) for both the RAW 264.7 and MC3T3-E1 cell lines. Briefly, in a 96 well polypropylene round bottom plate, approximately 100 cells per well were seeded in RPMI (supplemented with 10% FBS, 1% PenStrep and 0.1% 2mE) for RAW 264.7 cells or α-MEM (supplemented with 10% FBS and 1% PenStrep) for MC3T3-E1 cells

and incubated overnight at 37°C with 5% CO_2. The cells were washed with D-PBS and incubated with 100 µL of SAAP-148 solutions ranging from 10 µg/mL to 200 µg/mL for 24, 48 and 72 hours at 37°C with 5% CO_2. The peptide solutions were prepared in in α-MEM supplemented with 2% of the FBS. A control with this medium and without peptide was included. At each time point the media was removed and 100 µL of fresh α-MEM were added together with 10 µL of WST-1. The cells were incubated at 37°C with 5% CO_2 for 30 min and the supernatante was removed into a new 96 well polysterene round bottom plate and the absorbance was at 440 nm was determined in the plate reader (Synergy H1 multi-mode reader, BioTeck). Hundred µL per well lysis reagent 0.025% Triton X-100 (BioRad) in demi water (prepared at the VOBO department of the AMC) was added to the cells in the 96 well plate and incubated for 15 min at 37°C with 5% CO_2. The protein concentration was measured according to the manufactor instruction from the Pierce BCA (bicinchininic acid) protein assay kit (Thermo Fisher). Shortly, 12.5 µL of cell lysate were added to 100 µL of working reagent in an 96-well polysterene flat bootom plate and incubated for 30 min at 37°C protected from light. The absorbance at 562 nm was measured in the plate reader and the concentration of albumin was calculated based on a standard curve.

3.6 Calcium deposition assay

MC3T3-E1 cells were seeded in a 24 well plate (VWR) at concentration of $1x10^5$ cells/well and incubated at 37°C with 5% CO_2 until a confluenced layer was reached. Then, the cells were stimulated with α-MEM (control), osteogenic differention media (ODM; 50µg/mL of L-ascorbic acid (Sigma) and 10mM of β-glycerophosphate (Sigma)) (Langenbach and Handschel 2013), or 7.5, 15, 30 and 60 µg/mL of SAAP-148 for 14 and 21 days. All solutions were prepared in α-MEM supplemented with 2% of FBS and 1% of PenStrep. After each time point, the cells were washed twice with D-PBS and fixed in 4% paraformaldehyde for 15 minutes at room temperature. The fixative was removed and the cells were washed twice with demi water. Five hundred µL of filtered Alizarin Red S (40mM, Sigma) were added to each well and incubated at room temperature for 15 min with gentle shaking. The staining was washed 5 times with demi water, the water was removed and the cells were dryed and incubated at -20°C for at least 24 hours. The cells were defrosted and 400 µL of 10% acetic acid were added to each well and incubated at room temperature for 30 minutes with gentle shaking. The cells were collected and transferred to a microcentrifuge tube and vortexed for 30 seconds, followed by an incubation at 85°C for 10 min and 5 min on ice. The tubes were centrifuged at 20,000 g for 15 min. Two hundred µL of the supernatante were transferred to a new tube, to which 80 µL of 10% ammonium

hydroxide were added. Fifty µL aliquotes were transferred to a 96 well plate and the absorbance was measured at 405 nm in the plate reader. The amount of alizarin was calculated based on a standard curve.

3.7 Quantitative real time polymerase chain reaction (qPCR)

3.7.1 Cells stimulation

RAW 264.7 cells were seeded in a 24 well plate (VWR) with a concentration of $1x10^6$ cells/well and incubated at 37°C with 5% of CO_2 until a confluenced layer was reached. The cells were washed twice with D-PBS and stimulated with PBS (control) (He, Li et al. 2018), 20 ng/mL of LPS (Sigma) + 1 ng/mL of IFN-ɣ (StemCell) (He, Li et al. 2018), 2 ng/mL of IL-4 (StemCell) (He, Li et al. 2018), or 7.5, 15, 30 and 60 µg/mL of SAAP-148. All solutions were prepared in α-MEM supplemented with 2% of FBS and 1% of PenStrep. The cells were incubated for 1 and 5 days, with the medium changed after 3 days in the last group. After the stimulation period the cells were washed with D-PBS.

3.7.2 RNA extraction

The RNA was isolated with TRIzol reagent (Ambition) and purifyed with the Direct-Zol RNA MiniPrep kit (Zymo Research) according to the manufactor instructions. Briefly, after adding 290 µL TRIzol reagent to each well and verifying under the light microscope that the cells were lysed, 290 µL of ethanol (96%, filtered) were added to each well and mixed thoroughly. The mixture was transferred to a Zymo-Spin IICR column and centrifuged at 15,800 g for 30 seconds. Then, the RNA was washed twice with 400 µL of RNA pre-wash buffer and centrifuged at 15,800 g for 30 seconds. Next, the RNA is washed with 700 µL of RNA wash buffer and centrufuged at 15,800 g for 2 minutes. Finaly, the RNA was collected in a DNAse/RNAse free tube, by adding 50 µL of DNAse/RNAse free water and centrifuge at 15,800 g for 30 seconds.

After the RNA extraction, a DNAse treatment was performed by using the Turbo DNA-*free* kit (Invitrogen, Thermo Fisher) according to the manufactor instructions. Briefly, 5 µL of buffer, 2.8 µL of SUPERase-In RNAse inhibitor (Invitrogen) and 1.5 µL of DNAse was added to 50 µL of the RNA solution and incubated at 37°C for 30 min. Another 1.5 µL of DNAse were added and the samples were incubated at 37°C for another 30 min. Then 10 µL of DNAse inactivation agent were added and incubated for 5 min at room temperature, followed by a centrifugion at 10,000 g for 1.5 min. The supernatant was taken to a new RNAse free tube and the pellet was discarded. Finally, electrophoresis in a 1% agarose gel was performed in order to detect any residual genomic DNA still present.

3.7.3 cDNA synthesis

The amount of RNA was quantified in the Take3 Trio micro-volume plate function from the plate reader. The RNA purity was assessed through the determination of 260 nm/280 nm ratio, and only samples with a ration between 1.8 to 2.0 were used. The cDNA was synthesized according to the manufactor instructions from the SuperScript IV kit (Invitrogen, Thermo Fisher). Briefly, for an input of 1.0 µg of RNA it was added 1 µL of Random hexamers, 1 µL of Oligo d(T) and 2 µL of 10 mM dNTP mix was added, followed by an incubation at 65°C for 5 min, a centrifugion at 10,000 g for 10 seconds and an incubation for 1 min on ice. Then, 4 µL of 5x SSIV buffer, 1 µL of 0.1 mM DDT, 1 µL RNAse inhibitor, 1 µL MQ water and 1 µL SuperScript reverse transcriptase or 1 µL MQ water as a negative control were added. The mixture was incubated at 23°C for 10 min, followed by 45 min at 50°C and 5 minutes at 85°C. Finally, 1 µL of RNAse H was added and incubated at 37°C for 20 min.

3.7.4 Polymerase chain reaction (PCR)

As a control for the cDNA synthesis, the negative controls went through a PCR reaction for one of the reference gene, β-actin (Table 2), to confirm the lack of RNA. For the PCR reaction, the Go Taq PCR core system kit (Promega) was used according to the instructions from the manufactor. Briefly, 0.5 µL of the forward primer (10 µM), 0.5 µL of the reverse primer (10 µM), 0.5 µL of dNTP mix (10 mM), 2.5 µL $MgCl_2$ (25 mM), 5 µL Buffer green (5x), 0.12 µL Taq polymerase and 14.88 µL MQ water were added to 1 µL of cDNA. The samples were placed in the thermocycler (T3, Biometra) with the following program: initial denaturation at 95°C for 2 min, followed by 30 cycles of denaturation at 95°C during 30 seconds, anneling at 55°C during 30 seconds and extension at 72°C during 30 seconds, followed by a final extension at 72°C during 5 min.

3.7.5 qPCR

The LightCycler FastStart DNA Master SYBR Green I kit (Roche) was used according to the manufactor instructions. Briefly, 3 µL MQ water, 0.5 µL of primer forward (10 µM), 0.5 µL of primer reverse (10 µM) and 5 µL of Sybr green were added to 1 µL of 200 ng of cDNA in a 384 well plate (4titude). The plate was placed in the Thermal cycler (C100 Touch, CFX384 Real-Time System, Bio-Rad) with the following program: a pre-incubation at 95°C for 5 min, followed by 45 cycles of denaturation at 95°C for 10 seconds, anneling at 55°C for 10 seconds and extension at 72°C for 20 seconds. After each cycle, the level of flurescence was measured. For the melting curve the plate was at 95°C for 10 seconds followed by 65°C for 1 minute and with acquisition of data at 95°C.

3.7.6 Primers

Table 2 shows the primers used, designed using Primer-Blast (Ye, Coulouris et al. 2012), except for iNOS and β-actin that were retrieved from (He, Li et al. 2018). As reference genes for the RAW 264.7 cells were used β-actin, GADPH and HMBS (Bao, Huang et al. 2019) were used.

Table 2 - List of primers used in qPCR for RAW 264.7 cells.

Gene	**Primer sequence**		**Access code for NCBI or Reference**
iNOS	Forward	CAAGCTGAACTTGAGCGAGGA	(He, Li et al. 2018)
	Reverse	TTTACTCAGTGCCAGAAGCTGGA	
TNF-α	Forward	CCACGTCGTAGCAAACCAC	NM_013693.3
	Reverse	ACAAGGTACAACCCATCGGC	
CCR7	Forward	TGTACGAGTCGGTGTGCTTC	NM_007719.2
	Reverse	CCCACGAAGCAGATGACAGA	
Arg I	Forward	ATGGGCAACCTGTGTCCTTT	NM_007482.3
	Reverse	TTCCCCAGGGTCTACGTCTC	
CD206	Forward	GTGGACGCTCTAAGTGCCAT	NM_008625.2
	Reverse	GAATCTGACACCCAGCGGAA	
TGF-β	Forward	CTGCTGACCCCCACTGATAC	NM_011577.2
	Reverse	AAAGCCCTGTATTCCGTCTCC	
β-actin	Forward	CTCTTTTCCAGCCTTCCTTCTT	(He, Li et al. 2018)
	Reverse	GAGGTCTTTACGGATGTCAACG	
GADPH	Forward	TGTGAACGGATTTGGCCGTA	NM_001289726.1
	Reverse	ACTGTGCCGTTGAATTTGCC	
HMBS	Forward	ATGGCTCAGATAGCATGCAA	NM_013551.2
	Reverse	GGGCTCCTCTTGGAATGTTA	

3.8 SAAP-148 release from the PLGA coatings *in vitro*

For coating A, samples with a PLGA coating, samples with 1, 2 and 4 layers of 3D-printed PLGA coating containing SAAP 148. The samples were previously sterilized by gamma radiation. The samples were transferred into a new 12 well plate (Costar), sealed and incubated in PBS at 37°C. The supernatant was collected and replaced with fresh PBS at 1, 2, 4, 6, 24, 48, 72, 96 and 168 hours. The amount of SAAP-148 released from the coating was quantified by measuring the absorbance at 560 nm of 1:1 (v/v) of eluate and BCA working reagent from the Pierce BCA Protein assay kit after a 24 hour incubation at 37°C. The amount of SAAP-148 was calculated based on a standard curve. The eluates from the release were kept at -20°C for further analysis.

For coating B, samples with PLGA coating, samples with 1, 2 and 4 layers of 3D-printed PLGA coating containing SAAP-148 and samples produced by hand were

previously prepared, and sterlized with UV radiation for 45 minutes. The samples were transferred into a new 24 well plate (Costar), sealed and incubated in PBS at 37°C and 100 rpm in a humid atmosphere. The supernatant was collected and replaced with fresh PBS at 1, 24, 48, 72, 96, 144, 264 and 384 hours. The amount of SAAP-148 released from the coating was quantified by measuring the absorbance at 560 nm of 1:1 (v/v) of eluate and BCA working reagent from the Pierce BCA Protein assay kit after a 24 hours incubation at 37°C. The amount of SAAP-148 was calculate based on a standard curve. The eluates from the release were kept at -20°C for further analysis.

3.9 Antimicrobial activity of SAAP-148 released from PLGA coating *in vitro*

For coating A, the logarithmic phase inoculum in TSB was pelleted, washed twice with PBS and resuspended in RPMI and diluted in RPMI to $1x10^6$ CFU/mL, based on the OD_{620nm}. In a 96-wells polypropylene round bottom plate, 10 µL of the $1x10^6$ CFU/mL inoculum was added to 90 µL of eluates from the release assay or 90 µL of RPMI as a control. The plates were incubated overnight at 37°C and 120 rpm in a humid atmosphere. The number of viable bacteria was determined by quantitative cultures in blood agar plates.

To evaluate the remaining activity of the coating (2 cm diameter) after the release period of 168 hours, a modified version of the Japanese Industrial Standard test for surface microbicidal activity (JIS Z 2801:2000, (Association 2000)) was used. The logarithmic phase inoculum in TSB was pelleted, washed twice with PBS and resuspended in PBS with 1% of RPMI and diluted in PBS with 1% of RPMI to $5x10^5$ CFU/mL, based on the OD_{620nm}. Seventy-one µL of inoculum was placed on the middle of the coating ($3.55x10^4$ CFU/material) and covered with a sterile parafilm disc (2 cm diameter) to maximize the contact between the inoculum and the coating's surface. The samples were incubated at 37°C in a humid atmosphere for 24 hours. Subsequently, the samples were placed in 1.5mL PBS and vortexed for 30 seconds, sonicated in the water bath for 15 min (Elma Transsonic 460, frequency 35 kHz, Elma Schmidbauer GmbH) and vortexed again. A 100 µL aliquot was transferred to a 96 well polystyrene flat bottom plate and 10-fold serial dilutions were made and 10 µL droplets were plated on blood agar plates.

For coating B, the logarithmic phase inoculum in TSB was pelleted, washed twice with PBS and resuspended in RPMI and diluted in RPMI to $1x10^6$ CFU/mL, based on the OD_{620nm}. In a 96-well polypropylene round bottom plate, the eluates from the release assay were serial 2- to 2048-fold diluted in PBS. Ten µl of the $1x10^6$ CFU/mL inoculum were added to 90 µl of undiluted and diluted eluates from the release or 90

µL of PBS as a control. The plates were incubated overnight at 37°C and 120 rpm in a humid atmosphere. The number of viable bacteria were determined by quantitative cultures.

To quantify the SAAP-148 remaining in the coatings after the release assay, the samples were placed in 1.5 mL PBS and vortexed for 30 seconds, sonicated for 15 min and vortexed again. A 100 µL aliquot was place in a 96 well polypropylene round bottom plate and the peptide amount was measured by reading the absorbance at 560 nm of 1:1 (v/v) of eluate and BCA working reagent from the Pierce BCA Protein assay kit after a 24 hours incubation at 37°C. The amount of SAAP-148 was calculate based on a standard curve.

3.10 Statistical analysis

All data are expressed as mean ± standard deviation. Statistical analysis was performed with GraphPad Prism (GraphPad Software, version 8.0.2) using the Shapiro-Wilk test to assess the normal distribution of the results, and when shown to be normally distributed followed by the two way ANOVA test with the Tukey's test for multiple comparissons. The differences between the groups were considered statistacally significant when $p \leq 0.05$.

Chapter 4

4 Results

4.1 *In* vitro antimicrobial activity of SAAP-148

The sterilization of coatings can have an effect on its components that may lead to their inactivation. Therefore, to assure that the sterilization method used on the coatings from coating A, in this case gamma radiation, would not interfer with the antimicrobial activity of SAAP-148, the antimicrobial activity was assessed using the MIC and LC 99.9% assays.

Table 3 - Antimicrobial activity of SAAP-148 against *S. aureus* JAR 060131. Results are expressed as minimal inhibitory concentration (MIC), i.e. the lowest peptide concentration without visible growth and the lethal concentration (LC) 99.9, i.e. the lowest peptide concentration that kills ≥99.9% of the bacteria within 24 hours. The results represent the average and the range of three independent experiments

		MIC		LC 99.9	
		µM	µg/mL	µM	µg/mL
	SAAP-148	3.75	12.25	3.75	12.25
gamma radiated	SAAP-148 powder	3.75 (3.75-7.50)	12.25 (12.25-24.50)	3.75 (3.75-7.50)	12.25 (12.25-24.50)
	SAAP-148 solution	3.75 (1.88-3.75)	12.25 (6.14-12.25)	3.75 (3.75-7.50)	12.25 (12.25-24.50)

The concentration of SAAP-148 necessary to inhibit or to kill 99.9% of the inoculum remains simillar after gamma radiation when compared to the non-irradiated SAAP-148, both when radiated in powder or solution (Table 3). To evaluate if the gamma radiation led to a delay for the peptide to achive the LC 99.9% a time killing assay was performed.

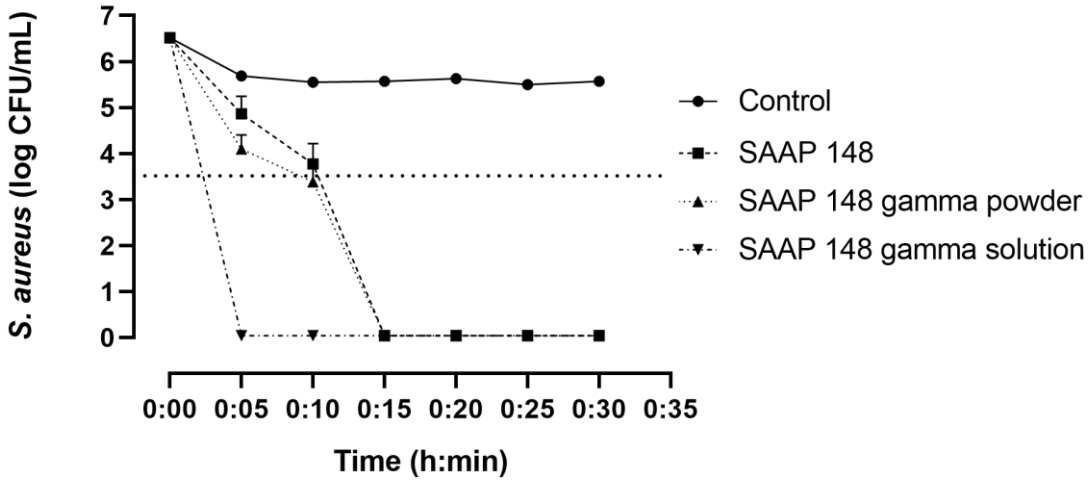

Figure 17 - Time killing assay. *S. aureus* JAR 060131 was challenged with a concentration corresponding to the LC 99.9% value of SAAP-148 concentration (i.e. 3.75 µM). As a control the bacteria were incubated with RPMI without peptide. The dotted line represents a 3-log reduction of the initial inoculum.

Gamma radiation does not reduce the peptide's activity over time (Figure 17). The same amount of time (<15 min) is necessary for both the irradiated and for the non-irradiated SAAP-148 to virtually kill all bacteria. It is, then, possible to conclude that using gamma radiation as a sterilization process for the coatings containing SAAP-148 will not affect the petide's activity.

FBS is an important supplement in media for cell cultures, because it provides growth factors and cytokines that support cellular growth. However, FBS also contains a variety of proteins that can inactivate SAAP-148. Therefore, a MIC and LC 99.9% assay was performed to establish the percentage of FBS that can be used for culturing cell without compromising the antimicrobial activity of SAAP-148.

Table 4 - Antimicrobial activity of SAAP-148 against *S. aureus* JAR 060131 in α-MEM media. The results express the MIC and LC 99.9%, i.e. the lowest peptide concentration needed to visually inhibit bacterial growth and the lowest peptide concentration needed to kill ≥99.9% of the inoculum, respectively.

	MIC		LC 99.9	
	µM	µg/mL	µM	µg/mL
α-MEM	0.94	3.07	1.88-3.75	6.14-12.25
α-MEM + 1% FBS	0.94	3.07	0.94	3.07
α-MEM + 2% FBS	0.94	3.07	1.88	6.14
α-MEM + 5% FBS	1.88 (0.94-1.88)	6.14 (3.07-6.14)	3.75 (0.94-3.75)	12.25 (3.07-12.25)

Addition of 1% of FBS shows the same MIC for SAAP-148 (0.94µM | 3.07µg/mL) as medium without addition of FBS and the LC 99.9% is even lower (Table 4). For the addition of 2% of FBS, both the MIC and the LC 99.9% are the same as for α-MEM without FBS. When 5% of FBS was added to the medium, the MIC is higher than the one from the control without FBS while the LC 99.9% is the same, however, there is a big variation in the results for the LC 99.9%. Thus, an addition of 2% FBS to the culture media is the best compromise between peptide activity and support for cellular grwoth (Puylaert 2018).

4.2 Influence of SAAP-148 on cell proliferation

Before stimulating the cells for futher analysis it is necessary to determine how different concentrations of SAAP-148 affects proliferation of the RAW 264.7 and MC3T3-E1 cells.

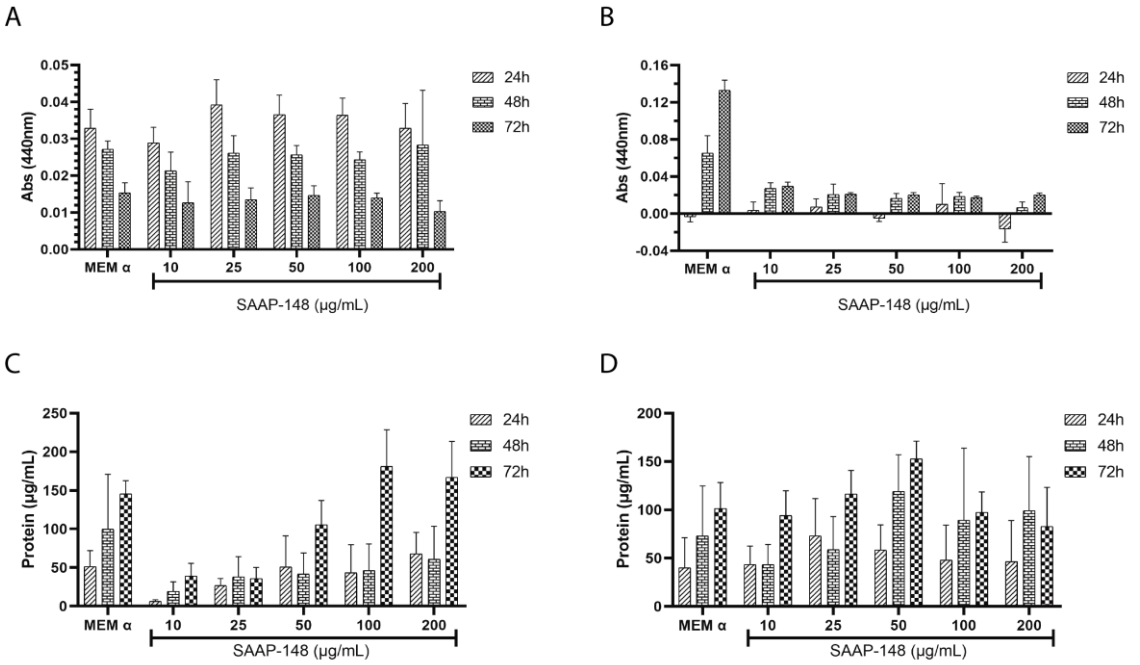

Figure 18 – Conversion of WST-1 into formazan by mitochondrial dehydrogenase as proliferation indicator after 24h, 48h and 72h for the cell lines (A) MC3T3-E1 cells and (B) RAW 264.7 cells. Colorimetric detection of protein concentration with the BCA assay in the cell lines (C) MC3T3-E1 cells and (D) RAW 264.7 cells, based on a standard curve (Supplementary Figure 1).

Tetrazolium salts are converted into formazan by the mithochondrial dehydrogenase from the cells. An increase in the amount of active cells results in a higher enzymatic activity which leads to higher amounts of formazan over time. SAAP-148 does not affect the proliferation of osteoblasts percursors MC3T3-E1 cells, because all the time points there is no significant differences between the samples with peptide and the control without peptide (α-MEM) (Figure 18A). Over time, there is a reduction in the converstion of WST-1 to formazan for all concentrations of SAAP-148 as well as for the control.

Macrophages are a type of cells that are present in many different tissues. Therefore, these cells have a good ability to adapt to different environements. Thus, in order to keep the same conditions for both cell lines, RAW cells were also incubated in α-MEM instead of the typically used RPMI medium. RAW 264.7 cells presented a very low activity during the first 24 hours with no significant differences between cells incubated with the peptide and the control (Figure 18B). However, there are significant diffrences between the highest peptide concentration of 200 µg/mL and the lower concentrations of 10, 25 and 100 µg/mL (p=0.090, p=0.0009 and p=0.0001, respectively). At 48 and 72 hours, the cells showed to recover, especially in the control. Nevertheless, SAAP-148 has a negative impact on the RAW cells proliferation, since

there is a significant difference between the samples with peptide and the control (p<0.0001 for all comparisons) at 48 and 72 hours. The increase in formazan concentration over time suggests that the cells need some time to adapt to a new environment, including in the presence of SAAP-148.

For protein quantification in MC3T3-E1 cells, an increase in protein concentration can be observed with the increase of SAAP-148 concentration and over time (Figure 18C). At 24 hours there are no significant differences between samples, while at 48 hours there is a significant higher protein concentration in the control when compared to the 10 µg/mL as well as 25 µg/mL of SAAP-148 (p=0.0017 and p=0.0317, respectively). At 72h, 10 µg/mL and 25 µg/mL of SAAP-148 are also showing significantly lower protein concentration compared to the control (p<0.0001). Hundred µg/mL and 200µg/mL of SAAP-148 gave significantly higher protein concentration compared to the remaining concentrations (p<0.0001 for 10 µg/mL and 25 µg/mL, while for 50 µg/mL the p values are 0.0039 for 100 µg/mL and 0.0328 for 200 µg/mL).

The RAW 264.7 cells show an increase in protein concentration over time in all concdition (Figure 18D). Similar to MC3T3-E1 cells, at 24 hours there are no significant differencenes in protein concentration between the different samples concentrations. At 48 and 72 hours the concentration of 50 µg/mL of SAAP-148 shows significant higher protein concentrations compared to the other conditions. Therefore, at 48 hours the concentration of 50 µg/mL is significantly different of α-MEM, 10 µg/mL, 25 µg/mL and 100 µg/mL SAAP-148 (p=0.0235, p=0.0006, p=0.0120 and p=0.0344, respectively), while at 72 hours the concentration of 50 µg/mL is significantly higher from 10 µg/mL and 200 µg/mL SAAP-148 (p=0.0425 and p=0.0076, respectively).

In short, SAAP-148 has a negative influnce on RAW 264.7 cells proliferation, therefor in the follow assays it was used low range concentrations of SAAP-148.

4.3 Calcium deposition assay

The main goal of a coating for orthopedic devices is to prevent infection and to potenciate osteointegration. Therefore, it is important to study how SAAP-148 affects the bone matrix deposition. To assess this matrix deposition, MC3T3-E1 cells exposed to graded concentrations of SAAP-148 were stained with Alizarin Red S, which binds to calcium phosphate, which is a vital component in the bone matrix.

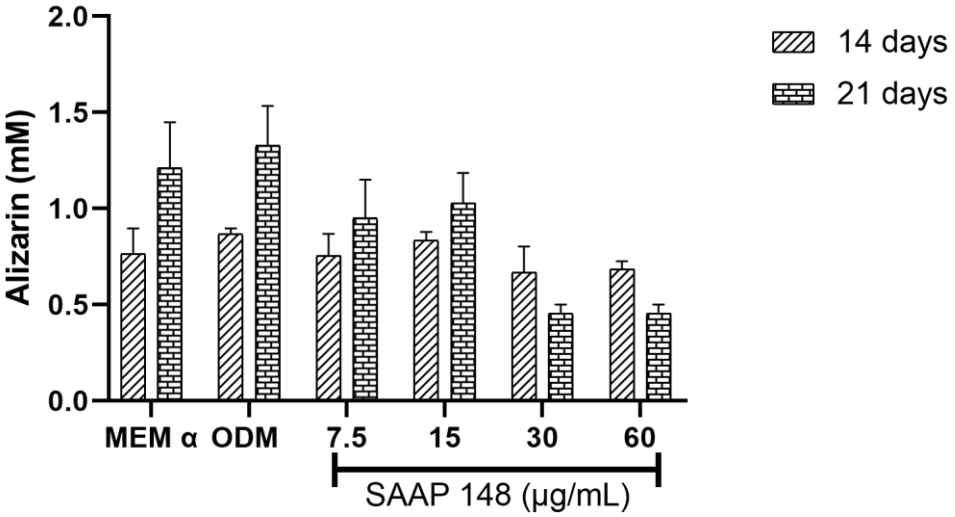

Figure 19 - Quantification of alizarin from MC3T3-E1 cells based on a standard curve with spectrophotometry at 405nm (Supplementary Figure 2).

There is an increase of calcium deposition over time for the controls and the lower concentrations of SAAP-148, while the the higher concentrations of SAAP-148 verified a reduction of calcium deposition (Figure 19). At 14 days there are no significant differences between all conditions. At 21 days, there is no significant difference between α-MEM and ODM (control for osteogenic differentiation of osteoblasts percursors), but the concentrations of 30 µg/mL and 60 µg/mL of SAAP-148 heve induced significantly lower calcium deposition compared to both α-MEM (p=0.0014, for both conditions) and ODM (p=0.0004, for both conditions). Overall, SAAP-148 interferes with the calcium deposition of MC3T3-E1 cells over timer at the higher concentrations (30µg/mL and 60µg/mL). In contrast, the lower concentrations (7.5µg/mL and 15µg/mL) of the peptide do not significantly reduce the calcium deposion.

4.4 qPCR

Macrophages are cells that are present in the fracture site and produce cytokines and chemokines that will determine the orientation of the inflammatory response as well as the success of the implant's integration. Therefore, RAW 264.7 cells were stimulated with a range of SAAP-148 concentrations and compared to controls for unstimulated cells (i.e. PBS), inflammatory stimulation (i.e. LPS and IFN-ɣ) and anti-inflammatory stimulation (i.e. IL-4).

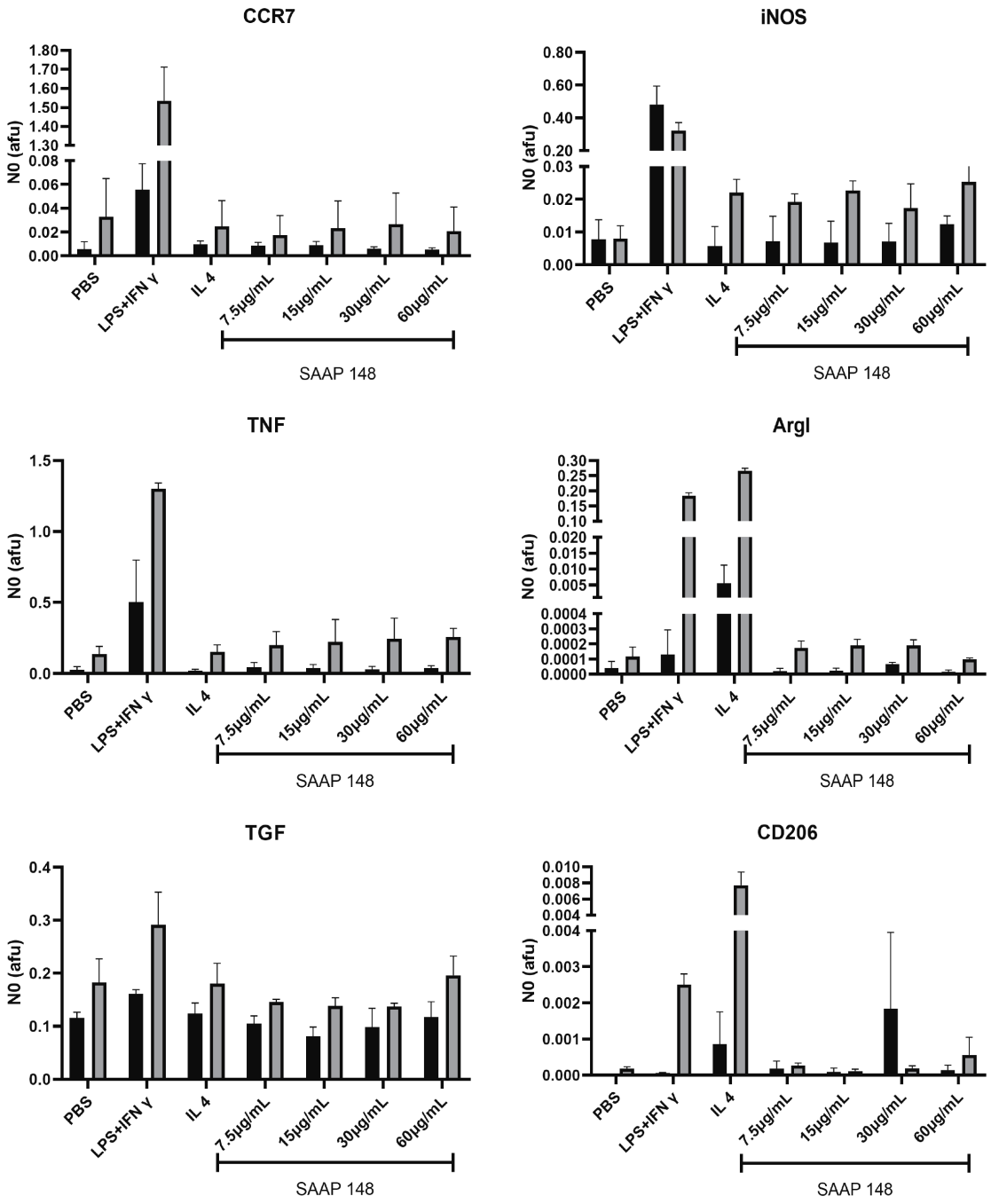

Figure 20 - RAW 264.7 cells gene expression of CCR7, iNOS, TNF-α, Arg I, TGF-β and CD206. The black bars represent the 1-day time point, while the grey bars represent the 5-days time point.

The gene expression of the inflammatory markers (nitric oxide synthase (iNOS), tumor necrosis factor alpha (TNF-α) and C-C chemokine receptor type 7 (CCR7)) and the anti-inflammatory markers (arginase I (Arg I), cluster of differentiation 206 (CD206) and transforming growth factor beta (TGF-β)) in RAW 264.7 cells at 1 and 5 days show all an increase over time (Figure 20).

For the inflammatory makers, iNOS, TNF-α and CCR7, the cells stimulated with LPS and IFN-ɣ have a significant higher expression than the other conditions in at both time points (p<0.0001).

At 1 day the cells stimulated with IL4 were significantly higher expressing Arg I than in the other conditions (p<0.0001, for all conditions). At 5 days, both cells stimulated with LPS and IFN-ɣ and cells stimulated with IL4 have a significant higher expression than the other conditions (p<0.0001, for all conditions). The peptide concentration of 60 µg/mL at 5 days is showing a higher Arg I concentration than the other concentrations, however the difference is not significant.

Cells stimulated with IL4 have a higher expression of CD206 than the other conditions (p<0.0001, for all conditions) at both time points. At 1 day, cells stimulated with LPS and IFN-ɣ also have a significant higher expression of CD206 than the other conditions (α-MEM, p=0.0026; 7.5 µg/mL SAAP-148, p=0.0013; 15 µg/mL SAAP-148, p=0.0010; 30 µg/mL SAAP-148, p=0.0012 and 60 µg/mL SAAP-148, p=0.0026).

Cells stimulated with LPS and IFN-ɣ have significant higher expression at 1 day of TGF-β from every condition except cells stimulated with IL4, while cells stimulated with IL4 are only significant higher expression than 15 µg/mL and 60 µg/mL SAAP-148 (p=0.0010 and p=0.0026, respectively). At 5 days, cells stimulated with LPS and IFN-ɣ have significantly higher expression of TGF-β when compared to every other condition.

4.5 SAAP-148 release from PLGA coatings *in vitro*

Before testing a coating in combination with cells, it is important to characterize the coating, such as performing release profiles. Thus, a release assay was performed for both PLGA-SAAP-148 coatings from both bioink formulations (coating A and coating B).

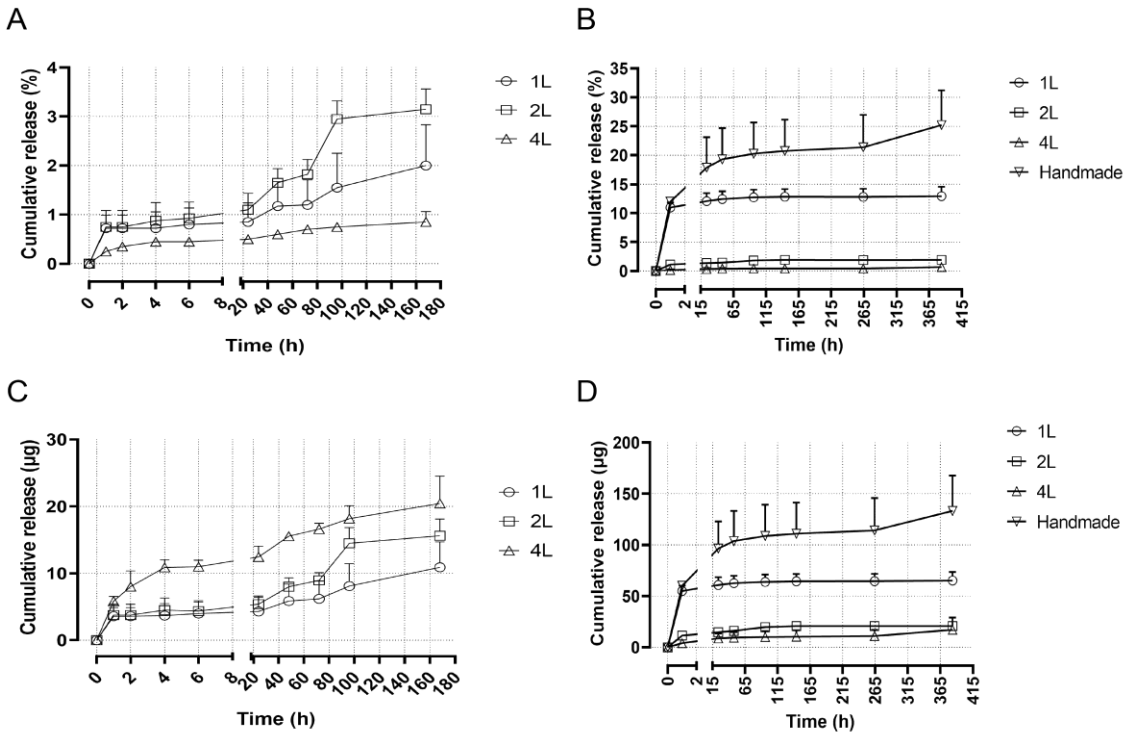

Figure 21 - Release profiles of SAAP-148 from PLGA coatings in PBS. (A) and (C) represent the cumulative release of SAAP-148 from coating A in percentage from the total amount of peptide in the coating and in µg, respectively. (B) and (D) represent the cumulative release of SAAP-148 from coating B in percentage from the total amount of peptide in the coating and in µg, respectively. 1L, 2L and 4L represents samples with one, two and four layer(s) of coating, respectively. Handmade represents samples that the coating was not made by the 3D printer. The calculations were based on standard curves (Supplementary Figure 3 and Supplementary Figure 4).

Coating A has an ineffective release, since after 168h (7 days) the highest release was 3.15% from the two-layers coating, followed by the one-layer coating with 2% of release and the four-layers coating with 0.85% of peptide release (Figure 21A). These results show a very slow release of the peptide from the PLGA matrix over time. A higher amount of peptide is released from coatings with more layers and therefore more peptide (4L, 20.45µg; 2L, 15.61µg and 1L, 10.90µg) (Figure 21).

Coating B shows a higher release from the handmade coatings, which is accompanied by bigger variations (Figure 21B). For the 3D-printed coatings, the release increases with the decrease of number of layers. Thus, after 384h (16 days) the highest release is from the handmade coatings (25.2%), followed by one-layer (12.93%), two-layers (1.93%) and four-layers (0.7%) coatings. The same tendency that the cumulative release is shown in the percentages (handmade (133.32µg) > one-layer (65.31 µg) > two-layers (20.78µg) > four-layers (17.21µg)).

Comparing coating A (Figure 21 A) with coating B (Figure 21 B), the difference in the production process increased the release only for one-layer coating, which passed from 2% to 12.8% after 7 days. For the two and four-layers coatings, coating B shows a slower release than coating A (3.15% to 1.93% and 0.85% to 0.43%, respectively).

4.6 Antimicrobial activity of SAAP-148 released from PLGA coating *in vitro*

4.6.1 Coating A

The eluates retrieved from the release assay were challenged with *S. aureus* JAR 060131 overnight and subsequently plated on blood agar plates. The bacteria were capable to fully grow in all conditions, with no reduction observed in any sample. In this way it was proved that there was not enough active peptide in each time point to reduce the number of bacteria.

Since the eluates from the release assay did not showed any activity, it was verified if the SAAP-148 in the PLGA matrix was still active against bacteria adhering to the surface after the release assay, using a modified version of the JIS Z 2801:2000 test.

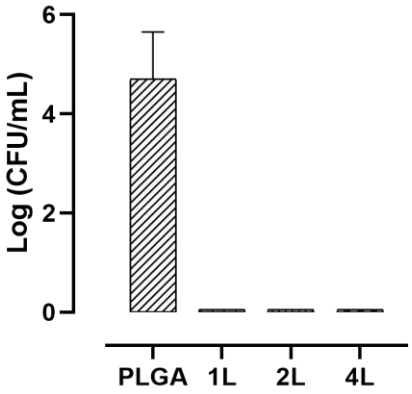

Figure 22 – JIS Z 2801:2000 assay of samples with coating A. The antimicrobial activity of the surface was assessed against *S. aureus* JAR060131 for 24h. PLGA represents the samples with the coating without SAAP-148; 1L, 2L and 4L represent the samples with one layer, two layers and four layers of the coating with SAAP-148, respectively. The samples value for Log (CFU)=0 had no growth; they are represented only for graphic visualization.

All the coatings with SAAP-148 have antimicrobial activity against *S. aureus* JAR060131 (Figure 22). These results corroborate the hypothesis that the peptide trapped in the PLGA matrix is still active.

In short, coating A did not release peptide in sufficiently high enough concentrations in the eluate to reduce the number of bacteria, but did shown surface antimicrobial activity.

4.6.2 Coating B

The eluates retrieved from the release assay were diluted and incubated over night with *S. aureus* JAR060131 to assess their microbicidal activity.

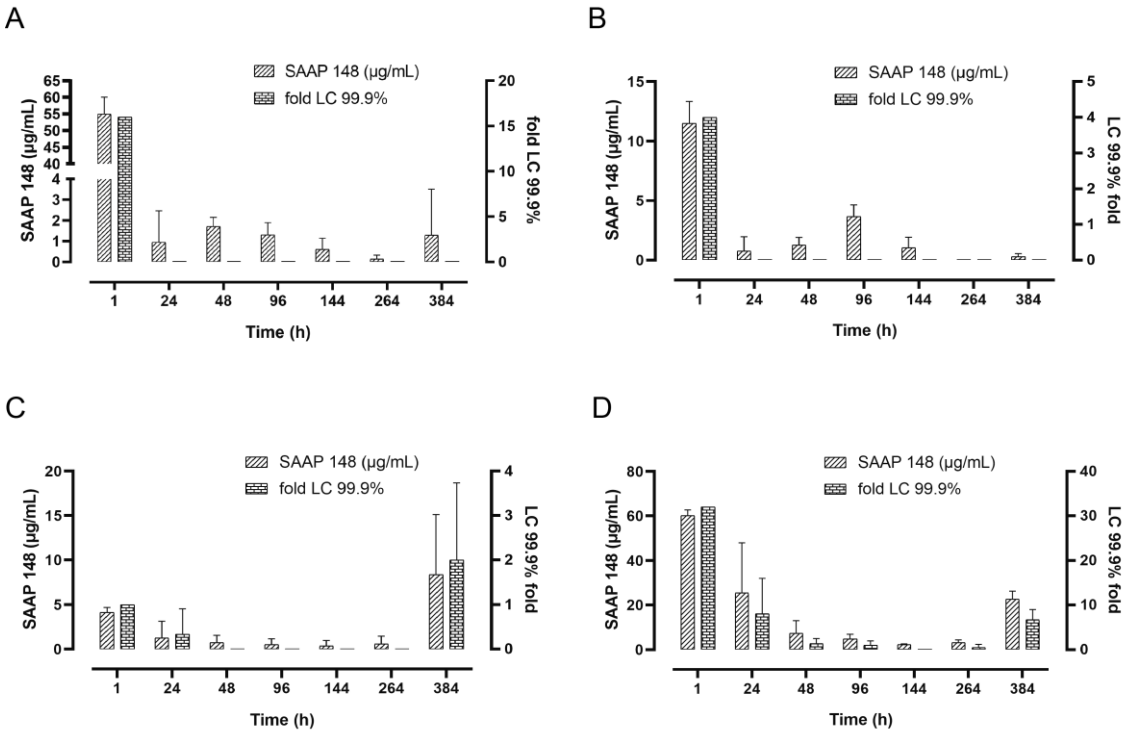

Figure 23 - Antimicrobial activity of eluates from coating B against *S. aureus* JAR060131. The graphs show the peptide concentration in the undiluted eluates for each time point and until which fold is possible to dilute and still kill ≥99.9% of the inoculum. (A) Samples with 1-layer coating. (B) Samples with 2-layers coating. (C) Samples with 4-layers coating. (D) Samples with handmade coating. The samples with LC 99.9%-fold with the value of zero had bacterial growth even in the undiluted sample, they are represented only for graphic visualization.

According to the Figure 23 A and B, for samples of one and two-layers coating only the eluate from the first hour of release has antimicrobial activity. However, these eluates presented an activity corresponding to 16 and 4-fold LC 99.9 concentration, respectively. Figure 23 C, representing the samples with four-layers coating, shows microbicidal activity in the eluates from 1 and 24 hours, where the peptide concentration equals the LC 99.9. At 384 hours (16 days), the samples seem to be starting a new burst of peptide release. With the increase of peptide concentration there is an increase in the antimicrobial activity reaching 2-fold of the LC 99.9. The handmade coating samples are represented in Figure 23 D, in which the eluates show antimicrobial activity in all the time points, with the exception for 144 hours (6 days). At 1h, with the initial burst of SAAP-148 release, the antimicrobial activity corresponds to 32-fold of the LC 99.9 concentration. After the first hour there is a decrease of the

peptide released as well as of the antimicrobial activity until 144 hours. At 264 and 384 hours there is an increase of peptide concentration together with an increase in the antimicrobial activity.

After characterizing the eluates from the release, it was estimated if still was SAAP-148 trapped in the coating (Figure 24) after sonicating and vertexing the materials.

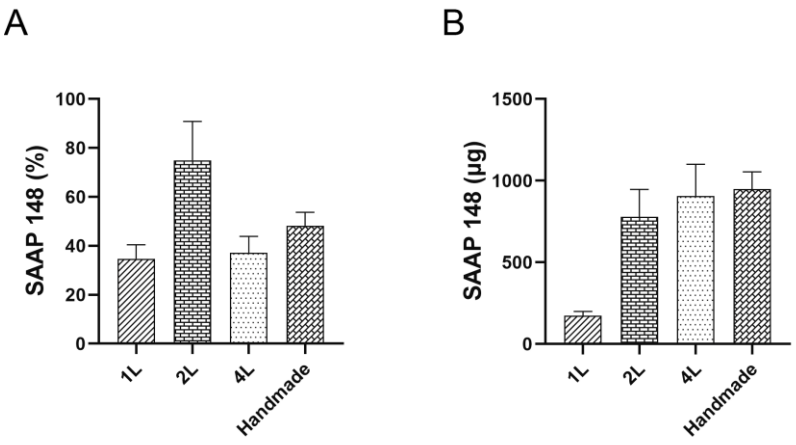

Figure 24 - Quantification of SAAP-148 in the PLGA coatings in percentage and in µg. The calculations were based on a standard curve (Supplementary Figure 5).

Figure 24 B shows that high amounts of SAAP-148 are still trapped in the PLGA coating. However, Figure 24 A shows that the peptide retrieved from the coating is a relatively small percentage for one and four-layers coatings as well as for the handmade coating (34.7%, 37.1% and 48.2%, of the incorporated amount, respectively). In contrast, for the two-layers coating samples, it was possible to retrieved a higher percentage of peptide (74.25%) from the PLGA matrix.

Chapter 5

5 Discussion

Bone fractures are a very common injury that, if not treated properly, can lead to infections and permanent disabilities. Therefore, there is a need for materials that are able to prevent and fight infections as well as enhance the bone healing. As a solution to this problem, in this work the antimicrobial peptide SAAP-148 in solution as well as incorporated in 3D-printed coatings of PLGA and SAAP-148 is studied.

5.1 Cell proliferation

The results from the WST-1 cell proliferation assay are not fully corroborated by the results from the protein quantification assay (Figure 18). One reason may be the presence of SAAP-148 intracellularly or bound to the cellular membrane, leading to higher protein concentration due ti the presence of the peptide itself. BCA is a colorimetric system where the number of peptide bonds, structure and the presence of amino acids such as cysteine, cystine, tryptophan and tyrosine are responsible for formation of color (Wiechelman, Braun et al. 1988). The peptide SAAP-148 has two tryptophans and one tyrosine in its primary stucture, as well as 23 peptide bonds, which means that if the peptide is present intracellularly or on the membrane, once the cells are lysated the peptide gets accesible to the BCA and therefore, there is a deviation of the results, i.e. a higher protein concentration than can be expected from the cells present.

In short, SAAP-148 has a negative effect on RAW 264.7 cells proliferation, especially at the long term. However, the peptide does not have a significative effect on

the proliferation of MC3T3-E1 cells. This is positive in view that in presence of SAAP-148 bone cells can still proliferate and therefore the peptide would not interfere with the bone regeneration. On the other hand, the presence of SAAP-148 negatively affects RAW 264.7 cells proliferation, which would be problematic, because it would compromise the number of macrophages around the implant and also the immune response to an infection. However, due to the differences between the two cell proliferation assays other viability assays should be performed in order to confirm the results obtained, e.g. a MTT assay, which is based on the same principle than the WST-1 or ATP assay, which measure ATP using firefly luciferase (Riss, Moravec et al. 2004). In addition, in this work was used cell lines, which are prone to mutations (Verma and Singh 2013) and therefore the responses from the cells to the peptide can be misleading, so, in order to get closer to the real system primary cells should be used (Verma and Singh 2013).

5.2 Calcium deposition assay

Higher, higher concentrations of SAAP-148 result in a significant reduction in calcium deposition by MC3T3-E1, with a decrease over time (Figure 19). However, the highest concentration of SAAP-148 that does not provoke a significant reduction in calcium deposition is 15 µg/mL, which is still higher than the concentration needed for killing (LC 99.9%, 12.25 µg/mL, Table 3). These results, suggest that the peptide is capable to maintain its antimicrobial activity without compromising the calcium deposition. However, local high concentration might reduce calcium deposition and should be avoided when designing an orthopedic implant coating.

5.3 qPCR

SAAP-148 does not promote a clear inflammatory or anti-inflammatory response, when looking at the gene expression of some inflammatory markers (Figure 20). However, cells stimulated by SAAP-148 have an expression profile of inflammatory markers closer to cells stimulated with IL4, representing M2 type of macrophages, than cells stimulated with the combination of LPS and IFN-ɣ, representing M1 type of macrophages. As for the expression profile of anti-inflammatory markers, cells stimulated with SAAP-148 are a more similar to non-stimulated cells. Unexpectedly, the cells stimulated LPS in combination with IFN-ɣ also present a high expression at 5 days, which is due to the use of LPS as an activator (Novak and Koh 2013, Jablonski, Amici et al. 2015). This is positive in view that the use of SAAP-148 in coatings would not enhance the inflammatory response allowing a proper healing of the bone.

5.4 PLGA-SAAP-148 coatings

5.4.1 Coating A

Coating A does not have the required release, independently of the number of layers by which the coating is formed (Figure 21A and C). However, the coating surface presents antimicrobial activity (Figure 22), which leads to the conclusion that the peptide is still trapped inside the PLGA matrix. Thus, these coatings are contact killing surfaces, which are ideal for situations where adhesion of bacteria to the implants surface is a fundamental step for an infection and biofilm development and where sustained release of the peptide is not required or beneficial, such as devices for situations that involve a flow, like stents and catheters.

5.4.2 Coating B

The coating B handmade shows the best release profile, however, it also presented bigger variation between samples, which is negative for the design of orthopedic implant coatings. The one-layer coating shows the best release profile from the 3D-printed coatings, however, only sufficient peptide to kill 99.9% of bacteria is released in the first hour (Figure 23). The amount of peptide released in the first hour is 16-fold the LC 99.9% (Figure 23), which is enough to kill all bacteria, while still peptide is residing inside the coating (Figure 24). The coatings with 2 and 4-layers show a very slow release compared to the one-layer coating, revealing that even the peptide distributed over the surface in these coatings is having difficulties to release from the PLGA matrix. This may be due to the interactions between the SAAP-148 and the PLGA or the peptide may be sinking in the previous layers and therefore having more troubles releasing.

However, by combining the percentage of SAAP-148 released and to the percentage of peptide still in the coating it does not reaches the 100% for any of the coatings, revealing that the extraction of the peptide from the PLGA matrix did not occurred properly. Therefore, it is necessary to optimize the extraction process in order to also quantify the amount of peptide that is lost during the production of the coating.

In short, the formulation from coating B is a very promising for application in orthopedic implants, where the release of an antimicrobial agent, such as SAAP-148, is very benefic in order to clear any bacteria on the site of the implant, preventing the adhesion of bacteria to the implant or infection of the peri-implant tissue.

Chapter 6

6 Conclusions and future work

6.1 Conclusions

In this dissertation we aimed to study the modulatory and antimicrobial activity of the synthetic antimicrobial peptide SAAP-148 as a possible solution to be applied in orthopedic devices against infection.

It was studied the modulatory activity of SAAP-148 over macrophages (RAW 264.7 cells). It is possible to conclude that SAAP-148 stimulates the gene expression of inflammatory markers similar to alternative activated macrophages and the gene expression of anti-inflammatory markers similar to non-stimulated macrophages. Therefore, according to the markers studied in this dissertation SAAP-148 does not promote an inflammatory response, allowing the establishment of a pro-healing environment and the bone regeneration. It was also studied the influence of SAAP-148 on calcium deposition by osteoblasts precursors (MC3T3-E1 cells). It is possible to conclude that there is a range of concentrations (7.5 and 15 µg/mL) of SAAP-148 where the deposition of calcium was not affected. The concentration of 15 µg/mL is still sufficiently high to kill 99.9% of bacteria, since it is higher than the LC 99.9 concentration for this peptide.

In this dissertation it was studied the antimicrobial activity of two formulations (coating A and coating B) of PLGA-SAAP-148 bio-ink for 3D-printed coatings. From the release and antimicrobial assays, it is possible to conclude that the formulation of coating B is the most adequate for orthopedic implants, because of the demonstrated

activity of the released SAAP-148, preventing the adhesion of bacteria to the implant's and the infection of the peri-implant tissue.

In short, SAAP-148 is a very promisor peptide with good antimicrobial activity and potential modulatory activity. However, during a bone fractures osteoblasts and macrophages do not act independently, but belong to a system and react to changes in the environment. Therefore, more studies should be performed to understand the influence of SAAP-148 on the cross-talk between macrophages and osteoblasts and consequently on the bone healing process.

6.2 Future work

For future work it would be interesting to see the influence of SAAP-148 (free form and on coatings) on the cross-talk between macrophages and osteoblast using co-culture systems. With the co-culture systems it would be interesting to:

i. analyze the differences on gene expression of macrophages and osteoblasts and compare it with mono-cultures;

ii. analyze the cytokines and proteins secreted

iii. analyze the gene expression and polarization change of macrophages previously stimulated.

iv. study the effect of plasma and the effect of an infection on the system

Supplementary data

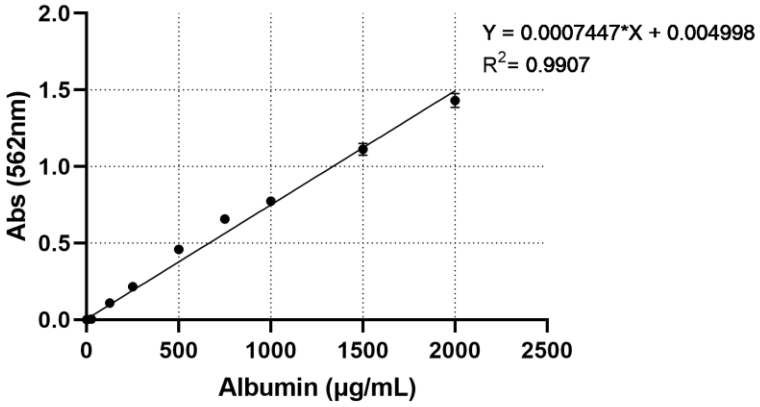

Supplementary Figure 1 - Standard curve for protein quantification.

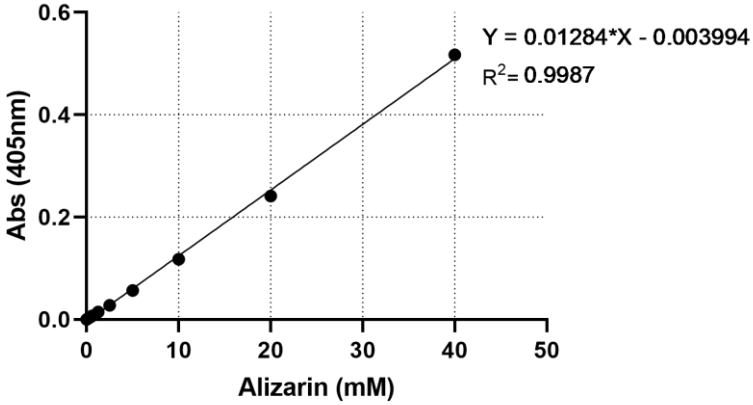

Supplementary Figure 2 - Standard curve for alizarin quantification

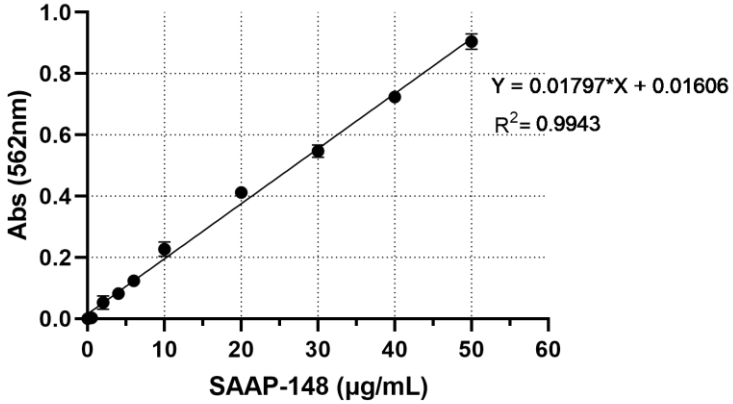

Supplementary Figure 3 - Standard curve for SAAP-148 quantification of the releases from coating A

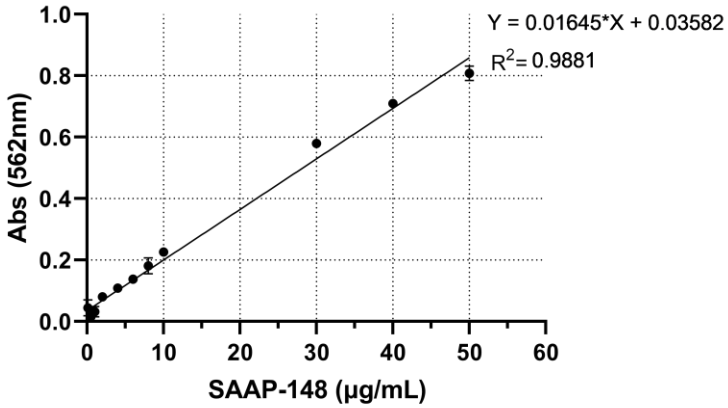

Supplementary Figure 4 - Standard curve for SAAP-148 quantification of the releases from coating 2

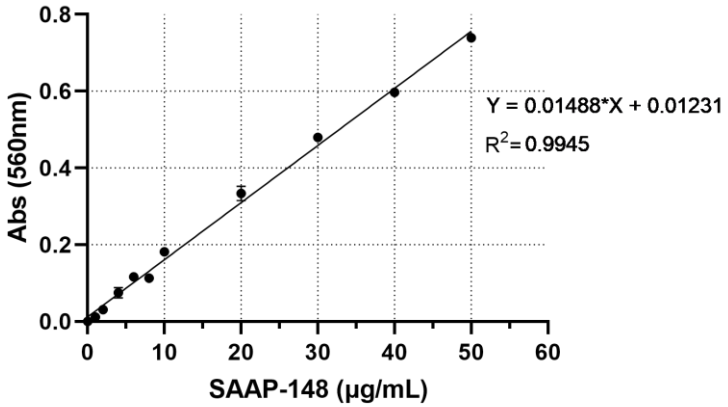

Supplementary Figure 5 - Standard curve for SAAP-148 quantification in coating B

References

Allan, C., A. Ker, C.-A. Smith, P. M. Tsimbouri, J. Borsoi, S. O'Neill, N. Gadegaard, M. J. Dalby and R. Dominic Meek (2018). "Osteoblast response to disordered nanotopography." Journal of tissue engineering **9**: 2041731418784098.

Andersson, D. I., D. Hughes and J. Z. Kubicek-Sutherland (2016). "Mechanisms and consequences of bacterial resistance to antimicrobial peptides." Drug Resistance Updates **26**: 43-57.

Arciola, C. R., D. Campoccia and L. Montanaro (2018). "Implant infections: adhesion, biofilm formation and immune evasion." Nature Reviews Microbiology **16**(7): 397-409.

Association, J. S. (2000). "JIS Z 2801:2000 Antimicrobial products - Test for antimicrobial activity and efficacy." Japanese Ind. Stand.

Baht, G. S., L. Vi and B. A. Alman (2018). "The role of the immune cells in fracture healing." Current osteoporosis reports **16**(2): 138-145.

Bang, S. M., H. J. Moon, Y. D. Kwon, J. Y. Yoo, A. Pae and I. K. Kwon (2014). "Osteoblastic and osteoclastic differentiation on SLA and hydrophilic modified SLA titanium surfaces." Clinical Oral Implants Research **25**(7): 831-837.

Bao, Z., Y. Huang, J. Chen, Z. Wang, J. Qian, J. Xu and Y. Zhao (2019). "Validation of Reference Genes for Gene Expression Normalization in RAW264. 7 Cells under Different Conditions." BioMed Research International **2019**.

Barlow, P. G., P. E. Beaumont, C. Cosseau, A. Mackellar, T. S. Wilkinson, R. E. Hancock, C. Haslett, J. R. Govan, A. J. Simpson and D. J. Davidson (2010). "The human cathelicidin LL-37 preferentially promotes apoptosis of infected airway epithelium." American journal of respiratory cell and molecular biology **43**(6): 692-702.

Bauer, M. E. and W. M. Shafer (2015). "On the in vivo significance of bacterial resistance to antimicrobial peptides." Biochimica et Biophysica Acta (BBA)-Biomembranes **1848**(11): 3101-3111.

Biomet. (2010). "LactoSorb® Resorbable Fixation System." Retrieved 23-10-2020, 2020, from https://www.zimmerbiomet.com/content/dam/zimmer-biomet/medical-professionals/cmf-thoracic/lactosorb-resorbable-fixation-system/lactosorb-resorbable-fixation-system-brochure.pdf.

Boonrungsiman, S., E. Gentleman, R. Carzaniga, N. D. Evans, D. W. McComb, A. E. Porter and M. M. Stevens (2012). "The role of intracellular calcium phosphate in osteoblast-mediated bone apatite formation." Proceedings of the National Academy of Sciences **109**(35): 14170-14175.

Brown, K. L. and R. E. Hancock (2006). "Cationic host defense (antimicrobial) peptides." Current opinion in immunology **18**(1): 24-30.

Brown, K. L., G. F. Poon, D. Birkenhead, O. M. Pena, R. Falsafi, C. Dahlgren, A. Karlsson, J. Bylund, R. E. Hancock and P. Johnson (2011). "Host defense peptide LL-37 selectively reduces proinflammatory macrophage responses." The Journal of Immunology **186**(9): 5497-5505.

Chen, Z., T. Klein, R. Z. Murray, R. Crawford, J. Chang, C. Wu and Y. Xiao (2016). "Osteoimmunomodulation for the development of advanced bone biomaterials." Materials today **19**(6): 304-321.

Chen, Z., C. Wu and Y. Xiao (2017). Convergence of osteoimmunology and immunomodulation for the development and assessment of bone biomaterials. The Immune Response to Implanted Materials and Devices, Springer**:** 107-124.

Ciumac, D., H. Gong, X. Hu and J. R. Lu (2019). "Membrane targeting cationic antimicrobial peptides." Journal of colloid and interface science **537**: 163-185.

Costa, D. O., P. D. Prowse, T. Chrones, S. M. Sims, D. W. Hamilton, A. S. Rizkalla and S. J. Dixon (2013). "The differential regulation of osteoblast and osteoclast activity by surface topography of hydroxyapatite coatings." Biomaterials **34**(30): 7215-7226.

Costa, F., I. F. Carvalho, R. C. Montelaro, P. Gomes and M. C. L. Martins (2011). "Covalent immobilization of antimicrobial peptides (AMPs) onto biomaterial surfaces." Acta biomaterialia **7**(4): 1431-1440.
Dalby, M. J., N. Gadegaard, R. Tare, A. Andar, M. O. Riehle, P. Herzyk, C. D. Wilkinson and R. O. Oreffo (2007). "The control of human mesenchymal cell differentiation using nanoscale symmetry and disorder." Nature materials **6**(12): 997-1003.
Davidson, D. J., A. J. Currie, G. S. Reid, D. M. Bowdish, K. L. MacDonald, R. C. Ma, R. E. Hancock and D. P. Speert (2004). "The cationic antimicrobial peptide LL-37 modulates dendritic cell differentiation and dendritic cell-induced T cell polarization." The Journal of Immunology **172**(2): 1146-1156.
de Breij, A., M. Riool, R. A. Cordfunke, N. Malanovic, L. de Boer, R. I. Koning, E. Ravensbergen, M. Franken, T. van der Heijde and B. K. Boekema (2018). "The antimicrobial peptide SAAP-148 combats drug-resistant bacteria and biofilms." Science Translational Medicine **10**(423): eaan4044.
de Mesy Bentley, K. L., R. Trombetta, K. Nishitani, S. N. Bello-Irizarry, M. Ninomiya, L. Zhang, H. L. Chung, J. L. McGrath, J. L. Daiss and H. A. Awad (2017). "Evidence of Staphylococcus aureus deformation, proliferation, and migration in canaliculi of live cortical bone in murine models of osteomyelitis." Journal of Bone and Mineral Research **32**(5): 985-990.
Dijksteel, G. S., M. M. Ulrich, M. Vlig, P. H. Nibbering, R. A. Cordfunke, J. W. Drijfhout, E. Middelkoop and B. K. Boekema (2019). "Potential factors contributing to the poor antimicrobial efficacy of SAAP-148 in a rat wound infection model." Annals of clinical microbiology and antimicrobials **18**(1): 38.
Donlan, R. M. (2001). "Biofilm formation: a clinically relevant microbiological process." Clinical Infectious Diseases **33**(8): 1387-1392.
Easton, D. M., A. Nijnik, M. L. Mayer and R. E. Hancock (2009). "Potential of immunomodulatory host defense peptides as novel anti-infectives." Trends in biotechnology **27**(10): 582-590.
Einhorn, T. A. and L. C. Gerstenfeld (2015). "Fracture healing: mechanisms and interventions." Nature Reviews Rheumatology **11**(1): 45.
Elmowafy, E. M., M. Tiboni and M. E. Soliman (2019). "Biocompatibility, biodegradation and biomedical applications of poly (lactic acid)/poly (lactic-co-glycolic acid) micro and nanoparticles." Journal of Pharmaceutical Investigation: 1-34.
Ghosh, C., P. Sarkar, R. Issa and J. Haldar (2019). "Alternatives to conventional antibiotics in the era of antimicrobial resistance." Trends in microbiology.
Gorbet, M., C. Sperling, M. F. Maitz, C. A. Siedlecki, C. Werner and M. V. Sefton (2019). "The blood compatibility challenge. Part 3: Material associated activation of blood cascades and cells." Acta Biomaterialia **94**: 25-32.
Guaní-Guerra, E., T. Santos-Mendoza, S. O. Lugo-Reyes and L. M. Terán (2010). "Antimicrobial peptides: general overview and clinical implications in human health and disease." Clinical immunology **135**(1): 1-11.
Gubin, A., V. Kuznetsov, D. Borzunov, A. Koryukov, A. Reznik and A. Chevardin (2016). "Challenges and perspectives in the use of additive technologies for making customized implants for traumatology and orthopedics." Biomedical Engineering **50**(4): 285-289.
Guihard, P., Y. Danger, B. Brounais, E. David, R. Brion, J. Delecrin, C. D. Richards, S. Chevalier, F. Rédini and D. Heymann (2012). "Induction of osteogenesis in mesenchymal stem cells by activated monocytes/macrophages depends on oncostatin M signaling." Stem cells **30**(4): 762-772.
Günther, F., G. H. Wabnitz, P. Stroh, B. Prior, U. Obst, Y. Samstag, C. Wagner and G. M. Hänsch (2009). "Host defence against Staphylococcus aureus biofilms infection: phagocytosis of biofilms by polymorphonuclear neutrophils (PMN)." Molecular immunology **46**(8-9): 1805-1813.

Hamlet, S., M. Alfarsi, R. George and S. Ivanovski (2012). "The effect of hydrophilic titanium surface modification on macrophage inflammatory cytokine gene expression." Clinical oral implants research **23**(5): 584-590.
Hancock, R. E., E. F. Haney and E. E. Gill (2016). "The immunology of host defence peptides: beyond antimicrobial activity." Nature Reviews Immunology **16**(5): 321.
Hancock, R. E. and H.-G. Sahl (2006). "Antimicrobial and host-defense peptides as new anti-infective therapeutic strategies." Nature biotechnology **24**(12): 1551-1557.
Haney, E. F. and R. E. Hancock (2013). "Peptide design for antimicrobial and immunomodulatory applications." Peptide Science **100**(6): 572-583.
Haney, E. F., S. K. Straus and R. E. Hancock (2019). "Reassessing the host defense peptide landscape." Frontiers in chemistry **7**.
He, X. T., X. Li, Y. Yin, R. X. Wu, X. Y. Xu and F. M. Chen (2018). "The effects of conditioned media generated by polarized macrophages on the cellular behaviours of bone marrow mesenchymal stem cells." Journal of cellular and molecular medicine **22**(2): 1302-1315.
Hilchie, A. L., K. Wuerth and R. E. Hancock (2013). "Immune modulation by multifaceted cationic host defense (antimicrobial) peptides." Nature chemical biology **9**(12): 761.
Hofstee, M. I., G. Muthukrishnan, G. J. Atkins, M. Riool, K. Thompson, M. Morgenstern, M. J. Stoddart, R. G. Richards, S. A. J. Zaat and T. F. Moriarty (2020). "Current concepts of osteomyelitis: from pathological mechanisms to advanced research methods." The American Journal of Pathology.
Hu, Z., T. Murakami, K. Suzuki, H. Tamura, K. Kuwahara-Arai, T. Iba and I. Nagaoka (2014). "Antimicrobial cathelicidin peptide LL-37 inhibits the LPS/ATP-induced pyroptosis of macrophages by dual mechanism." PloS one **9**(1).
Hu, Z., T. Murakami, K. Suzuki, H. Tamura, J. Reich, K. Kuwahara-Arai, T. Iba and I. Nagaoka (2016). "Antimicrobial cathelicidin peptide LL-37 inhibits the pyroptosis of macrophages and improves the survival of polybacterial septic mice." International immunology **28**(5): 245-253.
Hurtado, P. and C. A. Peh (2010). "LL-37 promotes rapid sensing of CpG oligodeoxynucleotides by B lymphocytes and plasmacytoid dendritic cells." The journal of immunology **184**(3): 1425-1435.
Iyer, K. M. and W. S. Khan (2019). General principles of orthopedics and trauma, Springer.
Jablonski, K. A., S. A. Amici, L. M. Webb, J. d. D. Ruiz-Rosado, P. G. Popovich, S. Partida-Sanchez and M. Guerau-de-Arellano (2015). "Novel markers to delineate murine M1 and M2 macrophages." PloS one **10**(12): e0145342.
Jenssen, H., P. Hamill and R. E. Hancock (2006). "Peptide antimicrobial agents." Clinical microbiology reviews **19**(3): 491-511.
Johnson, D. S. C. o. J. (2020). "RAPIDSORB® Fixation System." Retrieved 23-10-2020, 2020, from https://www.jnjmedicaldevices.com/en-US/product/rapidsorbr-rapid-resorbable-fixation-system.
Josse, J., F. Velard and S. C. Gangloff (2015). "Staphylococcus aureus vs. osteoblast: relationship and consequences in osteomyelitis." Frontiers in cellular and infection microbiology **5**: 85.
Kim, T., C. W. See, X. Li and D. Zhu (2020). "Orthopedic Implants and Devices for Bone Fractures and Defects: Past, Present and Perspective." Engineered Regeneration.
Koczulla, R., G. Von Degenfeld, C. Kupatt, F. Krötz, S. Zahler, T. Gloe, K. Issbrücker, P. Unterberger, M. Zaiou and C. Lebherz (2003). "An angiogenic role for the human peptide antibiotic LL-37/hCAP-18." The Journal of clinical investigation **111**(11): 1665-1672.
Koutsopoulos, S. (2017). Peptide applications in biomedicine, biotechnology and bioengineering, Woodhead Publishing.
Kuboki, Y., Q. Jin, M. Kikuchi, J. Mamood and H. Takita (2002). "Geometry of artificial ECM: sizes of pores controlling phenotype expression in BMP-induced osteogenesis and chondrogenesis." Connective tissue research **43**(2-3): 529-534.

Kumar, P., J. N. Kizhakkedathu and S. K. Straus (2018). "Antimicrobial peptides: Diversity, mechanism of action and strategies to improve the activity and biocompatibility in vivo." Biomolecules **8**(1): 4.
Kwakman, P. H., A. A. t. Velde, L. de Boer, D. Speijer, M. Christina Vandenbroucke-Grauls and S. A. Zaat (2010). "How honey kills bacteria." The FASEB Journal **24**(7): 2576-2582.
Lai, Y. and R. L. Gallo (2009). "AMPed up immunity: how antimicrobial peptides have multiple roles in immune defense." Trends in immunology **30**(3): 131-141.
Langenbach, F. and J. Handschel (2013). "Effects of dexamethasone, ascorbic acid and β-glycerophosphate on the osteogenic differentiation of stem cells in vitro." Stem cell research & therapy **4**(5): 1-7.
Lee, E. Y., M. W. Lee and G. C. Wong (2019). Modulation of toll-like receptor signaling by antimicrobial peptides. Seminars in Cell & Developmental Biology, Elsevier.
Lee, J., H. Byun, S. K. Madhurakkat Perikamana, S. Lee and H. Shin (2019). "Current advances in immunomodulatory biomaterials for bone regeneration." Advanced healthcare materials **8**(4): 1801106.
Lee, T.-H., K. N Hall and M.-I. Aguilar (2016). "Antimicrobial peptide structure and mechanism of action: a focus on the role of membrane structure." Current topics in medicinal chemistry **16**(1): 25-39.
Li, L.-Y., L.-Y. Cui, R.-C. Zeng, S.-Q. Li, X.-B. Chen, Y. Zheng and M. B. Kannan (2018). "Advances in functionalized polymer coatings on biodegradable magnesium alloys–A review." Acta biomaterialia **79**: 23-36.
Li, M., Y. Lai, A. E. Villaruz, D. J. Cha, D. E. Sturdevant and M. Otto (2007). "Gram-positive three-component antimicrobial peptide-sensing system." Proceedings of the National Academy of Sciences **104**(22): 9469-9474.
Löfgren, S., L. Miletti, M. Steindel, E. Bachere and M. Barracco (2008). "Trypanocidal and leishmanicidal activities of different antimicrobial peptides (AMPs) isolated from aquatic animals." Experimental parasitology **118**(2): 197-202.
Mader, J. S., C. Ewen, R. E. Hancock and R. C. Bleackley (2011). "The human cathelicidin, LL-37, induces granzyme-mediated apoptosis in regulatory T cells." Journal of Immunotherapy **34**(3): 229-235.
Madera, L. and R. E. Hancock (2012). "Synthetic immunomodulatory peptide IDR-1002 enhances monocyte migration and adhesion on fibronectin." Journal of innate immunity **4**(5-6): 553-568.
Mansour, S. C., O. M. Pena and R. E. Hancock (2014). "Host defense peptides: front-line immunomodulators." Trends in immunology **35**(9): 443-450.
Maria-Neto, S., K. C. de Almeida, M. L. R. Macedo and O. L. Franco (2015). "Understanding bacterial resistance to antimicrobial peptides: From the surface to deep inside." Biochimica et Biophysica Acta (BBA)-Biomembranes **1848**(11): 3078-3088.
Marsell, R. and T. A. Einhorn (2011). "The biology of fracture healing." Injury **42**(6): 551-555.
Mayer, M. L., C. J. Blohmke, R. Falsafi, C. D. Fjell, L. Madera, S. E. Turvey and R. E. Hancock (2013). "Rescue of dysfunctional autophagy attenuates hyperinflammatory responses from cystic fibrosis cells." The Journal of Immunology **190**(3): 1227-1238.
Metsemakers, W.-J., B. Smeets, S. Nijs and H. Hoekstra (2017). "Infection after fracture fixation of the tibia: analysis of healthcare utilization and related costs." Injury **48**(6): 1204-1210.
Mookherjee, N., K. L. Brown, D. M. Bowdish, S. Doria, R. Falsafi, K. Hokamp, F. M. Roche, R. Mu, G. H. Doho and J. Pistolic (2006). "Modulation of the TLR-mediated inflammatory response by the endogenous human host defense peptide LL-37." The Journal of Immunology **176**(4): 2455-2464.
Moravej, H., Z. Moravej, M. Yazdanparast, M. Heiat, A. Mirhosseini, M. Moosazadeh Moghaddam and R. Mirnejad (2018). "Antimicrobial peptides: features, action, and their resistance mechanisms in bacteria." Microbial Drug Resistance **24**(6): 747-767.

Moriarty, T. F., L. Debefve, L. Boure, D. Campoccia, U. Schlegel and R. G. Richards (2009). "Influence of material and microtopography on the development of local infection in vivo: experimental investigation in rabbits." The International journal of artificial organs **32**(9): 663-670.
Moriarty, T. F., S. A. Zaat and H. J. Busscher (2012). Biomaterials associated infection: immunological aspects and antimicrobial strategies, Springer Science & Business Media.
Muthukrishnan, G., E. A. Masters, J. L. Daiss and E. M. Schwarz (2019). "Mechanisms of Immune Evasion and Bone Tissue Colonization That Make Staphylococcus aureus the Primary Pathogen in Osteomyelitis." Current osteoporosis reports **17**(6): 395-404.
Nagaoka, I., H. Tamura and M. Hirata (2006). "An antimicrobial cathelicidin peptide, human CAP18/LL-37, suppresses neutrophil apoptosis via the activation of formyl-peptide receptor-like 1 and P2X7." The Journal of Immunology **176**(5): 3044-3052.
Nijnik, A. and R. Hancock (2009). "Host defence peptides: antimicrobial and immunomodulatory activity and potential applications for tackling antibiotic-resistant infections." Emerging health threats journal **2**(1): 7078.
Nijnik, A., J. Pistolic, A. Wyatt, S. Tam and R. E. Hancock (2009). "Human cathelicidin peptide LL-37 modulates the effects of IFN-γ on APCs." The Journal of Immunology **183**(9): 5788-5798.
Niyonsaba, F., K. Iwabuchi, H. Matsuda, H. Ogawa and I. Nagaoka (2002). "Epithelial cell-derived human β-defensin-2 acts as a chemotaxin for mast cells through a pertussis toxin-sensitive and phospholipase C-dependent pathway." International immunology **14**(4): 421-426.
Niyonsaba, F., L. Madera, N. Afacan, K. Okumura, H. Ogawa and R. E. Hancock (2013). "The innate defense regulator peptides IDR-HH2, IDR-1002, and IDR-1018 modulate human neutrophil functions." Journal of leukocyte biology **94**(1): 159-170.
Niyonsaba, F., H. Ushio, N. Nakano, W. Ng, K. Sayama, K. Hashimoto, I. Nagaoka, K. Okumura and H. Ogawa (2007). "Antimicrobial peptides human β-defensins stimulate epidermal keratinocyte migration, proliferation and production of proinflammatory cytokines and chemokines." Journal of Investigative Dermatology **127**(3): 594-604.
Novak, M. L. and T. J. Koh (2013). "Macrophage phenotypes during tissue repair." Journal of leukocyte biology **93**(6): 875-881.
Omardien, S., J. W. Drijfhout, H. van Veen, S. Schachtschabel, M. Riool, L. W. Hamoen, S. Brul and S. A. Zaat (2018). "Synthetic antimicrobial peptides delocalize membrane bound proteins thereby inducing a cell envelope stress response." Biochimica et Biophysica Acta (BBA)-Biomembranes **1860**(11): 2416-2427.
Omardien, S., J. W. Drijfhout, F. M. Vaz, M. Wenzel, L. W. Hamoen, S. A. Zaat and S. Brul (2018). "Bactericidal activity of amphipathic cationic antimicrobial peptides involves altering the membrane fluidity when interacting with the phospholipid bilayer." Biochimica et Biophysica Acta (BBA)-Biomembranes **1860**(11): 2404-2415.
Oono, T., Y. Shirafuji, W.-K. Huh, H. Akiyama and K. Iwatsuki (2002). "Effects of human neutrophil peptide-1 on the expression of interstitial collagenase and type I collagen in human dermal fibroblasts." Archives of dermatological research **294**(4): 185-189.
Otto, M. (2009). Bacterial sensing of antimicrobial peptides. Bacterial sensing and signaling, Karger Publishers. **16:** 136-149.
Ozbolat, I. T. (2016). 3D bioprinting: fundamentals, principles and applications, Academic Press.
Pajarinen, J., T. Lin, E. Gibon, Y. Kohno, M. Maruyama, K. Nathan, L. Lu, Z. Yao and S. B. Goodman (2019). "Mesenchymal stem cell-macrophage crosstalk and bone healing." Biomaterials **196**: 80-89.
Paul, N. E., C. Skazik, M. Harwardt, M. Bartneck, B. Denecke, D. Klee, J. Salber and G. Zwadlo-Klarwasser (2008). "Topographical control of human macrophages by a regularly microstructured polyvinylidene fluoride surface." Biomaterials **29**(30): 4056-4064.

Pavithra, D. and M. Doble (2008). "Biofilm formation, bacterial adhesion and host response on polymeric implants—issues and prevention." Biomedical Materials **3**(3): 034003.
Prevention, C. f. D. C. a. (2017). "National Hospital Ambulatory Medical Care Survey:2017 Emergency Department Summary Tables." Retrieved 02-10-2020, 2020, from https://www.cdc.gov/nchs/data/nhamcs/web_tables/2017_ed_web_tables-508.pdf.
Puylaert, P. (2018). Optimization of photochemical internalization of antimicrobial peptides targeting intracellular *Staphylococcus aureu*s. Master of Drug Development, University of Antwerp.
Reddy, K., R. Yedery and C. Aranha (2004). "Antimicrobial peptides: premises and promises." International journal of antimicrobial agents **24**(6): 536-547.
Riool, M., A. de Breij, J. W. Drijfhout, P. H. Nibbering and S. A. Zaat (2017). "Antimicrobial peptides in biomedical device manufacturing." Frontiers in chemistry **5**: 63.
Riss, T. L., R. Moravec, A. Niles, S. Duellman, H. Benink, T. Worzella and L. Minor (2004). "Cell viability assays assay guidance manual." Assay Guidance Manual: 1-23.
Scheinpflug, K., M. Wenzel, O. Krylova, J. E. Bandow, M. Dathe and H. Strahl (2017). "Antimicrobial peptide cWFW kills by combining lipid phase separation with autolysis." Scientific reports **7**(1): 1-15.
Scott, M. G., A. C. Vreugdenhil, W. A. Buurman, R. E. Hancock and M. R. Gold (2000). "Cutting edge: cationic antimicrobial peptides block the binding of lipopolysaccharide (LPS) to LPS binding protein." The Journal of Immunology **164**(2): 549-553.
Seebach, E. and K. F. Kubatzky (2019). "Chronic implant-related bone infections–can immune modulation be a therapeutic strategy?" Frontiers in immunology **10**: 1724.
Sevcsik, E., G. Pabst, A. Jilek and K. Lohner (2007). "How lipids influence the mode of action of membrane-active peptides." Biochimica et Biophysica Acta (BBA)-Biomembranes **1768**(10): 2586-2595.
Shprung, T., A. Peleg, Y. Rosenfeld, P. Trieu-Cuot and Y. Shai (2012). "Effect of PhoP-PhoQ activation by broad repertoire of antimicrobial peptides on bacterial resistance." Journal of Biological Chemistry **287**(7): 4544-4551.
Sjollema, J., S. A. Zaat, V. Fontaine, M. Ramstedt, R. Luginbuehl, K. Thevissen, J. Li, H. C. van der Mei and H. J. Busscher (2018). "In vitro methods for the evaluation of antimicrobial surface designs." Acta biomaterialia **70**: 12-24.
Smith, B. S., P. Capellato, S. Kelley, M. Gonzalez-Juarrero and K. C. Popat (2013). "Reduced in vitro immune response on titania nanotube arrays compared to titanium surface." Biomaterials Science **1**(3): 322-332.
Spiller, K. L., S. Nassiri, C. E. Witherel, R. R. Anfang, J. Ng, K. R. Nakazawa, T. Yu and G. Vunjak-Novakovic (2015). "Sequential delivery of immunomodulatory cytokines to facilitate the M1-to-M2 transition of macrophages and enhance vascularization of bone scaffolds." Biomaterials **37**: 194-207.
Steinmetz, S., D. Wernly, K. Moerenhout, A. Trampuz and O. Borens (2019). "Infection after fracture fixation." EFORT open reviews **4**(7): 468-475.
Stoodley, P., K. Sauer, D. G. Davies and J. W. Costerton (2002). "Biofilms as complex differentiated communities." Annual Reviews in Microbiology **56**(1): 187-209.
Takizawa, T., N. Nakayama, H. Haniu, K. Aoki, M. Okamoto, H. Nomura, M. Tanaka, A. Sobajima, K. Yoshida and T. Kamanaka (2018). "Titanium fiber plates for bone tissue repair." Advanced Materials **30**(4): 1703608.
Thakore, R. V., S. E. Greenberg, H. Shi, A. M. Foxx, E. L. Francois, M. A. Prablek, S. K. Nwosu, K. R. Archer, J. M. Ehrenfeld and W. T. Obremskey (2015). "Surgical site infection in orthopedic trauma: A case–control study evaluating risk factors and cost." Journal of clinical orthopaedics and trauma **6**(4): 220-226.
Thurlow, L. R., M. L. Hanke, T. Fritz, A. Angle, A. Aldrich, S. H. Williams, I. L. Engebretsen, K. W. Bayles, A. R. Horswill and T. Kielian (2011). "Staphylococcus aureus biofilms prevent

macrophage phagocytosis and attenuate inflammation in vivo." The Journal of Immunology **186**(11): 6585-6596.
Toben, D., I. Schroeder, T. El Khassawna, M. Mehta, J. E. Hoffmann, J. T. Frisch, H. Schell, J. Lienau, A. Serra and A. Radbruch (2011). "Fracture healing is accelerated in the absence of the adaptive immune system." Journal of Bone and Mineral Research **26**(1): 113-124.
van der Does, A. M., H. Beekhuizen, B. Ravensbergen, T. Vos, T. H. Ottenhoff, J. T. van Dissel, J. W. Drijfhout, P. S. Hiemstra and P. H. Nibbering (2010). "LL-37 directs macrophage differentiation toward macrophages with a proinflammatory signature." The journal of immunology **185**(3): 1442-1449.
VanEpps, J. S. and J. G. Younger (2016). "Implantable Device Related Infection." Shock (Augusta, Ga.) **46**(6): 597.
Verma, A. S. and A. Singh (2013). Animal Biotechnology: Models in discovery and translation, Academic Press.
Ward, W. K., E. P. Slobodzian, K. L. Tiekotter and M. D. Wood (2002). "The effect of microgeometry, implant thickness and polyurethane chemistry on the foreign body response to subcutaneous implants." Biomaterials **23**(21): 4185-4192.
Wei, F., Y. Zhou, J. Wang, C. Liu and Y. Xiao (2018). "The immunomodulatory role of BMP-2 on macrophages to accelerate osteogenesis." Tissue Engineering Part A **24**(7-8): 584-594.
Wiechelman, K. J., R. D. Braun and J. D. Fitzpatrick (1988). "Investigation of the bicinchoninic acid protein assay: identification of the groups responsible for color formation." Analytical biochemistry **175**(1): 231-237.
Yang, L., Y. Liu, H. Wu, Z. Song, N. Høiby, S. Molin and M. Givskov (2012). "Combating biofilms." FEMS Immunology & Medical Microbiology **65**(2): 146-157.
Yang, X., B. F. Ricciardi, A. Hernandez-Soria, Y. Shi, N. P. Camacho and M. P. Bostrom (2007). "Callus mineralization and maturation are delayed during fracture healing in interleukin-6 knockout mice." Bone **41**(6): 928-936.
Ye, J., G. Coulouris, I. Zaretskaya, I. Cutcutache, S. Rozen and T. L. Madden (2012). "Primer-BLAST: a tool to design target-specific primers for polymerase chain reaction." BMC bioinformatics **13**(1): 134.
Yuk, J.-M., D.-M. Shin, H.-M. Lee, C.-S. Yang, H. S. Jin, K.-K. Kim, Z.-W. Lee, S.-H. Lee, J.-M. Kim and E.-K. Jo (2009). "Vitamin D3 induces autophagy in human monocytes/macrophages via cathelicidin." Cell host & microbe **6**(3): 231-243.
Zhang, B. and J. Song (2018). "3D-Printed Biomaterials for Guided Tissue Regeneration." Small Methods **2**(9): 1700306.
Zhang, Z., K. Le, D. La Placa, B. Armstrong, M. M. Miller and J. E. Shively (2020). "CXCR2 specific endocytosis of immunomodulatory peptide LL-37 in human monocytes and formation of LL-37 positive large vesicles in differentiated monoosteophils." Bone reports **12**: 100237.
Zhang, Z. and J. E. Shively (2010). "Generation of novel bone forming cells (monoosteophils) from the cathelicidin-derived peptide LL-37 treated monocytes." PloS one **5**(11).
Zhang, Z. and J. E. Shively (2013). "Acceleration of bone repair in NOD/SCID mice by human monoosteophils, novel LL-37-activated monocytes." PloS one **8**(7).
Zimmerli, W. and P. Sendi (2011). Pathogenesis of implant-associated infection: the role of the host. Seminars in immunopathology, Springer.